Potential impact of temperature and carbon dioxide levels on rice quality

A thesis submitted in fulfilment of the requirements for admission to the degree of Doctor of Philosophy

School of Chemistry, The University of Sydney
March 2007

Rachelle Maree Ward

Abstract

A rice grain is composed of 90% starch, and amylose contributes to up 30% of the starch with the remainder as amylopectin. The structure of starch largely defines the quality of rice, yet the methods to characterise starch have not been reviewed recently. This thesis begins by using the simplest form of starch, debranched amylopectin, to detail and apply the principles of molecular weight theory using Size Exclusion Chromatography (SEC) to illustrate that without correct calibration the molecular weight distribution of starch has been underestimated. In contrast to amylopectin, amylose is difficult to isolate from flour without causing irrevocable damage, is unstable in an aqueous system and is believed to be impossible to debranch with isoamylase. Here an amylose-rich fraction was extracted directly from flour using hot water to avoid the structural–damaging isolation techniques used previously. The ability of isoamylase to debranch the amylose was shown through traditional methods of controlled enzyme degradation of the starch, ensuring that association of chains did not hinder access to the enzyme activation site, and through the contrast of 1H NMR spectra before and after the debranching event. Further, it was shown that 20% of carbohydrate was not recoverable from the SEC, and the unrecoverable carbohydrate is likely to be of high molecular weight and with long chains.

High temperatures during the grain filling period are known to impede on the rice quality of one classification of non-waxy varieties. That hypothesis was rigorously examined by growing rice from a wide genetic background in three temperature regimes, followed by analysis of amylose at a functional, structural and synthesis level. From that phenotypic data, the rice varieties could be divided into three distinct groups – two of poorer quality in an increasingly warmer climate. Candidate single nucleotide polymorphisms (SNPs) have been identified, and a mechanism proposed, to explain the phenotypes. Linking a phenotype to a SNP allows the opportunity for wide scale screening of varieties to predict the quality of rice in an increasing warmer environment.

Rice quality has the potential to change with elevated carbon dioxide levels, both alone and with increased temperature. Here, the quality traits of varieties grown in four combinations of temperature and carbon dioxide levels were assessed. The negative impact of temperature on grain quality was unable to be overcome by an increase in carbon dioxide in all but one quality. Chalk is the undesirable opaque belly of a grain that defines the market price of the grain. In elevated carbon dioxide, the proportion of grains containing a high amount of chalk per grain which will increase the market value of the grain and may help to alleviate the burden of climate change on rice farmers.

Declaration

I hereby declare that this thesis is my own work and that, to the best of my knowledge, it contains no material previously published or written by another person except where due acknowledgement is given in the text of this thesis.

Rachelle Ward

Thank You

It's often said that it is the journey, and not the end result that is important – my journey was touched by many people and experiences because it spanned four laboratories, two supervisors, two countries, one love and the support of my family.

The first of four labs was the cereal chemistry lab at the Yanco Agricultural Institute as part of the DPI, Margrit and Judy taught me the ways of growing and screening rice for many qualities explored on this thesis. For the next six months I was at the Key Centre for Polymer Colloids at The University of Sydney, lab trying to understand polymer principles, and happily working alongside Jef Castro and a visiting Chinese Professor QunYu Gao. At the International Rice Research Institute in the Philippines, I had a year in the Grain Quality lab with Dory, Ruby and Doug amongst many others to complete all my starch structure analysis, and the Grain Research Lab with Yvette and Ken to sequence the pesky *Wx* gene. Thanks to Jann Conroy and Shaoyu Wang at UWS for growing the CO2 plants. From this diversity of labs and people, I am fortunate to walk away with the research and morning tea approach of three different cultures, both lab and nationality, and with friendships and memories from each lab. Thank you.

Both supervisors, Bob Gilbert and Melissa Fitzgerald are hard task masters, but when you rise to the challenge the rewards are worth it. One of my proudest moments throughout my PhD was delivering my PhD seminar at Sydney Uni and Bob complementing me on good science and a great talk. What I have learnt from Melissa over a 6 year working relationship was summarised at the RTWG meeting we attended in Texas watching Melissa create opportunities through self confidence, timely science and, of course, wine! I want to thank Melissa and Bob for spending time fine tuning my writing and speaking ability and science acumen.

The most valued of journeys is that with Greg Halloran – the journey from meeting to marriage was a faster and more enjoyable journey than finishing this PhD!! Greg has experienced all of the highs and lows of this PhD right beside me. We met at the beginning of my PhD where Greg helped lug around my pots on hot Yanco weekends and prepare samples, Greg postponed his career and came to the Philippines with me for a year, and he has been my sounding board throughout the entire time – for this and much more I will love you forever.

My parents and family are at the centre of my entire life journey. The complete security of being part of a loving, supportive and caring family, I believe, makes anything possible. To my family, Mum, Dad, Dennis and Katrina, I dedicate this PhD.

Table of Contents

Chapter 1

The Rice Plant

An Introduction

1.1 BACKGROUND

Rice is easily the most important food crops in the world, providing over 21% of the calorific needs of the world's population, and up to 76 % of the calorific intake of people in south-east Asia [1]. In order to meet the world's demand for rice, a staggering 11% of the world's cultivated land is dedicated specifically to growing rice [2]. Rice is grown between the latitudes of 53°N and 35°S, and from elevations below sea level to above 2000 m [3]. From the Equator towards the Tropic of Capricorn and Tropic of Cancer, rainfall, solar radiation, air and soil temperature and soil organic matter all decrease, and diurnal variation increases. Similarly, from lowland towards upland rice, these climatic and soil nutrition features decrease in intensity. With the myriad different environments comes the enormous diversity of varieties held in the many rice gene banks around the world. Throughout the centuries, rice has adapted naturally or through breeding programs to cope with these varying climates while achieving increased yields alongside water and nutrient efficiency. The research presented in this thesis will look closely at the most recent adaptation to contend with – the increase in both global air temperatures and atmospheric carbon dioxide levels.

Rice farmers in tropical regions typically produce yields of 4 tonne per hectare, while farmers in more temperate regions can produce yields of more than 10 tonne per hectare. The lower yield in tropical regions is a result of low solar radiation, poor land and low-technology rice farming techniques available to the often poorer countries in these regions. When rice production does not match the population demands of each country, many regions need to import rice; for example, Indonesia, Philippines and Sub Saharan Africa. The quality of the rice is also a major contributor to rice trade. As a country becomes more developed, incomes rise, diets diversify, and the ability and the will to pay premiums for good quality rice causes rice trade to be driven by quality [4]. Several examples of quality-based trade are: Thailand commands the export market for soft-cooking fragrant rice, India and Pakistan export basmati rice for very high premiums, and Australia exports high-quality japonica rice to niche markets in developed and developing countries. Any adverse effects of climate change on the quality of rice can severely hamper the value of rice - a classic example of the potential influence of climate change presented to HM Treasury late last year [5].

The quality of a rice is gauged by its milling, aesthetic and cooking qualities. The milling quality is typically measured by the percent of wholegrain rice that remains after the grain is dehulled and milled. The desired aesthetic qualities are the consistency of the length and width and the lack of yellowness and chalkiness of the grain. The cooking qualities of the grain vary according to the cuisine of each country. Typical cooking qualities of the grain are the textural

mouth feel of the rice, which depends upon the less subjective measures of gelatinisation temperature, viscosity and hardness of the grain. These measurable cooking qualities depend upon the structure of the starch granules and starch molecules, and on the lipids and proteins within the grain. A revision of the methods to determine the molecular weight of starch is a high priority given the advances in polymer chemistry and availability of more sophisticated equipment. Much of the structures of starch are pre-determined by the genotype of the variety; however the climate has an enormous influence over the quality of rice [6-11]. In fact, the trade of rice between countries of different climates is common place to satisfy the diversity of grain qualities demanded by consumers of rice.

Attention to the impact of climate change on the world has recently evolved from the grass roots level to a bargaining tool in political fights for leadership, and the recent Stern Report [5] acknowledging the overwhelming evidence that climate change is actually happening. Sir Nicholas Stern reported to HM Treasury the need to assess the economic impact of climate change on agriculture [5]. Within the rice industry, the International Rice Research Institute has recently launched the 2007-2015 strategic plan that states in Goal 2 to "Ensure that rice production is sustainable and stable, has minimal negative environmental impact, and can cope with climate change." The Australian rice industry is also committed to recognising the impact of rice farmers on climate change through the implementation of the Environmental Champions Program. The objectives achieved in this thesis are a timely contribution to the potential social and scientific impact of climate change on the rice quality.

1.2 INTRODUCTION

1.2.1 Climate Trends

The depletion of our ozone layer, the melting of ice caps, the irregularity of La Niña and El Niño events such as drought, the occurrence of freak weather events such as tsunamis and typhoons, and the rapid changes to the gaseous balance in the stratosphere all contribute to global climate trends. In this subsection the climate trends of temperature and carbon dioxide levels will be highlighted. Using a town in the centre of the rice-growing region of Australia as the example, Yanco has experienced an increase in the minimum temperature of 0.03 °C each year and an increase in the maximum temperature of 0.01 °C per year [12]; a trend likely to continue in the future. The net effect of warmer ground and air temperature is common across the entire globe [13]. The average diurnal temperature variation at Yanco during the rice growing season is currently 14 °C and, according to the above trend, will continue to decrease by 0.02 °C each year. So while Yanco is typical of a temperate climate, as the daily average temperature continues to increase and diurnal variation to decrease, the climate may tend towards a tropical environment that experiences a narrower diurnal variation in temperature. Concurrently, atmospheric carbon dioxide levels have risen from 280 ppm to 350 ppm in the past 200 years [14], and from 330 to 375 ppm in the past 25 years in Australia [12]. Rather than reaching a plateau, this trend is expected to continue well into the future. The climate trend of increasing minimum and maximum temperature together with changes in carbon dioxide levels, are shown in Figure 1.1, from data collected by the Australian Bureau of Meteorology.

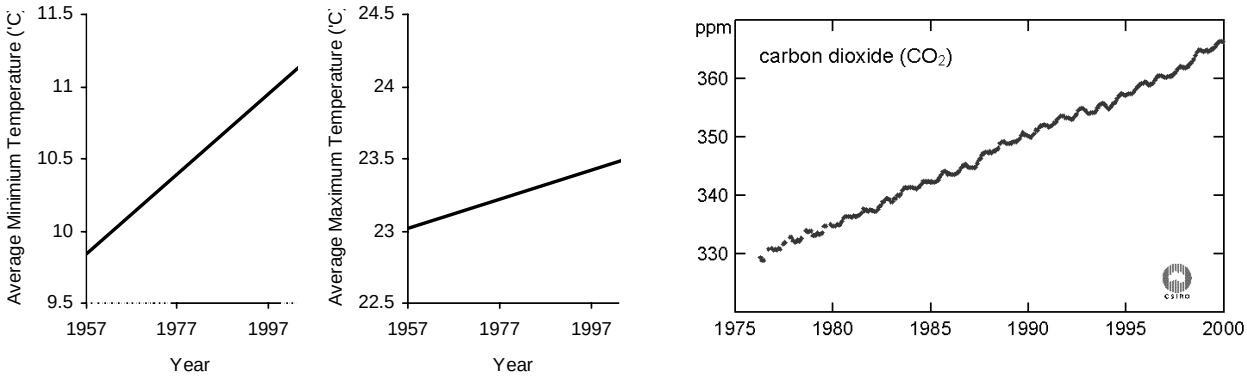

Figure 1.1. Minimum and maximum temperatures collected at Leeton Caravan Park, and carbon dioxide increase at Cape Grim, Tasmania (40.41 °S, 144.41 °E) [12].

1.2.2 The Three Phases of the Growth of a Rice Plant

The growth of a rice plant can be broadly divided into three phases: vegetative (1.2.2.1), reproductive (1.2.2.2) and ripening or grain filling (1.2.2.3)(Figure 1.2) [2,3]. The vegetative phase culminates with Panicle Initiation (PI), the reproductive phase with anthesis (flowering), and grain-filling at grain maturity. The genotype of the rice plant largely defines the characteristics of each phase, although the growth environment of the plant also contributes to the overall source-sink dynamics of the plant [15]. The impact of increased temperature and atmospheric-CO_2 (atm-CO_2) has an accumulative effect on the later phases of plant development; changes in the vegetative and ripening phase will alter the grain-filling phase and thus the grain quality of the rice. To account for this, in the following subsections, each growth phase and the known effects of temperature and carbon dioxide on each phase of the rice plant will be discussed. However, only a few studies report the combined effect of atm-CO_2 and temperature on the each phase of the rice plant.

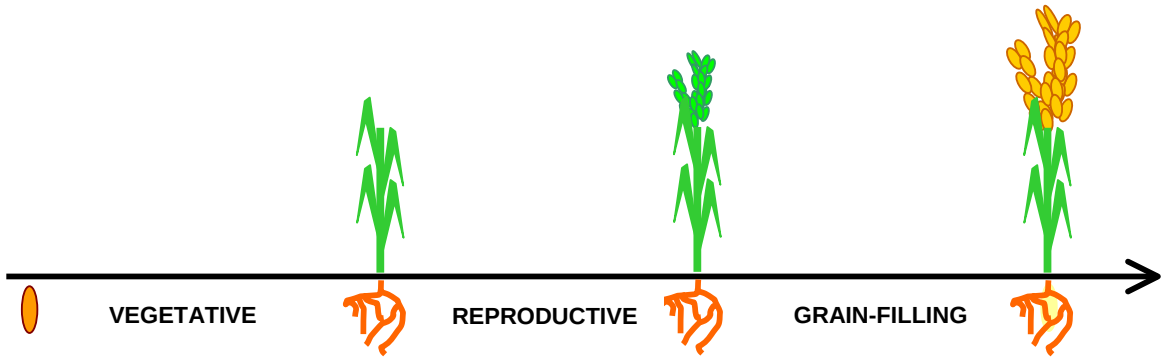

Figure 1.2: The three phases of plant development.

1.2.2.1 Effect of Temperature and atm-CO_2 on Vegetative Phase

The vegetative phase, from germination to PI, accounts for half of the plant life cycle. In this time the root mass increases below ground, while above ground the main culm elongates and produces a series of nodes and associated leaves. After the emergence of the 5th or 6th leaf on the main culm, the plant produces pairs of tillers and associated leaves. A panicle develops on each tiller [3]. Typically the tiller number reaches a maximum at PI [16].

The temperature during plant growth can affect the length of the vegetative period [15]. As temperatures increase the plant develops faster [17] resulting in an increase in biomass through an increase in leaf production [3], and the deposition of more starch in the chloroplast during the day [18]. Increased leaf production increases the tillering potential, although tillering can increase with temperature alone [19]. A critical minimum temperature of 16°C is required for germination and

panicle initiation. Below this temperature seeds can lie dormant, and below this temperature at PI, tillering is decreased. A significant amount of resources is being, and has been expended on solving the problem of cold susceptibility [20,21], and it is possible that increasing global temperatures could alleviate this problem [19]. Thus the main effect of high temperature on vegetative processes is to shorten the length of the vegetative phase; an effect capped at an optimal temperature of 28 °C [22]. The implications and mechanisms of a shorter vegetative phase on the processes of endosperm development, and thus grain quality, are unknown. It is expected that a reduction in the length of the vegetative phase limits the starch and nutrient accumulation into the plant, and that the small biomass will be rapidly exhausted during grain filling to reduce the yield and quality of the rice.

Increased atm-CO_2 has the greatest impact on C_3 plants such as rice [14]. A C_3 plant derives its name from the immediate synthesis of 3-phosphoglycerate during the CO_2 fixation step of photosynthesis (Calvin-Benson cycle), a reaction catalysed by rubisco (ribulose-1,5-biphosphate carboxylase). In elevated atm-CO_2, the amount [23] and activity of the rubisco protein is reduced [23,24], and photorespiration is inhibited, allowing a greater photosynthetic rate resulting in starch accumulation in the form of plant biomass and grain yield [14]. So at elevated atm-CO_2, the rate of CO_2 assimilated into the leaf drives growth during the vegetative stage [25].

When rice plants are grown in elevated atm-CO_2 the greatest response to the atm-CO_2 occurs within the first 16 DAP (Days After Planting), during the initial development of the shoot apex [26]. The effect is seen as an acceleration in the increase in tiller number and height at elevated atm-CO_2 (as compared to ambient atm-CO_2) [26]. After 16 DAP the observed difference in tiller height decreases so when elevated CO_2 is only applied after 15 DAP tiller number does not increase and grain yield is marginally better [26]. Canopy photosynthesis increases at elevated atm-CO_2 [22,27] to meet the increased requirement for carbohydrates for growth [26]. From germination to 35 DAP, at 700 ppm atm-CO_2, shoot growth and leaf expansion are greater than at ambient atm-CO_2 [27], with maximal leaf production having an upper atm-CO_2 limit of 500 ppm [22]. Further, tillering occurs after the emergence of the third leaf on the main culm [27], instead of the usual case, which is after emergence of the 5th or 6th leaf [3], resulting in fewer leaves per tiller. Extra tillering creates a greater potential for C sinks, and is a feature that is unique to rice and wheat [8]. In elevated atm-CO_2, tillering is at a maximum between 35 and 56 DAP and the relative leaf weight decreases [27] and more starch [28], soluble carbohydrate [26] and non-structural carbohydrate accumulates in the leaves [23]. Leaf nitrogen also decreases with long term elevated atm-CO_2 [17,24].

Nutrient supply also impacts on the apparent benefits of increased atmospheric CO_2. Nitrogen and water are the two restrictions for a positive plant response to CO_2 [29]. In conditions of limited N in the soil, there is no response of N accumulation to atm-CO_2 [30]. With sufficient N in the soil

(120 kg N ha^{-1}), N uptake and use is more efficient at elevated atm-CO_2 [30]. With a reduction in photosynthesis due to long term exposure to atm-CO_2, less N was in leaf blades because it was remobilised toward new leaf sheaths and roots [29]. Studies on the uptake of P at elevated atm-CO_2 have shown a positive relationship between increased P and yield at both ambient and elevated atm-CO_2 [25]. In summary, when rice plants are grown in elevated atm-CO_2, they produce fewer leaves, more leaf area and more tillers, implying that during the vegetation stage, the tiller is the preferential sink for carbon [27]. The increase in tiller starch is valuable since grain-filling relies on the mobilisation of that starch [3]. The benefit of increased tillering does not translate into an increase in grain yield as the associated decrease in percent full grains and grain weight results in a decreased grain yield [31].

The impact of temperature and atm-CO_2 on grain quality is largely dependent upon the nutrient and starch accumulated into the leaf material during this vegetative phase that can be potentially remobilised to the panicle during grain-filling. Studies conducted so far have directed the way for future studies, although more work is needed to confirm the predicted flow-on effects of temperature and atm-CO_2 during the vegetative phase using varieties from a wide genetic background and a range of temperature, nutritional and atm-CO_2 levels. To prepare for the rapidly changing conditions of the environment, this work is particularly urgent if the accepted grain quality and yield of rice is to be secured in the future.

1.2.2.2 Effect of Temperature and atm-CO_2 on the Reproductive Phase

The beginning of the reproductive stage is defined by the initiation of the panicle primordia (PI), followed by booting whereby the panicle is seen as a bulge at the base of the leaf sheath. Internodes lengthen, resulting in increased plant height, and the last leaf - flag leaf - emerges. Tillering can still occur during this stage, although generally these 'late stage' tillers do not produce panicles [32]. Heading - the emergence of the panicle - occurs approximately 30 days after PI, and spikelet anthesis (flowering) follows. A single panicle can take up to 10 days to complete anthesis and a crop can take up to 14 days [33]. PI and anthesis are the critical stages of plant growth and if water is limiting, the amount of assimilates that enter the plant decreases [3].

Fertilisation of the anther is the stage of reproductive growth following elongation of the panicle, and it is a stage also susceptible to high temperature [3]. If the hour of anthesis for a particular spikelet coincides with temperature above about 35 °C, fertilisation of that spikelet is highly unlikely to occur [3,31]. The critical maximum temperature for sterility thus determines potential rice yield. Once fertilisation occurs, the first stage of grain development begins, and several days later starch granules are initiated. The temperature of the panicle contributes to the initiation of the mobilisation of assimilates from the flag leaf to the panicle; this occurs most

efficiently when the temperature of the panicle is below about 30 °C [34]. This suggests that, if environmental conditions place the panicle at temperatures above 30 °C, the processes driving the supply of assimilates to the grain will be less, with implications for yield and quality. In the two weeks prior to heading (defined as 90% of panicle emergence from the stem), the temperature difference between the canopy and air temperature has been associated with yield [35]. Varieties that can increase canopy diffusion through stomatal control, reduce the canopy temperature by as much as 1.4 °C compared to the air temperature [35]. In a warming world, the selection of germplasm that tolerates anthesis in warmer conditions, or can maintain cooler canopy temperatures is one way to ensure that yield is maintained in higher temperatures.

In conditions of all atm-CO_2 levels above 500 ppm, PI occurred 12 days earlier [22], while anthesis was reported to occur 7 days earlier for Jarrah rice grown at atm-CO_2 of 700 ppm [36]; presumably this was due to the accelerated vegetative phase rather than any interaction between atm-CO_2 and the reproductive phase of development. Stem elongation around flowering [36] and was reported to increase with atm-CO_2 [27] particularly the length of the first two internodes [26], thus adding to the starch store ready for mobilization into the grain as it fills. In elevated atm-CO_2, biomass continued to increase, reaching a peak at heading [17]. Elevated CO_2 coupled with high temperature improves water-use efficiency within the plant as a result of stomatal closure and decreased evapotranspiration [37,38], but this is offset by the increased temperature in the canopy [39].

Overall, the potential increase in grain yield due to increased tillering caused by atm-CO_2 is promising if the increase in yield is not hampered by high temperatures during the reproductive phase, inhibiting biomass accumulation and low fertility rates. The unpredictable temperatures throughout the reproductive stage suggest that the only way to combat this problem is to enable breeders to select actively for temperature-resistant germplasm featuring, for example, rice with the ability to control its canopy temperature [35], temperature-resistant flowering[40], and efficient starch mobilisation to the grain. Any reduction in the effects of temperature and carbon dioxide on the reproductive stage should, in turn, limit the effects on the grain-filling period to minimise the potential loss of grain quality.

1.2.2.3 Effect of Temperature and atm-CO_2 on Grain-filling Phase of Rice

The grain-filling phase of the rice plant takes approximately 30 to 65 days and begins with the mobilisation of sucrose, nitrogen and starch from the leaf into the grain, a process termed senescence. All cell division within the endosperm occurs within the first 10 days after fertilisation [41] thus defining the potential sink size. Available assimilates during the cell division phase determine cell number [33].

The structure of starch is greatly influenced by temperatures during the active period of grain-filling, which is 5-15 days after anthesis [42]. The time required to reach maximum grain weight can halve at higher temperatures [3]. The increased growth rate results in inferior grain quality compared to grain grown at ambient temperatures [43]. High temperatures during grain-filling could either inhibit sucrose transport into the peduncle [15] or cause substrate to be redirected into cell maintenance [34]. The minimum critical temperature is 15 °C, below which rice will not mature [34]. Therefore the main reason for decreased grain yield with temperature [44] is increased spikelet sterility. For full grains, seed weight increased with temperature till 26.7 °C but declined at higher temperatures [15,45].

In conditions of elevated atm-CO_2, leaf area increases [27] and, as leaf area is linearly related to juvenile spikelets [46], the number of spikelets should also increase. Grain yield is influenced by tiller number, panicle number, spikelet number, sterility rate, grain size, grain number and ultimately grain weight. So far we know that at elevated atm-CO_2 (i) early-stage tiller number increased, resulting in increased panicles per plant; and (ii) leaf number decreased but leaf area increased resulting in increased number of spikelets. Sterility depends upon temperature at anthesis and is largely unaffected by elevated atm-CO_2. Typically, grain weight is uniform for each variety [46], however, grain weight and grain number increased with atm-CO_2 and phosphorous so increased yield [27]. Therefore it is expected that yield per plant increases with atm-CO_2. Nevertheless, the response of increased grain yield in elevated atm-CO_2 is variety-dependent [47] and can on occasion decrease [30].

Very few studies have looked at the combined effects of high temperature and elevated atm-CO_2 levels during the grain-filling stage. Atm-CO_2 is projected to increase, but temperatures, at least in Australia, typically peak during the grain-filling period. Therefore experiments should be designed to be able to predict the impact of these two factors of climate change on rice quality.

1.2.3 Beneath the hull

The act of milling polishes the pericarp layers off the rice grain to reveal the white endosperm, which, unlike other cereals, is commonly consumed without further processing. In the milling process within a breeding program and at the commercial mill, the percent of whole grains, grain shape, grain weight, yellowness and the chalky/opaque appearance of the grain are all recorded. The desired value for each of these parameters depends entirely on the targeted market. For example, a rice suitable for making risotto should be bold with a chalky (opaque) belly, whereas a Basmati rice should be long and slender with no chalk at all (that is, the grain should be transparent).

There are multiple levels of organisation within the rice grain (see Figure 1.3). Milled rice is composed of ~93 % starch, ~6 % protein and ~1 % lipids. Cells are arranged radially in narrow, slender indica grains (7 mm by 1.6 mm) whereas in shorter and wider *japonica* grains cells are arranged along the dorsiventral axis [48]. Amyloplasts reside within cells whereby the width of an amyloplast at the widest point (centre) is about 40 µm and at the narrowest point (periphery) is about 10-20 µm [41]. Amyloplasts are arranged into blocklets of starch granules [49] with dimensions of 100 µm by 400 µm [50]. Individual starch granules are packed within the compound amyloplast (starch granule, see Figure 1.4). The compound starch granules of rice are typically 2-10 µm in size.

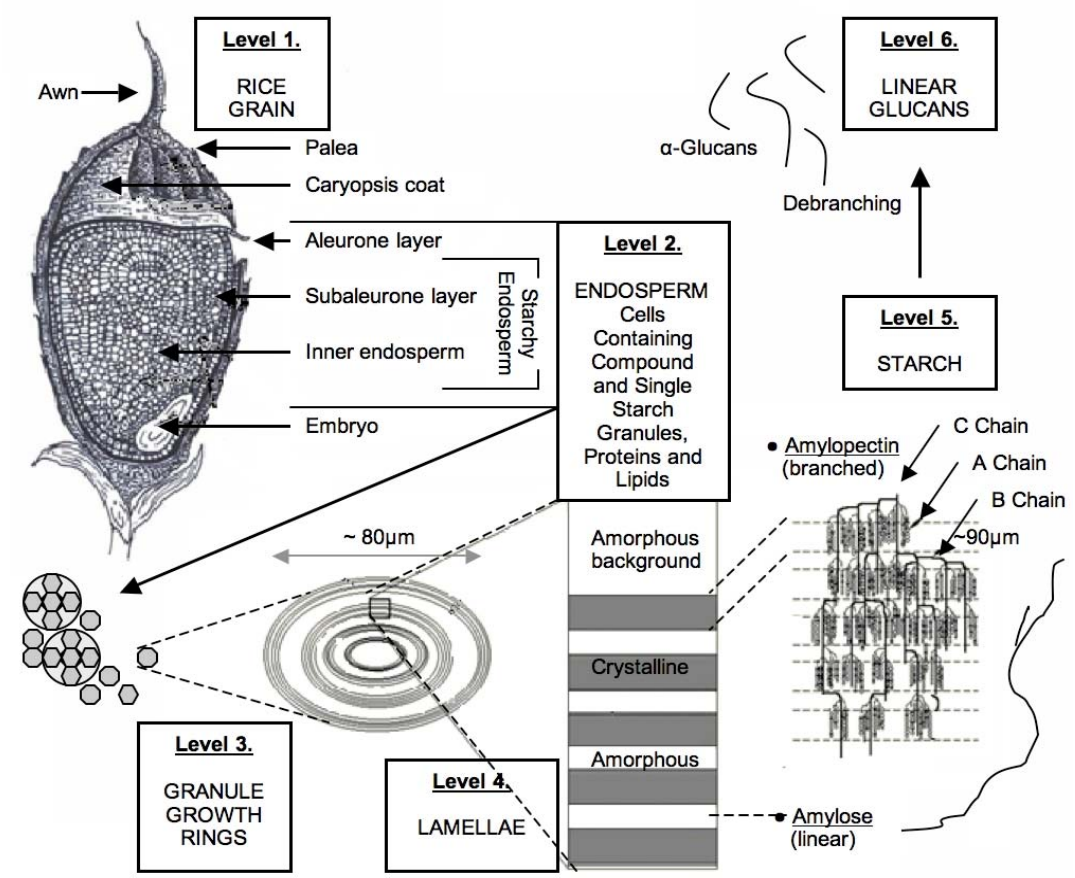

Figure 1.3: Multiple levels of order within the starch granule.

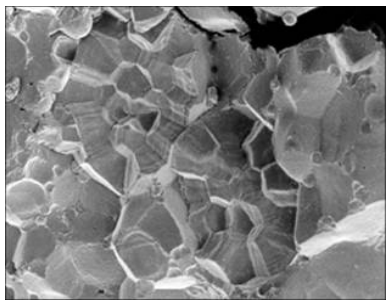

Figure 1.4: Rice starch granule (SEM).

Proteins and lipids are also present in the endosperm. There are four major groups of proteins in rice, with around 70 % of the storage protein is oryzenin [51]. Lipids can be free throughout or bound to starch [52]. After the physical properties of grain dimensions, grain weight and the chalky appearance of a grain, the balance between starch, proteins and lipids is the next benchmark for defining grain quality, with different cultures preferring different compositions.

1.2.4 Rice Starch

Starch is one of the most studied natural polymers, yet many questions about the synthesis, the exact structure of starch and the influence of structure on the functional parameters of starch still remain unanswered. A recent study of the family of starch synthase genes has mapped the level of conservation of these genes over 10 cereals to show clearly that each cereal shares at least one isoform of each starch synthase gene [53]. The suite of alleles found in each species defines the structure of starch that accumulates in the storage organ of each species. A granule requires amylopectin for its structure [54]. Amylose can range from 0 % in waxy rice to a highest observed value of about 30 % in non-waxy rice, and amylose is not required for the structure of the granule. Given rice starch governs many of the cooking qualities of rice, the synthesis, structure and function of amylose and amylopectin will be discussed further.

1.2.4.1 Amylose

Amylose is synthesised by the action of Granule Bound Starch Synthase 1 (GBSS1) which adds glucose-1-phophate molecules to the non-reducing end of chains through an α-(1, 4) bonds glycosidic linkage [55]. The final product is a molecule with a weight average degree of polymerisation of approximately 1110 [56]. The location of amylose within the starch granule has been suggested (Figure 1.3) but has not been resolved. One possibility is that amylose molecules occupy the amorphous lamellae that occur between the crystalline lamellae [42], but other studies show it at the central core of the starch granule [57], and in the amorphous growth rings of the granule [58] which alternate with the semi-crystalline growth rings. The percent of amylose synthesised is effectively determined by the availability of adenosine diphosphoglucose (ADP-glucose), the activity of the ADP/ATP transporter proteins [59], the available space in the granule, and the capacity of GBSS1 protein to be expressed in the endosperm [60].

The amount of GBSS1 protein produced in the endosperm has formed the basis for the classification of the waxy locus into two major alleles – Wx^a and Wx^b (see Figure 1.5). Intermediate and high amylose cultivars carry the Wx^a allele that produces more GBSS1 protein and amylose, and low amylose varieties typically carry the Wx^b allele that encodes for less GBSS1 and less amylose [60]. Both alleles are found in indica rice [61] and only the Wx^b allele has so far been found in temperate japonica rice. With the availability of genotyping technology, these

alleles are now defined by a G → T polymorphism at the 5` splice site of the leader intron 1 (+1, or +126 after the transcription initiation site) [62] which post-transcriptionally alters the expression of the GBSSI protein [63]. In varieties carrying the AGgt sequence, a transcript of 2.3 kB is transcribed and translated [64]. Varieties carrying the AGtt sequence use at least six different splicing patterns to generate a proportion of correctly and incorrectly spliced 2.3 kB GBSSI transcript, only some of which can be translated [65]. Those varieties also accumulate an incompletely spliced transcript of 3.3 kB, which contains intron 1, and cannot be translated [64]. This molecular information all suggests that interferences to the production of 2.3 kB transcript contribute the most to the variability in amylose content by altering the amount of GBSS1 protein that can be translated.

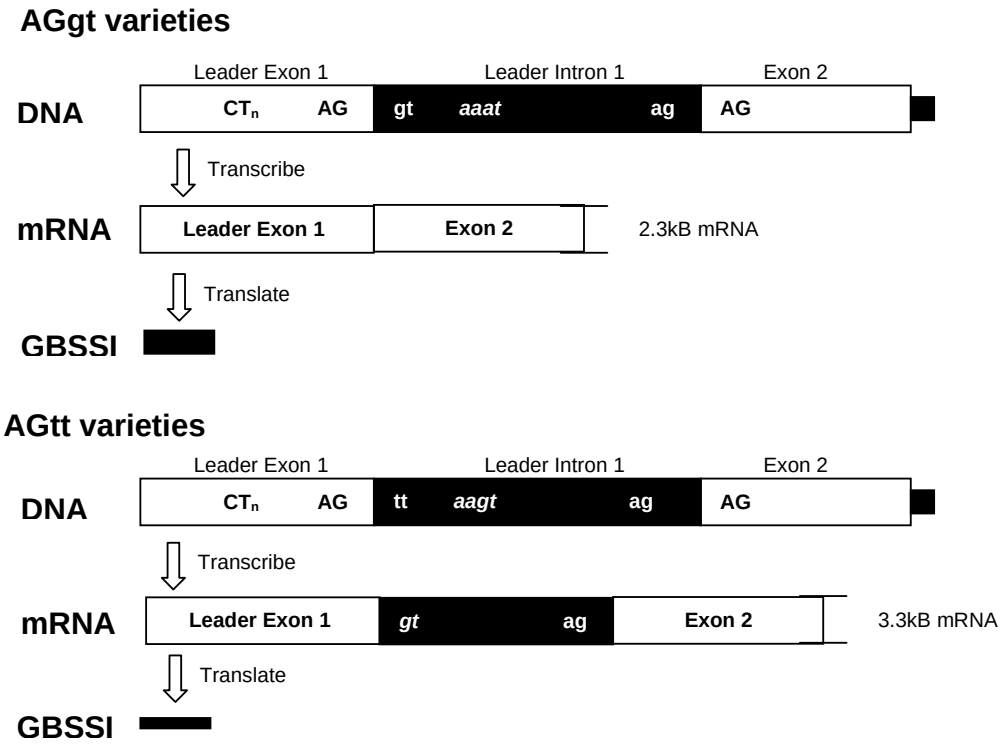

Figure 1.5: Diagram of the published splice site mechanisms of the *Wx* gene.

The temperature during grain filling is known to affect the synthesis of amylose. At cool temperatures, the amount of Wx^b protein expressed is greater, and the amylose content is correspondingly greater [7,66]. At high temperatures the splicing efficiency at the mutation at the 5′ splice site at intron1 of the Wx^b pre-mRNA is reduced [63,66] and an untranslatable Wx^b transcript is produced, decreasing the amylose content. The Wx^a protein is insensitive to cool temperatures and is not disturbed by high temperatures [67].

Interestingly, the domestication of rice can be tracked through the genotype of the *Waxy* gene that encodes GBSS1 protein. Wild rices (*O. rufipogon*, *O. barthii* and *O. glaberrima*) and *indica* subspecies of *O. sativa*, from Africa and India and surrounds, carry the Wx^a allele [63,67]. The Wx^b mutation occurred after domestication of the Wx^a allele [63]. The Wx^b cannot splice properly, but the splicing efficiency does increase in cooler conditions [7,63,66]. In warmer conditions, Wx^b has inefficient splicing at either 1 bp from the authentic splice site, or 100 bp upstream of the authentic splice site [68]. The null mutant, recessive gene, of the *Wx* gene is the *wx* allele and is not capable of making GBSS1 or producing amylose [63] because it contains an extra 23 base pairs within intron 1 which prevent transcription [69].

The classification of rice as Wx^a and Wx^b only accounts for 79.7 % of variation of amylose [70]. Therefore, further characterisation of cultivars is required. On the flanking end of the *Wx* allele, 145 base pairs downstream of the splice site of intron 1, there is a polymorphic region of dinucleotide (CT_n) repeats that can predict up to 88 % of variation in amylose content [63,66,71,72]. That rate of prediction is likely to be successful only when narrow germplasm pools are used because most of the polymorphisms of CT_n occur with both isoforms of the *Wx* allele. The 12 – 20 % of non-waxy rice varieties that cannot be classified, and the narrow genetic background on which this classification is based, places a bias on the reliability of the single nucleotide polymorphism (SNP) and simple sequence repeat (SSR) to predict amylose content, strongly suggesting that a revision of the *indica* / Wx^a style and CT style classification system is warranted.

Amylose content is routinely determined by colormetric analysis of amylose–iodine complexes, amylose structure is much more difficult to ascertain. The structure of amylose can be determined only after isolating the amylose from rice flour. In 1957, the ability to separate linear amylose at a temperature just above gelatinisation was established [55,73]. Linear and branched amylose can be leached from starch with a hot aqueous solution [73-76], hot water [77,78] or extracted from a dispersed, gelatinised starch solution[55], and recrystallised with 1-butanol [75,78]. These solubilisation / recrystallisation steps can distort the *in situ* (natural) structure of the amylose [76,79].

Amylose structure has been quantified from the determination of weight-average molecular weight (M_w), number-average molecular weight (M_n) and branch number of both whole and β-limit dextrins of amylose by wet chemistry and chromatography [55,73-75,78,80]. To obtain the branch number, the whole starch needs to be de-branched, that is, to be hydrolysed at the α-(1,6) branch linkages to produce linear α-(1,4) linked chains. Typically this is done by using isoamylase from *Pseudomonas* sp. (EC 3.1.2.9) [81,82] however it is generally accepted that isoamylase is not able to access some of the branch points of amylose [83,84]. The basis for this inference is that after treating the debranched amylose with β-amylase (EC 3.2.1.2) (to cleave alternate α-(1,4) bonds to

produce maltose) high molecular weight molecules remain [85-87]. However, after hydrolzing the starch with isoamylase and *β*-amylase it was found that amylose exists as both linear and partially branched chains [88] with an average chain length degree of polymerisation (DP) = 980-1110 comprised of 2-5 branches with lengths DP of 250-730 [80]. Due to the amylose-extraction method, the questionable effectiveness of enzymes to degrade the starch, and the lack of correlation between molecules of such structure and functional properties, it is imperative to utilise new technologies to re-visit the method to determine the structure of amylose molecules.

1.2.4.2 Amylopectin

The first component of starch to be deposited in the starch granule is amylopectin. The highly branched structure of amylopectin is synthesized by multiple enzymes: ADP-glucose pyrophosphorylase, starch synthases (SS), starch branching enzymes (SBE), starch debranching enzymes (SDE).

There are four classes of SS that elongate glucan chains via linear α-(1, 4) bonds by transferring glucose from ADP-glucose to a non-reducing end of the starch [53,89], and at least 3 alleles of each SS gene exist. Each class of SS and allele determine the amylopectin classification of S-, M- and L-type on the basis of the proportion of A and B_1 (short) chains relative to B_2 (long) chains. Chains with DP 8-12 and 6-7 are elongated by SSI [53,89], if more than 24% of chains are DP < 10 the product is defined as S-type amylopectin [90]. Starch synthase IIa produces chains with a DP > 24, within a cluster of A and B_1 chains, and its activity is reduced in *japonica* varieties [91]. Chains of DP between 25 and 35 are synthesised by SSIII [92] and are classified as L-type amylopectin when less than 20% of chains are DP < 10[90], typical of *indica* varieties [89]. Essentially, SSIIa determines the amylopectin type, as this enzyme produces intermediate chain lengths [90].

Branching enzymes transfer lengths of glucose chains from donor to acceptor via an α-(1, 6) bond [93], The differences between isoforms reflect each preference of substrate, for example, in *in vitro* studies, BEI transfers longer chains [94] around dp 16 [95] to form a slightly branched structure [96], while BEII prefers shorter chains [94] of DP 10-12. There are two isoforms of BEII, BEIIa is responsible for the synthesis of short chains and BEIIb contributes to the synthesis of short A-chains of amylopectin chains [95]. *In vitro*, the optimal temperature for BEI activity is 33°C and for BEII activity it is less than 20°C [94]; the situation *in vivo* is unknown. The activity for BEII isoforms is the same [96]. All BE isoforms are capable of shifting the glucan-iodine complexes to lower wavelengths [96]. A rice with a mutation in the BEIIb gene is termed an amylose extender mutant due to a lack of chain DP ≤ 13 [95].

The role of starch debranching enzyme (SDE) is to hydrolyse α-(1, 6) branch bonds [89]. The two isoforms of SDE are pullulanase, that debranches α-(1, 6) linkages and β-limit dextrins, and isoamylase that attacks α-(1, 4) structures such as denatures amylopectin and glycogen [89,97]. Without SDE, glucosyl units are diverted to a highly branched structure [97]. The second hydrolysing enzyme, the D-enzyme, transfers glucose units with α-(1, 4) bonds to trim the amylopectin to promote crystallisation [97], but is most likely involved in starch degradation (see Review [98]).

Different isoforms of the SS enzymes act at different times in the grain-filling period, however the co-ordination of several enzymes, and pleiotropic effects of enzymes also play a significant role in the synthesis of amylopectin. For example, SBEIIb can only be activated when complexed with a phosphorylase and SBEI, while SBEIIa must be in a complex with phosphorylase to be activated [99].

Amylopectin is a high MW and highly branched molecule. Rice amylopectin molecules have an average DP of 700-2100, 4400- 8400 and 13400-26500 with an increasing number of clusters per molecule [100], comprising many chains ranging in length from DP 10 up to 130 [101]. A-chains are held in parallel and form the crystalline lamellae [89], B_1 span one cluster, B_2 span 2 clusters, etc [54,89]. The C-chain carries the only reducing end in the molecule [89]. Branch points lie in the amorphous regions [102].

During cooking and processing, starch undergoes gelatinisation. Knowing the gelatinisation temperature (GT) enables prediction of the shelf-life stability and sensory attributes of rice products [103]. Gelatinisation temperature (GT) is the temperature required to reach glass transition of the amorphous region (second order) and melt starch crystals (first order)[104]. Gelatinisation is an irreversible, endothermic reaction involving the swelling of the amorphous region, compaction and alignment of the crystalline region, followed by the denaturing of the amylopectin [102] (Figure 5).

The structure of amylopectin has been related to GT [90], in particular the length of the A-chains and the depth of the amorphous region [91,104,105]. Gelatinisation temperature is positively correlated to the ratio of chains DP < 10 to DP < 24; therefore, L-type amylopectin has higher GT than S-type [90]. Small helices as in S-type starch have broad endotherms [106], because less crystallinity means lower enthalpy. Conversely, large amorphous regions show low GT [104]. SSIIa has been identified as the enzyme that contributes the most to defining gelatinisation temperature class [91].

Temperature can affect the structure of amylopectin. In a test tube, SS1 activity peaked at 25 °C, above which activity is considerably reduced and synthesis is decreased [107]; the activity of

other enzymes remained unchanged [107]. In a glasshouse, the SS1 activity peaked at 7 DAF when exposed to an average temperature of 32 °C decreasing rapidly to 15 DAF, whereas at 25 °C the activity of SS1 peaks between 7 and 11 DAF [108]. The activity of SBE was also reduced at 32 °C [108]. Overall, changes in the activity of starch synthesis enzymes in increased temperatures result in a greater amount of long B chains and decrease in short chains as compared to at low temperatures in both non-waxy [109] and waxy rice varieties [42]. The gelatinisation temperature endosperm widens with increased exposure to temperatures of 30 °C from 5 to 15 days after pollination [42] due to changes in the structure of amylopectin.

1.2.5 Rice and the climate

The impact of climate change on grain quality is best understood by gathering information at synthesis, structural and functional level as depicted in Figure 1.6. Then travelling this pathway from synthesis to structure, and structure to synthesis insists that connections are made between each information level. Applying abiotic stresses to the rice plant and observing how the pathway changes can hold an enormous amount of information. Rice breeders can begin to exclude quality traits that are vulnerable to temperature and carbon dioxide to secure accepted grain qualities in the future, and to limit the economic cost of climate change on the agricultural sector. Industrial and food chemists can utilise the functional properties of starch to create value-added food products or renewable, starch-based polymer products to sequester carbon into paints and plastics. Cereal chemists can link the range of phenotypes created by the trials to the genetic background of each variety to glean mechanistic information about the control of each phenotype, and can link structural data to cooking qualities of the grain to provide information to both rice breeders and industrial chemists.

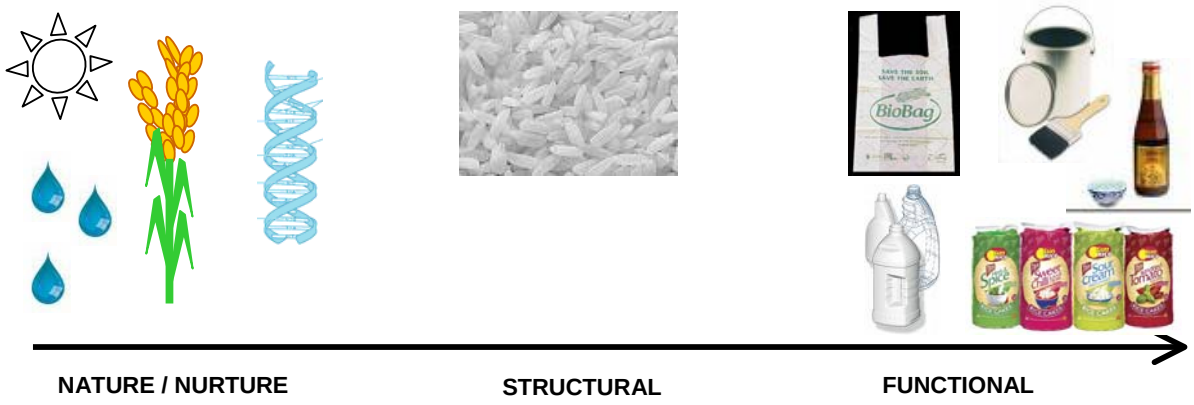

Figure 1.6. The flow of information from synthesis to structural to functional data.

Rice quality is related to the molecular structures of starch, but methods to measure these structures are antiquated and fraught with critical problems. Chapter 2 aims to use principles developed within polymer chemistry to improve the interpretation of Size Exclusion Chromatography (SEC) data [82]. Chapter 3 is focused on the betterment of the problems associated with the isolation, debranching and measurement of amylose by SEC, and to use the interpretation of SEC data developed in Chapter 2.

The new techniques to characterise starch will be used in Chapters 4 and 5 to understand the impacts of increased temperature and carbon dioxide levels on rice quality (see Figure 1.6). Chapter 4 is primarily focused on the impact of temperature on rice qualities related to amylose by using the results and problems of a previous study as the hypothesis [66]. Chapter 5 aims to be the first comprehensive study that combines the two aspects of climate change that pose an immediate threat to the global rice industry – temperature and carbon dioxide.

1.3 REFERENCES

1. *Rice Almanac* (eds. Maclean, J. L., Dawe, D. C., Hardy, B. & Hettel, G. P.) (2002).
2. IRRI, WARDA, CIAT & FAO. *Rice Almanac: Source Book for the Most Important Economic Activity on Earth.* (eds. Maclean, J. L., Dawe, D. C., Hardy, B. & Hettel, G. P.) (CABI Publishing, 2002).
3. Yoshida, S. *Fundamentals of Rice Crop Science* (International Rice Research Institute, Los Banos, Laguna, 1981).
4. http://www.ifc.org/ifcext/mekongpsdf.nsf/AttachmentsByTitle/MDB1/$FILE/MDB1-EN.pdf.
5. Stern, N. *Stern Review: The Economics of Climate Change* (Cambridge University Press, Cambridge, 2006).
6. Resurreccion, A. P., Hara, T., Juliano, B. O. & Yoshida, S. Effect of temperature during ripening on grain quality of rice. *Soil Sci. Plant Nutr.* **23**, 109 - 112 (1977).
7. Sano, Y., Maekawa, M. & Kicuchi, H. Temperature effects on the *Wx* protein level and amylose content in the endosperm of rice. *J. Hered.* **6**, 221 -222 (1985).
8. Seneweera, S. P. & Conroy, J. P. Growth, grain yield and quality of rice (*Oryza sativa* L.) in response to elevated CO_2 and phosphorus nutrition. *Soil Sci. Plant Nutr.* **43**, 1131-1136 (1997).
9. Lisle, A., Martin, M. & Fitzgerald, M. A. Chalky and translucent rice grains differ in starch composition and structure and cooking properties. *Cereal Chemistry* **77**, 627 - 632 (2000).
10. Zhong, L.-j., Cheng, F.-m., Wen, X., Sun, Z. X. & Zhang, G. P. The deterioration of eating and cooking quality caused by high temperature during grain filling in early-season *indica* rice cultivars. *Journal of Agronomy and Crop Science* **191**, 218 - 225 (2005).
11. Philpot, K., Martin, M., Burtado Jr., V., Willoughby, D. & Fitzgerald, M. A. Environmental factors that affect the ability of amylose to contribute to retrogradation in gels made from rice flour. *J. Agric. Food Chem.* **54**, 5182-5190 (2006).
12. http://www.bom.gov.au.
13. Karl, T. R., Kukla, G., Razuvayev, V. N., Changery, M. J., Quayle, R. G., Heim, R. R. & Easterling, D. R. Global warming: Evidence for asymmetric diurnal temperature change. *Geophys. Res. Lett.* **18**, 2253 - 2256 (1991).
14. Amthor, J. S. Perspective on the relative insignificance of increasing atmospheric CO_2 concentration to crop yield. *Fields Crop Research* **58**, 109-127 (1998).
15. Dingkuhn, M. & Kropff, M. in *Photoassimilate distribution in plants and crops: Source-sink relationships* (eds. Zamski, E. & Schaffer, A. A.) 519-547 (Marcel Dekker Incorporated Publishers, 1996).
16. Batten, G. & Blakeney, A. Using NIR to monitor crop energy reserves. *In Advances in Near Infrared Spectroscopy* **Ed: Murray I and Cowe IA**, 303 - 308 (1992).
17. Sakai, H., Yagi, K., Kobayashi, K. & Kawashima, S. Rice carbon balance under elevated CO_2. *New Phytologist* **150**, 241-249 (2001).
18. Preiss. Regulation of the biosynthesis and degradation of starch. *Annual Review of Plant Physiology* **54**, 431 - 454 (1982).

19. Baker, J. T., Allen, L. H. & Boote, K. J. Response of rice carbon dioxide and temperature. *Agricultural and Forest Meteorology* **60**, 153-166 (1992).
20. Farrell, T. C., Fukai, S. & Williams, R. L. Minimising cold damage during reproductive development among temperate rice genotypes. I. Avoiding low temperature with the use of appropriate sowing time and photoperiod-sensitive varieties. *Aust. J. Agric. Res.* **57**, 75 - 88 (2006).
21. Farrell, T. C., Fox, K. M., Williams, R. L. & Fukai, S. Minimising cold damage during reproductive development among temperate rice genotypes. II. Genotypic variation and flowering traits related to cold tolerance screening. *Aust. J. Agric. Res.* **57**, 89 - 100 (2006).
22. Baker, J. T. & Allen, L. H. Assessment of the impact of rising carbon dioxide and other potential climate changes on vegetation. *Environmental Pollution* **83**, 223 - 235 (1994).
23. Rowland-Bamford, A. J., Baker, J. T., Allen Jr, L. H. & Bowes, G. Acclimation of rice to changing atmospheric carbon dioxide concentration. *Plant, Cell and Environment* **14**, 577 - 583 (1991).
24. Nakano, H., Makino, A. & Mae, T. The effect of elevated partial pressure of carbon dioxide on the relationship between photosynthetic capacity and N content in rice leaves. *Plant Physiol.* **115**, 191-198 (1997).
25. Conroy, J. P., Seneweera, S. P., Basra, A. S., Rogers, G. & Nissen-Wooller, B. Influence of rising atmospheric CO_2 concentrations and temperature on growth, yield and grain quality of cereal crops. *Aust. J. Plant Physiol.* **21**, 741 - 758 (1994).
26. Jitla, D. S., Rogers, G. S., Seneweera, S. P., Basra, A. S., Oldfield, R. J. & Conroy, J. P. Accelerated early growth of rice at elevated CO2: is it related to developmental changes in the shoot apex ? *Plant Physiol.* **115**, 15 - 22 (1997).
27. Seneweera, S. P., Blakeney, A., Milham, P., Basra, A. S., Barlow, E. W. R. & Conroy, J. P. Influence of rising atmospheric CO_2 and phosphorus nutrition on the grain yield and quality of rice (*Oryza sativa* cv. Jarrah). *Cereal Chemistry* **73**, 239 - 243 (1996).
28. Ziska, L. H., Namuco, O., Moya, T. & Quilang, J. Growth and yield response of field-grown tropical rice to increasing carbon dioxide and air temperature. *Agron. J.* **89**, 45- 53 (1997).
29. Makino, A., Harada, M., Sato, T., Nakano, H. & Mae, T. Growth and N allocation in rice plants under CO_2 enrichment. *Plant Physiol.* **115**, 199- 203 (1997).
30. Kim, H. Y., Lieffering, M., Miura, S., Kobayashi, K. & Okada, M. Growth and nitrogen uptake of CO_2-enriched rice under field conditions. *New Phytologist* **150**, 223-229 (2001).
31. Baker, J. T., Allen Jr, L. H. & Boote, K. J. Temperature effects on rice at elevated CO_2 concentration. *J. Experimental Botany* **43**, 959 - 964 (1992).
32. Sheehy, J. E., Mnzaya, M., Cassman, K. G., Mitchell, P. L., Pablico, P., Robles, R. P., Samonte, H. P., Lales, J. S. & Ferrer, A. B. Temporal origin of nitrogen in the grain of irrigated rice in the dry season: the outcome of uptake, cycling, senescence and competition studied using a ^{15}N-point placement technique. *Field Crops Research* **89**, 337 - 348 (2004).
33. Mohapatra, P. K., Patel, R. & Sahu, S. K. Time of flowering affects grain quality and spikelet partitioning within the rice panicle. *Aust. J. Plant Physiol.* **20**, 231-241 (1993).
34. Chowdhury, S. I. & Wardlaw, I. F. The effect of temperature on kernel development in cereals. *Aust. J. Agric. Res.* **29**, 205-223 (1978).
35. Horie, T., Matsuura, S., Takai, T., Kuwasaki, K., Ohsumi, A. & Shiraiwa, T. Genetic difference in canopy diffusive conductance measured by a new remote-sensing method

and its association with the difference in rice yield potential. *Plant Cell and Environment*, 1-8 (2005).
36. Seneweera, S. P., Milham, P. & Conroy, J. P. Influence of elevated CO_2 and phosphorus nutrition on the growth and yield of a short duration rice (*Oryza sativa* cv. Jarrah). *Aust. J. Plant Physiol.* **21**, 281 - 92 (1994).
37. Hunsaker, D. J., Hendrey, G. R., Kimball, B. A., Lewin, K. F., Mauney, J. R. & Nagy, J. Cotton evapotranspiration under field-grown conditions with CO_2 enrichment and variable soil moisture regimes. *Agricultural and Forest Meteorology* **70**, 247 - 258 (1994).
38. Kimball, B. A. & Idso, S. B. Increasing atmospheric CO_2: effects on crop yield, water use, and climate. *Agric. Water Manag.* **7**, 55 - 72 (1983).
39. Yoshimoto, M., Oue, H. & Kobayashi, K. Energy balance and water use efficiency of rice canopies under free-air CO_2 enrichment. *Agricultural and Forest Meteorology* **133**, 226 - 246 (2005).
40. Matsui, T., Kobayashi, K., Kagata, H. & Horie, T. Correlation between viability of pollination and length of basal dehiscence of the theca in rice under hot and humid condition. *8* **2** (2005).
41. Matsuo, T. & Hoshikawa, K. *Science of the rice plant* (eds. Matsuo, T. & Hoshikawa, K.) (Food and Agriculture Policy Research Center., Tokyo, Japan, 1993).
42. Asaoka, M., Okuno, K. & Fuwa, H. Effect of environmental temperature at the milky stage on amylose content and fine structure of amylopectin of waxy and nonwaxy endosperm starches of rice (*Oryza sativa L.*). *Agric. Biol. Chem.* **49**, 373 - 379 (1985).
43. Baker, J. T., Allen, L. H., Boote, K. J., Jones, P. & Jones, J. W. Developmental responses of rice to photoperiod and carbon dioxide concentration. *Agricultural and Forest Meteorology* **50**, 201-210 (1990).
44. Baker, J. T., Allen Jr, L. H., Boote, K. J. & Pickering, N. B. Rice responses to drought under carbon dioxide enrichment. 1. Growth and yield. *Global Change Biology* **3**, 119 - 128 (1997).
45. Tamaki, M., Ebata, M., Tashiro, T. & Ishikawa, M. Physio-ecological studies on quality formation of Rice Kernel. I. Effects of nitrogen top-dressed at full heading time and air temperature during ripening period on quality of rice kernel. *Japanese Journal of Crop Science* **58**, 653 - 658 (1989).
46. Sheehy, J. E., Dionora, M. J. A. & Mitchell, P. L. Spikelet numbers, sink size and potential yield in rice. *Fields Crop Research* **71**, 77- 85 (2001).
47. Ziska, L. H., Manalo, P. A. & Ordonez, R. A. Intraspecific variation in the response of rice (*Oryza sativa* L.) to increased CO_2 and temperature: growth and yield reponse of 17 cultivars. *J. Experimental Botany* **47**, 1353 - 1359 (1996).
48. Juliano, B. O. *Rice: Chemistry and Technology* (ed. Juliano, B. O.) (St. Pauls, Minnesota, 1985).
49. Gallant, D. J., Bouchet, B. & Baldwin, P. S. Microscopy of starch: evidence of a new level of granule organisation. *Carbohydrate Polymers* **32**, 177 - 191 (1997).
50. Dang, J. M. C. & Copeland, L. Imaging of rice grains using atomic force microscopy. *Jounal of Cereal Science* **37**, 165-170 (2003).
51. Chrastil, J. & Zarins, Z. M. Influence of storage on peptide subunit composition of rice oryzenin. *J. Agric. Food Chem.* **40**, 927 - 930 (1992).

52. Slade, L. & Levine, H. Non-equilibrium melting of native granular starch: Part I. Temperature location of the glass transition associated with gelatinisation of A-type cereal starches. *Carbohydrate Polymers* **8**, 183 - 208 (1998).
53. Hirose, T. & Terao, T. A comprehensive expression analysis of the starch synthase gene family in rice (*Oryza sativa* L.). *Planta* **220**, 9 - 16 (2004).
54. Hizukuri, S. Polymodal distribution of the chain lengths of amylopectin, and its significance. *Carbohydrate Research* **147**, 342 - 347 (1986).
55. Banks, W., Greenwood, C. T. & Thomson, J. The properties of amylose as related to the fractionation and subfractionation of starch. *Edinburgh University Press*, 197 - 213 (1959).
56. Takeda, Y. & Hizukuri, S. Structures of branched molecules of amylose of various origins, and molar fractions of branched and unbranched molecules. *Carbohydrate Research* **165**, 139 - 145 (1987).
57. Blennow, A., Hansen, M., Schulz, A., Jorgensen, K., Donald, A. M. & Sanderson, J. The molecular deposition of transgenically modified starch in the starch granule as imaged by functional microscopy. *Journal of Structural Biology* **143**, 229 - 241 (2003).
58. Atkin, N. J., Cheng, S. L., Abeysekera, R. M. & Robards, A. W. Localisation of amylose and amylopectin in tarch granules using enzyme-gold labelling. *Starch/Staerke* **51**, 163 - 172 (1999).
59. Emes, M. J., Bowsher, C. G., Hedley, C., Burrell, M. M., Scrase-Field, E. S. F. & Tetlow, I. J. Starch synthesis and C partitioning in developing endosperm. *J. Experimental Botany* **54**, 569-575.
60. Sano, Y. Differential regulation of waxy gene expression in rice endosperm. *Theor. Appl. Genet.* **68**, 467-473 (1984).
61. Prathepha, P. & Baimai, V. Variation of *Wx* microsatellite allele, waxy allele distribution and differentiation of chloroplast DNA in a collection of Thai rice (*Oryza sativa* L.). *Euphytica* **140**, 231-237 (2004).
62. Isshiki, M., Morino, K., Nakajima, M., Okagaki, R. J., Wessler, S. R., Izawa, T. & Shimamoto, K. A naturally occurring functional allele of the rice waxy locus has a GT to TT mutation at the 5` splice site of the first intron. *The Plant Journal* **15**, 133 - 138 (1998).
63. Hirano, H.-Y., Eiguchi, M. & Sano, Y. A single base change altered the regulation of the *Waxy* gene at the posttranscriptional level during the domestication of rice. *Molecular Biology and Evolution* **15**, 978 - 987 (1998).
64. Wang, Z.-Y., Zheng, F.-Q., Shen, G.-Z., Gao, J.-P., Snustad, D.-P., Li, M.-G., Zhang, J.-L. & Hong, M.-M. The amylose content in rice endosperm is related to the post-transcriptional regulation of the *waxy* gene. *Plant Journal* **7**, 613 - 622 (1995).
65. Cai, X.-L., Wang, Z.-Y., Xing, Y.-Y., Zhang, J.-L. & Hong, M.-M. Aberrant splicing of intron 1 leads to the heterogeneous 5` UTR and decreased expression of *waxy* gene in rice cultivars of intermediate amylose content. *The Plant Journal* **14**, 459-465 (1998).
66. Larkin, P. D. & Park, W. D. Transcript accumulation and utilisation of alternate and non-concensus splice sites in rice granule-bound synthase are temperature-sensitive and controlled by a single-nucleotide polymorphism. *Plant Molecular Biology* **40**, 719-727 (1999).
67. Sano, Y., Hirano, H. Y. & Nishimura, M. in *Rice Genetics II* 11-20 (IRRI, 1991).

68. Isshiki, M., Nakajima, M., Satoh, H. & Shimamoto, K. *dull*: rice mutants with tissue-specific effects on teh splicing of the *waxy* pre-mRNA. *The Plant Journal* **23**, 451 - 460 (2000).
69. Wanchana, S., Toojinda, T., Tragoonrung, S. & Vanavichit, A. Duplicated coding sequence in the *waxy* allele of tropical glutinous rice (*Oryza sativa* L.). *Plant Science* **165**, 1193-1199 (2003).
70. Ayres, N. M., McClung, A. M., Larkin, P. D., Bligh, H. F. J., Jones, C. A. & Park, W. D. Microsatellites and a single-nucleotide polymorphism differentiate apparent amylose classes in an extended pedigree of US rice germ plasm. *Theoretical and Applied Genetics* **94**, 773 - 781 (1997).
71. Bligh, H. F. J., Till, R. I. & Jones, C. A. A microsatellite sequence closely linked to the *waxy* gene of *Oryza sativa*. *Euphytica* **86**, 83-85 (1995).
72. Bergman, C. J., Delgado, J. T., McClung, A. M. & Fjellstrom, R. G. An improved method for using a microsatellite in the rice waxy gene to determine amylose class. *Cereal Chemistry* **78**, 257-260 (2001).
73. Cowie, J. M. G. & Greenwood, C. T. *J. Chem. Soc.*, 4430-4437 (1957).
74. Hizukuri, S. Properties of hot-water-extractable amylose. *Carbohydrate Research* **217**, 251-253 (1991).
75. Murugesan, G., Shibanuma, K. & Hizukuri, S. Characterisation of hot-water-soluble components of starches. *Carbohydrate Research* **242**, 203-215 (1993).
76. Ramesh, M., Ali, Z. S. & Bhattacharya, K. R. Structure of rice starch and its relation to cooked-rice texture. *Carbohydrate Polymers* **38**, 337 - 347 (1999).
77. Banks, W. & Greenwood, C. T. *Starch and its components* (Edinburgh University Press, Edinburgh, 1975).
78. Mizukami, H., Takeda, Y. & Hizukuri, S. The structure of hot-water soluble components in the starch granules of new Japanese rice cultivars. *Carbohydrate Polymers* **38**, 329-335 (1999).
79. Chiou, H., Martin, M. & Fitzgerald, M. A. Effect of purification methods on rice starch structure. *Starch/Staerke* **54**, 415-20 (2002).
80. Takeda, Y. & Hizukuri, S. Purification and structure of amylose from rice starch. *Carbohydrate Research* **148**, 299 - 308 (1986).
81. Yokobayashi, K., Misaki, A. & Harada, T. Specificity of *Pseudomonas* Isoamylase. *Agric. Biol. Chem.* **33**, 625 - 627 (1969).
82. Batey, I. L. & Curtin, B. M. Measurement of amylose/amylopectin ratio by high-performance liquid chromatography. *Starch* **48**, 338-344 (1996).
83. Banks, W. & Greenwood, C. T. Physicochemical studies on starches. XXXII. Incomplete b-amylolysis of amylose. Discussion of its cause and implications. *Starch* **19**, 197 - 206 (1967).
84. Takeda, Y., Maruta, N. & Hizukuri, S. Structures of indica rice varieties (IR48 and IR64) having intermediate affinities for iodine. *Carbohydrate Research* **187**, 287 - 294 (1989).
85. Hizukuri, S., Takeda, Y., Yasuda, M. & Suzuki, A. Multi-branched nature of amylose and the action of de-branching enzymes. *Carbohydrate Research* **94**, 205 - 213 (1981).
86. Takeda, Y., Maruta, N. & Hizukuri, S. Examining the structure of amylose by tritium labelling of the reducing terminal. *Carbohydrate Research* **227**, 113-120 (1992).
87. Takeda, Y., Maruta, N. & Hizukuri, S. Structures of amylose and subfractions with different molecular sizes. *Carbohydrate Research* **226**, 279 - 285 (1992).

88. Hizukuri, S., Takeda, Y., Maruta, N. & Juliano, B. O. Molecular structures of rice starch. *Carbohydrate Research* **189**, 227-235 (1989).
89. Nakamura, Y. Towards a better understanding of the metabolic system for amylopectin biosynthesis in plants: rice endosperm as a model tissue. *Plant Cell Physiol.* **43**, 718-725 (2002).
90. Nakamura, Y., Sakurai, A., Inaba, Y., Kimura, K., Iwasawa, N. & Nagamine, T. The fine structure of amylopectin in endosperm from cultivated rice can be largely classified into two classes. *Starch* **54**, 117-131 (2002).
91. Umemoto, T., Yano, M., Satoh, H., Shomura, A. & Nakamura, Y. Mapping of a gene responsible for the difference in amylopectin structure between japonica-type and indica-type rice varieties. *Theor. Appl. Genet.* **104**, 1-8 (2002).
92. Edwards, A., Fulton, D. C., Hylton, C. M., Jobling, S. A., Gidley, M., Rossner, U., Martin, C. & Smith, A. M. A combined reduction in activity of starch synthases II and III of potato has novel effects on the starch of tubers. *Plant J.* **17**, 251-261 (1999).
93. Borovsky, D., Smith, E. E. & Whelan, W. J. On the mechanism of amylose branching by potato Q-enzyme. *Eur. J. Biochem.* **62**, 307 - 312 (1976).
94. Takeda, Y., Guan, H. P. & Preiss. Branching of amylose by the branching isoenzymes of maize endosperm. *Carbohydrate Research* **240**, 253-263 (1993).
95. Nishi, A., Nakamura, Y., Tanaka, N. & Satoh, H. Biochemical and genetic analysis of the effects of amylose-extender mutation in rice endosperm. *Plant Physiology* **127**, 459-472 (2001).
96. Guan, H. P. & Preiss, J. Differentiation of the properties of the branching isozymes from maize (Zea mays). *Plant Physiology* **102**, 1269-1273 (1993).
97. Myers, A. M., Morell, M. K., James, M. G. & Ball, S. G. Recent progress toward understanding biosynthesis of the amylopectin crystal. *Plant Physiol.* **122**, 989-997 (2000).
98. Smith, A. M., Zeeman, S. C., Thorneycroft, D. & Smith, S. M. Starch mobilisation in leaves. *Journal of Experimental Botany* **54**, 577 - 583 (2003).
99. Tetlow, I. J., Wait, R., Lu, X., Akkasaeng, R., Bowsher, C. G., Esposito, S., Kosar-Hashemi, B., Morell, M. K. & Emes, M. J. Protein phosphorylation in amyloplasts regulates starch branching enzyme activity and protein-protein interactions. *The Plant Cell* **16**, 694 - 708 (2004).
100. Takeda, Y., Shibahara, S. & Hanashiro, I. Examination of the structure of amylopectin molecules by fluorescent labelling. *Carbohydrate Research* **338**, 471 - 475 (2003).
101. Hanashiro, I., Tagawa, M., Shibahara, S., Iwata, K. & Takeda, Y. Examination of molar-based distribution of A, B and C chains of amylopectin by fluorescence labelling with 2-aminopyridine. *Carbohydrate Research* **283**, 151 - 159 (2002).
102. Donald, A. M., Kato, K. L., Perry, P. A. & Waigh, T. A. Scattering studies of the internal structure of starch granules. *Starch* **53**, 504-512 (2001).
103. Biliaderis, C. G. The structure and interactions of starch with food constituents. *Can. J. Physiol. Pharmacol.* **69**, 60 -78 (1989).
104. Biliaderis, C. G., Page, C. M., Maurice, T. J. & Juliano, B. O. Thermal characteristion of rice starches: A polymeric approach to phase transitions of granular starch. *J. Agric. Food Chem.* **34**, 6-14 (1988).
105. Gidley, M. J. & Bulpin, P. V. Crystallisation of malto-oligosaccharides as models of the crystalline forms of starch: minimum chain-length requirement for the formation of double helices. *Carbohydrate Research* **161**, 291-300 (1987).

106. Waigh, T. A., Kato, K. L., Donald, A. M., Gidley, M. J., Clarke, C. J. & Riekel, C. Side-chain liquid-crystalline model for starch. *Starch* **52**, 450-460 (2000).
107. Keeling, P. L., Banisadr, R., Barone, L., Wasserman, B. P. & Singletary, G. W. Effect of temperature on enzymes in the pathway of starch biosynthesis in developing wheat and maize grain. *Aust. J. Plant Physiol.* **21**, 807-827 (1994).
108. Jiang, H., Dian, W. & Wu, P. Effect of high temperature on the fine structure of amylopectin in rice endosperm by reducing the activity of the starch branching enzyme. *Phytochemistry* **63**, 53 - 59 (2003).
109. Asaoka, M., Okuno, K., Sugimoto, Y., Kawakami, J. & Fuwa, H. Effect of environmental temperature during development of rice plants on some properties of endosperm starch. *Starch/Starke* **36**, 189 - 193 (1984).

Chapter 2

Characterisation of the amylopectin structure

This material is an edited version of material presented in

Measurement of the molecular weight distribution of debranched starch

JV Castro, RM Ward, RG Gilbert, MA Fitzgerald

Biomacromolecules, 2005, 6 (4), 2260-2270

2.1 INTRODUCTION

Starch is a native polymer. Principles validated and developed within polymer chemistry can be transferred to the measurement of starch. This transfer of knowledge across two disciplines is relatively new and laden with heavy equations, and as such a number of inaccuracies within literature have emerged. This chapter aims to provide a detailed explanation of the principles of molecular weight theory, and use this knowledge to highlight errors found within literature to provide the platform for Chapter 3. Debranched amylopectin will be used to explain molecular weight theory because, unlike amylose, amylopectin is relatively stable in aqueous systems, can be completely debranched with isoamylase and can be separated on an Ultrahydrogel 250 column.

The simplest analysis of debranched starch (glucans) is by Capillary Electrophoresis (CE) which is independent of calibration and provides a simple number distribution. CE is useful for the analysis of chains with up to 80 glucose units [1] but unable to detect the longer chains of amylopectin and amylose. Size Exclusion Chromatography (SEC, also known as Gel Permeation Chromatography) is capable of analysing amylose and amylopectin [2], although SEC requires calibration and considered treatment and interpretation of the data to account for band broadening, baseline correction and quantitative calculations. The basic SEC system comprises a pump, column, a mass-sensitive Differential Refractive Index Spectrometer (DRI) and a multi- or low- angle light scattering detector (MALLS, or LALLS). The mobile phase (eluent) and the column used to separate the starch sample are the two most important considerations for the SEC system. The mobile phase needs to be compatible with the sample solvent and should maximise the hydrodynamic volume of the sample. The pore size of the column packing needs to be able to separate the sample of interest. A mobile phase of ammonium acetate and an Ultrahydrogel 250 column (Waters) have been identified as suitable for the separation of each chain of the amylopectin molecule, [2] and is used throughout this research. Columns are packed with material of specific pore sizes for separating molecules on the basis of their hydrodynamic volume. For illustrative purposes, we consider a hypothetical bimodal sample (Figure 2.1); larger molecules (molecular weight W_1) will elute before smaller molecules (W_2) as the smaller molecules will, on average, explore a longer path through the porous packing material, and thus elute later than larger molecules. The SEC trace obtained directly and without manipulation from this system is a plot of differential refractive index (DRI) signal as a function of elution time (or equivalently to elution volume). The two groups of molecules, W_1 and W_2, do not elute at one discrete elution time, but as a continuous elution profile over several elution times, as depicted in Figure 2.1. This phenomenon is known as band broadening and is, as yet, there is no general method for

correcting this in SEC systems (although new developments are moving towards a solution of this problem[3,4]).

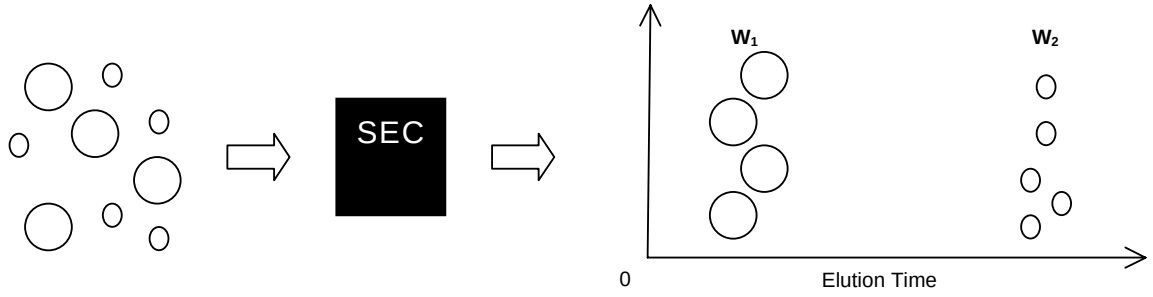

Figure 2.1: Schematic view of the separation of a bimodal solution by SEC.

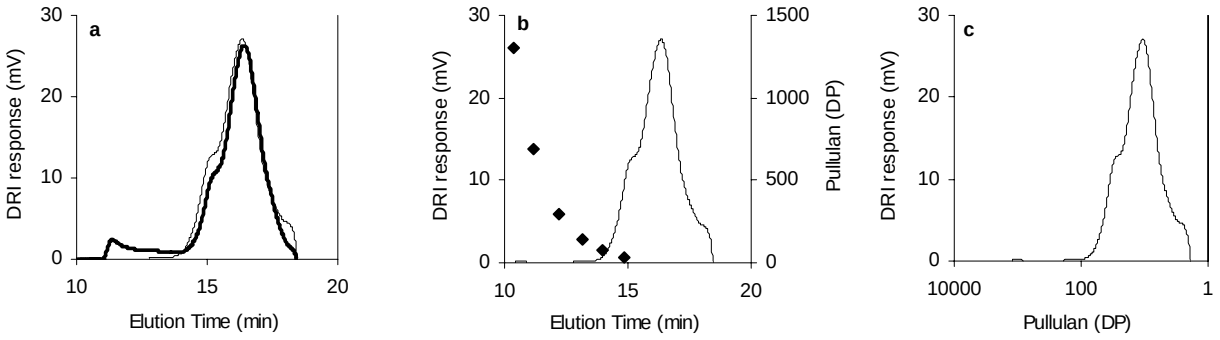

Figure 2.2: Typical representations of SEC traces of debranched starch. The three examples are (a) a comparison of two SEC traces, (b) SEC trace plotted with the elution time of pullulan standards, and (c) SEC trace plotted against a pullulan calibration.

There are three ways in which an SEC trace of debranched starch is typically presented in the literature [5-7]. Commonly, SEC traces of two samples are overlaid as in Figure 2.2a. In this case, as the detector is mass sensitive, qualitative comparisons of the amounts of chains in each sample. For example, in Figure 2.2a, the sample represented by the thick black line has more high molecular weight material compared to the sample represented by the thin line, with no high molecular weight material. The second presentation of SEC traces is in the form of molecular weight (MW) or degree of polymerization (DP) of pullulan standards also plotted against the time axis. An example of this plot is shown in Figure 2.2b. While this plot provides an estimate of the DP of the sample, no accurate quantitative inferences can be drawn from this mode of presentation. Finally, Figure 2.2c plots the SEC trace against a calibration curve created directly

from the pullulan standards. As the hydrodynamic volume of the α-(1,6) linked glucans of pullulan differs from that of the α-(1,4) linked glucans of linear starch, plots 2.2b and 2,2c do not allow for any specific references to the absolute MW, or DP, of the sample at all. Without improving these inaccurate presentations of SEC data of starch, incorrect interpretations regarding the structures of starch are inevitable. Thus, it is imperative to place some emphasis on the development of more accurate methods to allow qualitative and quantitative inferences to be drawn about the structures of starch.

2.2 MATERIALS AND METHODS

Two varieties of rice (*Oryza sativa* L.), Amaroo and Shimizu mochi, were sourced from the Department of Primary Industries at Yanco. Paddy rice of each was dehulled (THU35A 250V 50Hz Test Husker, Satake), milled (McGill No.2 Mill) and a sub-sample was ground (Cyclotec 1093 sample mill, Tecator) to pass through a 0.5 mm sieve. Flour (50 mg) was solubilised by dispersing with ethanol (500 µL), gelatinising with sodium hydroxide (0.25 M, 2 mL), and refluxing for 10 min at 150 °C. The ethanol was allowed to evaporate and the weight of the solution adjusted to 4 g with water. An aliquot (794 µL) of this solution was mixed with sodium acetate solution (0.05 M, pH 4, 206 µL) and glacial acetic acid (6 µL). Starch in the solution was debranched with isoamylase (7 µL, 250 U mL^{-1}) and the mixture incubated at 40 ºC for 2 hours. For SEC, the debranched mixture was boiled, then desalted (1 h) with mixed bed resin (Biorad ,1 mg), and centrifuged (10 500 *g*, 10 min). The supernatant containing debranched starch was retained for analysis [2].

SEC of the debranched flour solution and the pullulan standards was performed on a Waters system consisting of an Alliance (2695) and Differential Refractive Index Detector (Waters 2410) with Waters software (Empower®) to control the pump, and to acquire and process data. The eluent was ammonium acetate (0.05 M, pH 5.2) flowing at 0.5 mL min^{-12}. Separation columns packed with a hydroxylated poly(methyl methacrylate)-based gel Ultrahydrogel 250 (UH 250, from Waters), was used, and the column was held at 60 °C. Injection volume was 40 µl and the run time was 40 min. Elution time of amylose and amylopectin were determined by comparing the elution profile of the waxy rice (Shimizu mochi), which contains only amylopectin, with that of the non-waxy rice (Amaroo).

A calibration curve for linear starch separated by the UH 250 column was created using pullulan standards and universal calibration (see below). The Mark-Houwink parameters used for this conversion in an ammonium acetate (0.05 M, pH 5.2) solvent at 60°C were recently found to be K = 0.00126 mL g^{-1} and α = 0.733 for pullulan, and K = 0.0544 mL g-1 and α = 0.486 for linear starch [8].

2.3 RESULTS AND DISCUSSION

To obtain the molecular weight distribution (MWD) of linear, α-(1,4) linked amylose chains, a calibration is required to relate elution time (or volume) to molecular weight (M), or degree of polymerization (DP, or X). To obtain such a calibration, narrow standards of known molecular weight (M) such as pullulan – an α-(1,6) linked glucose polymer – are injected into the SEC system and the elution time is noted for each pullulan standard. The hydrodynamic volume of pullulan and starch differ, although the two can be related by the Mark-Houwink-Sakurada equation (Equation 1), where K and a are specific to polymer, eluent and temperature; M is the molecular weight of each polymer, in this case, starch (S) and pullulan (P). Recently, these values for starch (K = 0.0544 mL g^{-1} and α = 0.486) relative to pullulan (K = 0.0126 mL g^{-1} and α = 0.733) were determined for the aqueous system used in this study [8]. So by knowing the M_P, the correct value of M_S can be calculated.

$$K_P M_P^{a_P + 1} = K_S M_S^{a_S + 1} \qquad 1$$

This conversion of elution time (or volume) to M is known as "universal calibration", which enables the experimental SEC trace to be transformed into the SEC distribution. The experimental SEC trace, $G(V_{el})$, and the number distribution $P(M)$ are related by Equation 2, whereby the kernel of the integral equation, $K(V_{el},M)$, describes the elution profile of a molecule with a certain M (see Figure 2.1). There are two possible elution profiles; with or without band broadening.

$$G(V_{el}) = \int_0^\infty K(V_{el},M)P(M)M\mathrm{d}M \qquad 2$$

In the ideal case of no band broadening (as seen in CE), a molecule with a given M elutes at a unique time (or volume, V_{el}). This elution profile is best described by a delta function as described by Equation 3. The kernel, or elution profile, becomes $K(V_{el},M) = \delta(V_{el} - V(M)) = 1$.

$$\int_0^\infty \delta(V_{el} - V(M)) = 1 \qquad 3$$

Equation 2 is an unsolvable integral of the observable elution volume, V_{el}, as a function of M. It is thus necessary to convert the integral to a function of V_{el}. From observation, a non-linear correlation (i.e. calibration) between M and V_{el} is defined through the following proof by Equation 4.

$$\text{Using } \log_{10}x = \frac{\ln x}{\ln 10} \approx 2.303 \text{ and } \frac{\mathrm{d}}{\mathrm{d}x}(\ln x) = \frac{1}{x}$$

$$\text{the observable } V(M) = a + b\log_{10}M \text{ becomes } \frac{\mathrm{d}V}{\mathrm{d}M} = \frac{b}{2.303M}$$

$$\mathrm{d}M \propto M\mathrm{d}V \qquad 4$$

The substitution of the elution profile defined by the delta function in Equation 3, and the non-linear relationship between M and V_{el} in Equation 4 into the experimental SEC trace is given in Equation 5. This equation defines SEC distribution in a situation of no band broadening.

$$G(V_{\mathrm{el}}) = P(M(V_{\mathrm{el}}))M(V_{\mathrm{el}})^2 = P(M)M^2 \qquad 5$$

Band broadening inevitably occurs in real experiments whereby molecules of molecular weight M elute across a range of elution volumes, as observed in Figure 2.1. This elution profile, or band broadening effect, is described by using a kernel with the form of a non-Gaussian Spreading Function (*SF*) [9]. Once the $G(V_{\mathrm{el}})$ is known from the experimental SEC trace and the $P(M)$ is obtained from a non-SEC source (for example, capillary electrophoresis), the *SF* for a column can be determined. To apply this *SF* to a SEC trace is to deconvolute the trace into a distribution without the effect of band broadening (i.e. obtain $P(M)$). The $P(M)$ for molecules less than a DP of 80 can be determined by CE [1], but no tool is available to obtain $P(M)$ for molecules longer than DP 80 such as amylose and long chains of amylopectin. Thus, the only option available is to determine the *SF* over the CE range, and extrapolate this *SF* to higher molecular weights assuming that this extrapolation is valid. The solution to band broadening for SEC systems currently being explored [3,4].

It is important to realise the significance of calibrating directly to a pullulan standard and to a linear starch standard after universal calibration. In a plot of DP of the standard and calibrated standard against elution time (Figure 2.3 a), it is clear that the calibration against pullulan standards underestimates the DP of starch by as much as 30% at early elution times and 60% at later elution times. To gauge the error on a "real" sample, a debranched sample was injected into the SEC and the signal calibrated to pullulan and calibrated to starch using Mark-Houwink

parameters and universal calibration (Figure 2.3 b and c, respectively), without correcting for band broadening. In Figure 2.3b, all amylopectin chains elute below a DP of 100; however, when the SEC is calibrated using Mark-Houwink parameters, the chains are shown to elute below a DP of 130. The lower limit of the calibration is dependent on the size of the smallest pullulan standard which is DP 40 for pullulan, and after calibration this limit becomes DP 60 for linear starch.

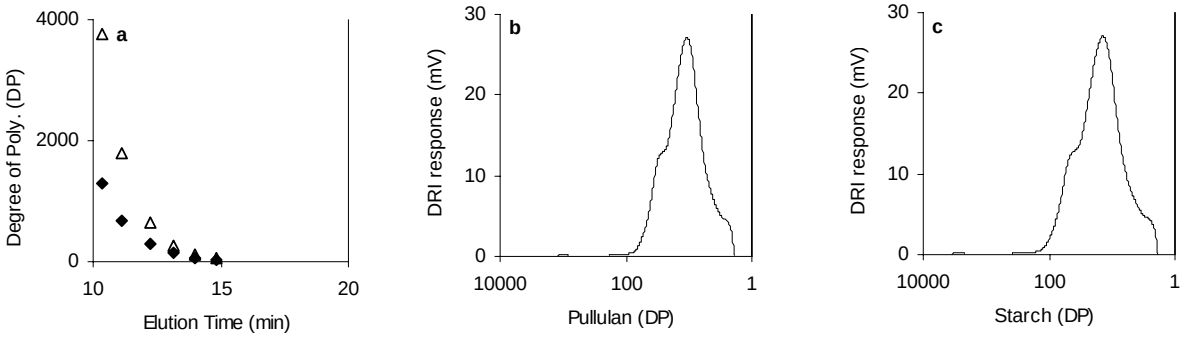

Figure 2.3: The DP of pullulan (diamonds) and the starch (triangles) after calibration with Mark-Houwink parameters, and a MWD of a debranched sample of the waxy variety Shimizu mochi plotted against (b) pullulan standards, and (c) after calibration with Mark-Houwink standards.

From this SEC distribution, i.e. $P(M)M^2$ from Equation 5, cereal chemists tend to quote the $dp_{\max}$ as the peak DRI response of the experimental distribution, but to infer anything from the maximum of a plot of $P(M)M^2$ against M is misleading. Far more meaningful is the weight-average molecular weight, $\overline{M}_{\mathrm{w}}$, derived from the weight distribution (MWD), and the number-average molecular weight, $\overline{M}_{\mathrm{n}}$, derived from the number distribution. Literature indicates that cereal chemists prefer to communicate in terms of degree of polymerisation (DP or X) of monomer units of glucose. The average DP and the corresponding average molecular weight are trivially related by multiplying or dividing by the molecular weight of the monomer unit according to Equation 6 (dehydroglucose, molecular weight = 162).

$$X = \frac{M}{M_o} \qquad 6$$

The weight distribution, MWD ($W(M) = MP(M)$), is the weight of a population of chains $P(M)$ of a certain M, and can be derived directly from the SEC distribution by dividing $P(M)M^2$ by M and plotting the resultant $P(M)M$ against M. The weight-average, $\overline{M}_w$ (or $\overline{X}_w$ using Equation 6), of this distribution or resolved segments within the distribution, can be calculated in the continuous or discrete case using Equation 7.

$$\overline{M}_w = \frac{\int_0^\infty M\,W(M)\,dM}{\int_0^\infty W(M)\,dM} = \frac{\int_0^\infty M^2\,P(M)\,dM}{\int_0^\infty M\,P(M)\,dM} = \frac{\Sigma\,M^2\,P(M)\,\Delta M}{\Sigma\,M\,P(M)\,\Delta M} \qquad 7$$

The number distribution is the population (P) by number of chains of a certain M, and can be derived directly from the SEC distribution by dividing $P(M)M^2$ by M^2 and plotting $P(M)$ against M. Alternatively for DP < 80, this distribution can be determined by capillary electrophoresis.[1] From this number distribution, the number-average, $\overline{M}_n$ (or $\overline{X}_n$ using Equation 6), of this distribution can be calculated using Equation 8. Cereal chemists occasionally refer to this number distribution as the chain length distribution (CLD), and the average simply as the chain length (CL).[10] Caution must be used in comparisons with earlier reports, as the $\overline{X}_n$ quoted is of the $\overline{X}_{re}$ (the $\overline{X}$ of glucose units per reducing end, re, using the modified Park-Johnson method in conjunction with a method to measure total carbohydrate), and CL is incorrectly interchanged with $\overline{X}_{nre}$ (the $\overline{X}$ of the non-reducing ends, nre, using the rapid-Smith degradation method).[5-7]

$$\overline{M}_n = \frac{\int_0^\infty M\,P(M)\,dM}{\int_0^\infty P(M)\,dM} = \frac{\Sigma\,M\;P(M)\,\Delta M}{\Sigma\,P(M)\,\Delta M} \qquad 8$$

The last definition useful to cereal chemists is polydispersity (Q, Equation 9). Polydispersity describes the range of molecular species within a sample whereby a polydispersity of 1 describes a perfectly monodisperse sample. A value above 1 is considered a polydisperse sample and is seen as a broad SEC distribution.

$$Q = \frac{\overline{M}_w}{\overline{M}_n} \qquad 9$$

The $\overline{X}_n$, $\overline{X}_w$ values and Q of the waxy variety Shimizu mochi (Figure 2.3b) and a non-waxy variety Amaroo (Figure 2.4) calculated from the SEC distributions are presented in Table 2.1. All starch in the waxy variety elutes below DP 130 (Figure 2.3b). This observation has been seen in a range of other waxy varieties, thus debranched amylopectin elutes below DP 130. For reasons that will be outlined in further detail in Chapter 3, the UH 250 column is not suitable for separating the amylose chains which elute in the void volume above a DP of 130. However, for the exercise of understanding the concept of $\overline{X}_n$, $\overline{X}_w$ values the SEC distribution will be considered as bimodal: debranched amylopectin below DP 130 and debranched amylose above DP 130. The $\overline{X}_n$, $\overline{X}_w$ values and Q in the range DP 130 to 4 are similar for both Shimizu mochi and Amaroo to suggest that the structure of amylopectin is conserved between varieties. The $\overline{X}_n$, $\overline{X}_w$ values for Amaroo between 1800 and 130 are inaccurate as these chains elute outside the calibration range, and in the void volume which is the region of limited separation. As seen in Table 2.1 the $\overline{X}_n$, $\overline{X}_w$ values for Amaroo in the range DP 1800 to 4 are more comparable to the amylopectin than amylose because, in addition to earlier inaccuracies of measuring amylose on the UH250 column, the amylose content for Amaroo is only 18% of the whole starch component. Thus, quantitative information from the $\overline{X}_n$, $\overline{X}_w$ values and Q calculated from a bimodal trace or from molecules that elute within the non-separating, void volume must be used with discretion.

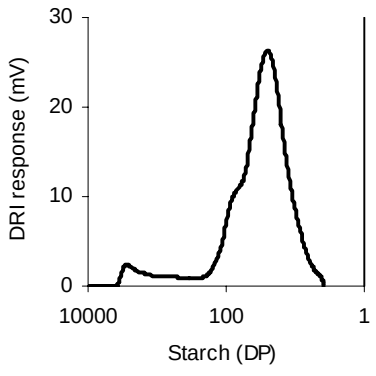

Figure 2.4: SEC distribution of debranched Amaroo separated on a UH 250 column and calibrated by universal calibration

Table 2.1: The $\overline{X}_n$, $\overline{X}_w$ values and Q for the whole SEC distribution of Shimizu mochi and for several DP ranges for Amaroo across

Variety	DP range	$\overline{X}_n$	$\overline{X}_w$	Q
Shimizu mochi	130 - 4	10	21	2.1
Amaroo	130 - 4	10	19	1.9
Amaroo	1800 - 130	453	785	1.7
Amaroo	1800 - 4	11	70	6.4

A correct calibration, detailed derivation of the SEC distribution, and a comparison of the nomenclature of polymer and cereal chemists allows a smooth transfer of principles in polymer chemistry to measuring starch. From qualitative information in a SEC trace, it is now possible to obtain quantitative information from a calibrated SEC distribution. However, the limitations of these calculations for the $\overline{X}_n$, $\overline{X}_w$ and Q values are that they (i) can be calculated only within the separation and calibrated range of the distribution, (ii) are meaningless when calculated for a whole debranched starch (that is, the bimodal trace), and (iii) remain subject to the effects of band broadening.

2.4 CONCLUSION

A more accurate method to determine the SEC distribution of linear chains of amylopectin is possible through the implementation of universal calibration. A comparison of universal calibration against traditional methods to calibrate an SEC system shows that without accounting for the difference in hydrodynamic volume of linear starch and the pullulan standards, the distribution of DP is underestimated. The ability to correct for band broadening will further improve the accuracy of measuring the distribution of linear chains of amylopectin. The SEC column used in this study is restricted to the measurement of amylopectin and Chapter 3 is aimed at improving methods to measure amylose.

2.5 REFERENCES

1. O'Shea, M. G., Samuel, M. S., Konik, C. M. & Morell, M. K. Fluorophore-assisted carbohydrate electrophoresis (FACE) of oligosaccharides: efficiency of labelling and high-resolution separation. *Carbohydrate Research* **307**, 1 - 12 (1998).
2. Batey, I. L. & Curtin, B. M. Measurement of amylose/amylopectin ratio by high-performance liquid chromatography. *Starch* **48**, 338-344 (1996).
3. Castro, J. V., van Berkel, K. Y., Russell, G. T. & Gilbert, R. G. General solution to the band-broadening problem in polymer molecular weight distributions. *Aust. J. Chem.* **58**, 178 - 81 (2005).
4. Konkolewicz, D., Taylor II, J. W., Castignolles, P., Gray-Weale, A. & Gilbert, R. G. Towards a more general solution to the band-broadening problem in size separation of polymers. *Macromolecules* **submitted** (2007).
5. Hizukuri, S., Takeda, Y., Yasuda, M. & Suzuki, A. Multi-branched nature of amylose and the action of de-branching enzymes. *Carbohydrate Research* **94**, 205 - 213 (1981).
6. Takeda, Y. & Hizukuri, S. Purification and structure of amylose from rice starch. *Carbohydrate Research* **148**, 299 - 308 (1986).
7. Mizukami, H., Takeda, Y. & Hizukuri, S. The structure of hot-water soluble components in the starch granules of new Japanese rice cultivars. *Carbohydrate Polymers* **38**, 329-335 (1999).
8. Castro, J. V. PhD Thesis in *School of Chemistry, Key Centre for Polymer Colloids* (The University of Sydney, Sydney, 2005).
9. Castro, J. V., Ward, R. M., Gilbert, R. G. & Fitzgerald, M. A. Measurement of the molecular weight distribution of debranched starch. *Biomacromolecules* **6**, 2260 - 2270 (2005).
10. Thompson, D. B. On the non-random nature of amylopectin branching. *Carbohydrate Polymers* **43**, 233 - 239 (2000).

Chapter 3

Characterisation of the amylose structure

This material is an edited version of material presented in

Improved methods for the structural analysis of the amylose-rich fraction from rice flour

RM Ward, Q Gao, H deBruyn, RG Gilbert, MA Fitzgerald

Biomacromolecules, 2006, 7 (3) 866 – 876

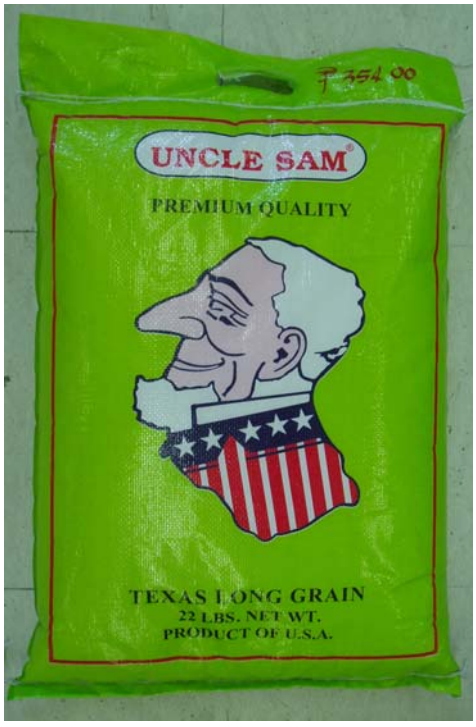

3.1 INTRODUCTION

Starch is the major component of rice grains, and the amylose content of the starch is considered to be the most important factor affecting the cooking quality of rice. However, amylose content is not sufficient to explain variability in cooking properties (e.g.[1-3]), and the molecular architecture of the amylose molecules is also likely to contribute to these properties. The validity of any structure-function relation is entirely dependent on the quality of the method used to acquire the data. An outstanding problem in rice chemistry is the development of a improved method for the accurate determination of amylose structure. In order to perform such a study, the following are required: (a) the ability to determine amylose structure with a calibrated SEC system, (b) experimental size exclusion chromatography (SEC) data that are representative of the true hydrodynamic volume distribution of amylose-rich fractions, (c) the ability to debranch an amylose-rich fraction completely, and (d) a method to obtain an amylose-rich fraction of rice flour with minimal degradation of the starch structure and minimal contribution from amylopectin. Even though in this work only rice is used, it is reasonable to assume that the general methodologies and conclusions will find application in other grains.

A complication of obtaining an accurate amylose structure is that pullulan standards have generally been used to calibrate the SEC. The problem with this is two-fold. First, amylose molecules are branched [4] and the elution profile of branched molecules does not directly translate to the MWD of the amylose [5]. Second, since pullulan standards are not of the same composition as starch, their elution profile will differ from that of starch, and so a calibration curve generated from pullulan standards cannot be used in isolation to measure the MWD of either amylose molecules or amylose chains. Here we use and build on earlier techniques[5,6] to quantitatively convert SEC traces to MWDs. The particular system for the methodologies discussed here is SEC with differential refractive index (DRI) detection. Additional detector systems are available, such as in-line multi-angle laser light scattering (MALLS) and in-line viscometry, which provide more information than a DRI system alone: respectively the weight average degree of polymerization ($\bar{X}_W$) for each slice of elution volume (from MALLS) and hydrodynamic volume (from viscometry), the latter being extremely complex to interpret for branched polymers and indeed only able to be interpreted with semi-empirical relations and parameters [7,8]. No combination of these can provide a complete specification of the architecture of a branched polymer.

Aqueous SEC can provide structural information by separating the components based on their hydrodynamic volume and on their molecular weight (after meeting certain conditions). However, it is important to ensure that the SEC data are representative of the true hydrodynamic volume distribution of the sample, as some studies have suggested that recovery of carbohydrate

following SEC is incomplete [9-11]. One approach is to measure the recoverable carbohydrates after a sample passes through the SEC system. An alternate approach is to use multi-angle laser light scattering (MALLS) to compare the $\overline{X}_w$ value of the initial sample to the sample collected after passage through the SEC column, or again, by iodine assay to identify any differences in the absorbance spectra between the pre- and post-SEC samples. Many studies (e.g.[12,13]) describe the measurement of amylose by SEC, but few of the methods have been widely adopted, perhaps because none for rice amylose have been rigorously validated [12,14]. This complicates efforts to draw comparisons between different studies.

The analysis of the structure of amylose requires analysis of the components of amylose molecules. Amylose molecules are essentially long linear chains that carry a few long branches [12,14]. Investigation of the chains constituting the molecules is typically done using isoamylase from *Pseudomonas* sp. (EC 3.1.2.9) to hydrolyse the α-(1,6) branch linkages to produce linear α-(1,4) linked chains [15,16]. However it is generally accepted that isoamylase is not able to access some of the branchpoints of amylose [17,18]. The basis for this inference is that after treating the debranched amylose with β-amylase (EC 3.2.1.2) (to cleave alternate α-(1,4) bonds to produce maltose), high molecular weight molecules remain [4,14,19]. This problem is revisited by exploring the effect of molecular association and pH on the efficiency of both enzymes using ^{1}H NMR analysis[20] and SEC. After optimizing the method to collect a fraction from rice flour that is rich in intact amylose molecules, and determining the conditions required to debranch it completely, we obtain the MWD's, the weight and number-average degrees of polymerization ($\overline{X}_w$ and $\overline{X}_n$), and the polydispersity (Q) of the debranched amylose.

Previous methods which have isolated starch from flour using variations of the alkaline precipitation/steeping method[21] have been shown to cause degradation of the large amylose chains [22]. Precipitation of amylose from the starch, using butanol or concavalin A, is not absolute, with incomplete recovery of the amylose[23] and precipitation of some residual amylopectin [9,12,14,19]. The common feature of many methods[6] is to leach out the amylose molecules at a temperature above the gelatinization temperature; this feature will be used to develop a new procedure to extract an amylose-rich fraction directly from rice flour. The compromise with this method is while existing lipid-amylose complexes will remain in the insoluble fraction, some free lipids may complex with the leached amylose; the data generated here be applied in Chapters 4 and 5 to understanding cooking properties, and formation of lipid amylose complexes is one of the processes of cooking. Here we will investigate the following: how the concentration of the rice flour in the solution influences the proportion of amylose in the leached fraction (supernatant); ways to minimize the contribution of amylopectin to the supernatant; the relationship between gelatinization temperature and amount of amylose leached; and a method to

measure the hot-water-soluble and hot-water-insoluble fractions using SEC. The absorbance of the complex between iodine and the leached compounds, and comparison with the iodine complex between both amylose and amylopectin, can give some indication of the composition of the leached components [12,24].

Currently, a full description of the complex structure of amylose, on all its levels of organization, is well beyond present technology, but many structure-property relations may hopefully be understood using the descriptors of structure available from current technology, for example, the distribution of the hydrodynamic volume of amylose molecules together with the molecular weight distribution (MWD) of the chains comprising the amylose molecules. Not only could such data be used for structure-property relations for purposes of cooking quality and industrial applications of starch (e.g.[25]), but it could also be used to make qualitative and quantitative inferences about the enzymatic processes in starch biosynthesis [26]. In this chapter, methodologies are examined so that these and other quantitative measures of architecture can be obtained reliably for amylose from rice, so that eventually structural information of starch can be related to both physical properties of the starch and to the enzymatic processes of the *in vivo* starch synthesis [26].

3.2 MATERIALS AND METHODS

3.2.1 Materials

Samples of rice (*Oryza sativa*), Shimizu mochi, Amaroo and Doongara, were obtained from the 2002/3 harvest at NSW Agriculture, Yanco, Australia. Shimizu mochi is a waxy Japanese variety, and Amaroo and Doongara are both non-waxy Australian varieties. Paddy of each variety was dehulled (THU35A 250V 50Hz Test Husker, Satake), milled (McGill No.2 Mill) and then ground (Cyclotec 1093 sample mill, Tecator) to pass through a 0.5 mm sieve. Amylose content [27], and protein content were determined (Dumas method, ASTM E191-64). Gelatinisation temperature was determined using a Differential Scanning Calorimeter (Q Series Instrument, Q Series Explorer software, TA Instruments) increasing in temperature from 35-120˚C,in increments of 4˚C/min.

The hot water soluble fraction (HWSF) was collected from the flour of each variety, at two concentrations (1.96 % and 3.85 % w/w). Rice flour (250 mg or 500 mg) from the three varieties was mixed with water (12.5 g), and the HWSF was separated from the flour by Rapid Visco Analysis (RVA 3 – Newport Scientific) (AACC standard method (61-02)). Briefly, the RVA runs for 12.5 min at 160 rpm and follows a temperature profile of 50 °C for 2.5 min, ramps to 95°C and cools to 50 °C for a final 2.5 min. After each run, the mixture was centrifuged immediately (10^4 *g*, 10 min). The supernatant contained the HWSF and the pellet contained the hot water insoluble fraction (HWIF).

Isoamylase (*Pseudomonas* sp., EC 3.1.2.9, 105 U/mg), *β*-amylase (Barley, EC 3.2.1.2, 1400 U/mg), *α*-amylase (*Bacillus licheniformis,* EC 3.2.1.1, 54 U/mg) and a Total Starch Assay Kit were obtained from Megazyme and used as supplied. Pullulan standards (from Shodex) were used for SEC calibration, using the universal calibration. High purity water (MilliQ) was used for all SEC experiments, and D_2O was used for all ^{1}HNMR experiments. All chemicals used were reagent grade.

3.2.2 Calibration and Validation of SEC for HWSF of Flour

Size Exclusion Chromatography SEC of the HWSF was performed either on a Waters system consisting of an Alliance (2695) and Differential Refractive Index (DRI) Detector (Waters 2410) with Waters software (Empower®) to control the pump, and to acquire and process data, or with a Shimadzu system: a Wyatt OPTILAB EOS interferometric refractometer and Astra software. For both systems, the eluent was ammonium acetate (0.05 M, pH 5.2) flowing at 0.5 mL min^{-1}.[19] SEC columns packed with a hydroxylated poly(methyl methacrylate)-based gel, an Ultrahydrogel 500 (UH500) or an Ultrahydrogel 250 (UH250, both from Waters),

were used independently, and held at 60 °C during each run. Aliquots (40 μL) of the HWSF were injected without further processing, and the run time was 40 min.

Calibration of SEC Shodex standards (P800, P400, P200, P100, P50, P20, P10, P5) were injected into the SEC into the UH500 and the UH250 column separately. Based on retention time, a calibration curve for linear starch was created using the Mark-Houwink-Sakaruda equation and universal calibration [5]. The Mark-Houwink parameters used for this conversion, with ammonium acetate (0.05 M, pH 5.2) as the solvent, and the column at 60 °C were recently found to be K = 0.00126 mL g^{-1} and α = 0.733 for pullulan, and K = 0.0544 mL g^{-1} and α = 0.486 for linear starch [5]. The value of α is close to the value of ½ for a θ solvent: that is, the solvent system chosen here behaves ideally [28].

Validation of the SEC As amylose is best separated by the UH500 [16], validation was performed on this system. Reproducibility of the SEC and of the UH500 column were tested by replicate collections, on different days, of the HWSF of Amaroo, prepared at both concentrations. In order to determine whether or not the chromatogram represents all the starch molecules in the injection, carbohydrate recovery, $\overline{X}_W$ by MALLS, and λ_{max} of starch-iodine complexes, was measured pre- and post-SEC. The pre-SEC sample was prepared by mixing an aliquot of each sample (40 μL) with eluent (5.96 mL) to give the same concentration as the material that eluted from the column. As starch eluted from the DRI detector, the post-SEC sample was collected from the beginning of the void volume until the end of the separating phase (8-20 min) (manually or with a Waters Fraction Collector III).

For measurement of total starch, the pre-SEC and post-SEC samples were evaporated under vacuum (Jouan RCT 60 and RC 10.09) to a weight of 500 mg, and then starch in the samples was measured with the Total Starch Assay Kit (Megazyme). Recovery is reported as the difference in the glucose content pre- and post-SEC.

For $\overline{X}_W$ determination, a Photon Correlation Spectrometer (Brookhaven Instruments comprising a BI-200SM Version 2 goniometer with BI-APD avalanche photodiode detector, and PC1 B1-9000AT EN correlator) in static (MALLS) mode, with a 35 mW He-Ne laser light, λ = 633 nm, and 400 μm aperture was used. To obtain reproducible $\overline{X}_W$ data using this technique, filtered eluent (0.1 μm) was used to prepare the samples and as the reference. Defects in sample tubes, coupled with impurities in the decalin solvent used for MALLS, required that each sample be measured in triplicate. Berry plots[28,29] were generated with BIC Zimm Plot Software (Version 3.17). For the pre-SEC Berry plot, the HWSF was diluted with eluent to a concentration range from 0.11 to 0.02 mg mL^{-1}. For the post-SEC Berry plot, different injection volumes were used to create a similar range of concentrations, and the Berry plot was determined from five

concentrations measured at six angles (30°, 45°, 55°, 65°, 75°, and 90°). Each value is the average of three replicates.

For starch-iodine complexes, an aliquot of the injection pre- and post- SEC (1 mL) was mixed with citric acid (0.1 M, 2 mL) and iodine solution (1 mL), and then the volume adjusted to 20 mL with water. Absorbance was measured every 1.25 nm over the visible spectrum using a scanning spectrophotometer (GBC UV/VIS 918).

3.2.3 Is debranching complete of the HWSF from flour?

Amylose was debranched as follows. The HWSF (795 µL, 1.96%) from each variety was mixed with sodium acetate buffer (0.2 M, pH 4, 205 µL) together with glacial acetic acid (6 µL), and isoamylase (10 µL). This mixture was incubated at 50 ºC for 2 h, boiled to denature the enzyme, and centrifuged (10000 *g*, 5 min). The supernatant was desalted with mixed bed resin (BioRad AG 501-X8) for 60 min at 50 ºC.

Isoamylase was also incubated with aliquots of the HWSF of flour (795 µL) mixed with sodium acetate buffer either at pH 4 or 5 (0.2 M, 205 µL) together with glacial acetic acid (6 µL), or with milliQ water (205 µL) to maintain a pH of 6. Each reaction mixture (pH 4, 5 and 6) was debranched as above. To one sample with a pH of 4, NaOH (1 M, 200 µL) was added to change the pH to 6. *β*-amylase (20 µL) was added directly to these mixtures (pH 4, 5, 6 and to the one with a pH change from 4 to 6), and the mixtures were incubated (60 ºC, 20 min). Samples were then boiled to denature the enzyme, centrifuged to remove precipitates (10^4 *g*, 5 min), and desalted (as above). Aliquots of each supernatant (40 µL) were analyzed by SEC.

Analysis of the *α*-(1,6) linkages was completed on HWSF (1.96%) prepared from the three flours, using deuterium oxide (D_2O) as the solvent instead of milliQ water, and debranched at pH 4 (as above). ^{1}H NMR (Bruker 300 Ultrashield) was used to detect the proportion of *α*-(1,4) and *α*-(1,6) linkages in each sample before and after debranching. Removal of salt by using the mixed bed resin caused poor peak resolution, and was therefore not used in sample preparation. ^{1}H NMR were measured at 300.13 MHz, and 360 K [20]. XWIN PLOT Software was used for processing data. Chemical shifts were referenced to an internal standard of 3-(trismethylsilyl) sodium propionate-d_4(TSP) with a chemical shift of 0 ppm. The lower limit of resolution of *α*-(1,6) linkages was determined by subsequent dilution of the sample with D_2O.

Evidence of association, aggregation or retrogradation of freshly prepared HWSF and debranched HWSF (as above at pH 4) from Doongara (1.96%) was examined. Aliquots of both were injected into the SEC immediately after preparation, and a second aliquot of each was treated in the following way to disassociate any associated chains. The second aliquot of each

was diluted by half, and kept at 50 ºC for one week with constant, gentle shaking, during which aliquots were removed daily and injected into the SEC.

An additional α- amylase incubation between the isoamylase and β-amylase incubations was performed. To one sample debranched at pH 6, α-amylase (20 µL) was added directly. To another sample debranched at pH 4, α-amylase (20 µL) was added after the pH of the debranched sample was changed to 6 by the addition of NaOH (1 M, 200 µL). Samples were incubated (60 ºC, 60 min), then boiled and centrifuged (10000 g, 5 min); β-amylase was then added to the supernatant and the samples were incubated and treated as above.

3.2.4 Characterizing starch in the HWSF from flour

Identification of starch in the HWSF The HWSF of flour (1.96 %) from the three varieties was collected as described earlier, but both the supernatant and the pellet were retained after centrifugation. An aliquot of the HWSF (795 µL) was debranched as described above. To a sub-sample (40 mg) of each HWIF, NaOH (0.25 M, 1 mL) was added and the samples were solubilized by heating and refluxing (2 min). The weight of each solubilized HWIF was adjusted to 4 g with water. An aliquot (795 µL) of each solubilized HWIF was debranched as described above. The Waters SEC was used, the injection volume was 40 µL and the run time was 40 min. The yield of the HWSF was determined gravimetrically after drying aliquots of the HWSF (~50ºC, ~24 hours), and the contribution of amylose and amylopectin to both the HWSF and HWIF was determined by SEC using the UH250, which suitably separates debranched amylose and amylopectin chains [16].

3.3 RESULTS AND DISCUSSION

3.3.1 Calibration and Validation of SEC for HWSF of Flour

Size Exclusion Chromatography (SEC) separates *branched* and *linear* molecules on the size of the molecule in an aqueous mobile phase. Regardless of composition, the elution time is a function of the hydrodynamic volume [8,30]. The SEC distribution can be expressed simply as hydrodynamic volume, but is more informative if expressed as degree of polymerization (DP, or X). Multi-Angle Laser Light Scattering (MALLS) measures the *weight-average* degree of polymerization ($\bar{X}_W$) for each elution volume; while such information is useful, it gives only an average molecular weight for branched polymers, because SEC separates by hydrodynamic volume, not molecular weight. Moreover, use of MALLS was found to be impractical for the present system, as the concentration high enough for a good DRI response was found to swamp the very sensitive MALLS detectors. Universal calibration[30] assigns a true hydrodynamic volume to the sample eluting at a given elution volume; this relies on the assumption that SEC separation depends only on hydrodynamic volume, not composition. The Mark-Houwink parameters relate the intrinsic viscosity (or hydrodynamic volume) and DP of a *linear* standard such as pullulan, to the viscosity (or hydrodynamic volume) and DP of a second *linear* polymer such as starch [5]. So for a *linear* system, elution time is related to hydrodynamic volume, hydrodynamic volume is related to intrinsic viscosity, and intrinsic viscosity related to the DP. For a branched system its has been shown[8] that hydrodynamic volume correlates well with elution volume. Here, the SEC distribution is expressed as "Linear Equivalent DP" whereby the DP is for a *linear* molecule that has the same hydrodynamic volume of a *branched* molecule. A full description of universal calibration and derivation of K and α values (which relate hydrodynamic volume and X) has recently been published [5].

The calibration curves created for both columns used in this study, the UH250 and the UH500, are shown in Figure 3.1. When pullulan standards are used in the calibration, the UH250 has a separating range of DP 60 to 1800, but when additional, lower molecular weight standards, like polyethylene oxide are used, the UH250 can separate linear starch to DP 10 [26]. The UH500 has a separating range from DP 60 to 17000, and it is suitable for the measurement of amylose molecules. It is also of interest to examine the size of the error that arises. Figure 3.2a shows the SEC distributions of a starch sample (debranched Amaroo at 1.96% concentration on the UH500) with the molecular weight relative to pullulan, and the true molecular weight found by universal calibration using the above Mark-Houwink parameters. It is seen that determining the molecular weight from pullulan ("relative molecular weight") without universal calibration significantly under-estimates the actual molecular weight by a factor of 10. If the UH500 calibration curve is

fitted with a linear curve (Figure 3.2b), as is the case with the UH250 column, rather than a third-order polynomial then the difference between the pullulan and starch standard is also distorted at the high MW end of the chromatogram.

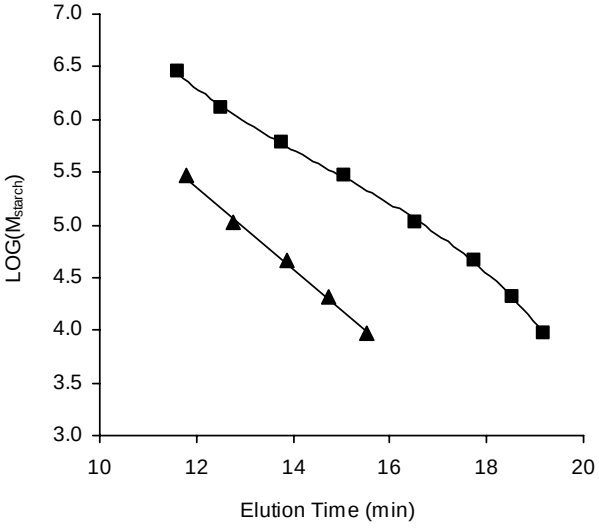

Figure 3.1. Calibration curves of linear starch for the Waters system using UH250 column (triangles) and the UH500 column (squares) created from the Mark – Houwink parameters of pullulan (K = 0.00126 mL g^{-1} and α = 0.733) and linear starch (K = 0.0544 mL g^{-1} and α = 0.486) in ammonium acetate solution (0.05 M, pH 5.2) at 60 °C [5].

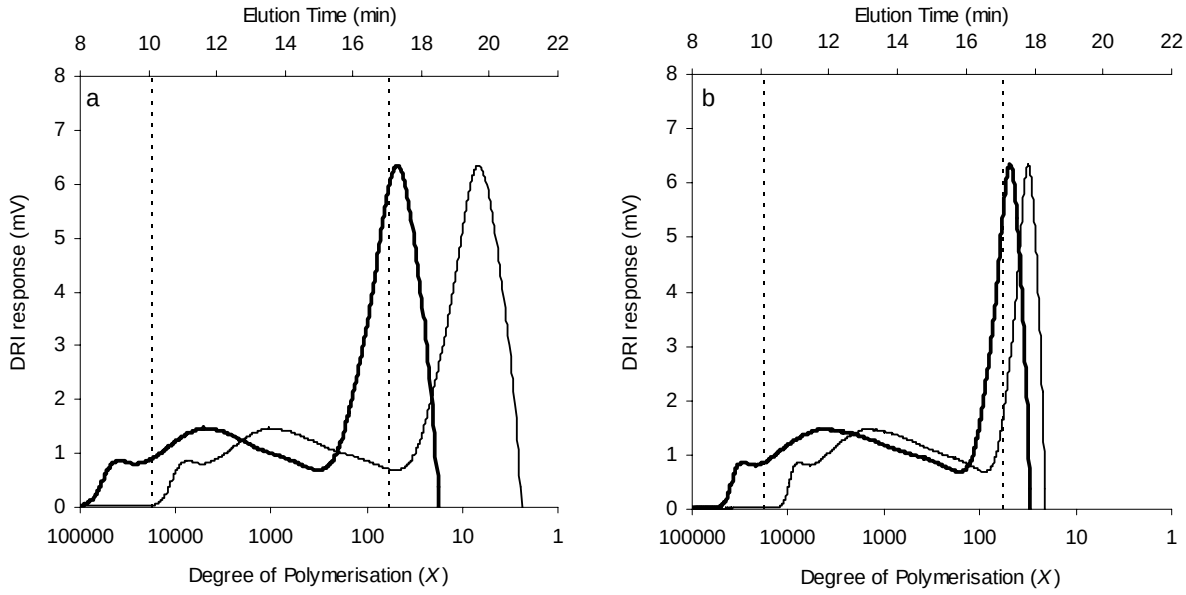

Figure 3.2. SEC distribution for debranched Amaroo (1.96%) starch, showing two scales: molecular weight relative to pullulan standards (thin line), and absolute molecular weight from universal calibration (thick line). Part a is with a linear calibration, and Part b is with a third order calibration. The vertical dashed lines show the limit of calibration for the UH 500 column.

Both the separation technique and the SEC technique are very reproducible for both concentrations (Figure 3.3). However, it is important to ensure that the SEC signal obtained represents the distribution of all the starch in the injection. The first check was to examine the recovery (%) of carbohydrate in HWSF collected post-SEC. The results in Table 3.1 show a 77-82 % recovery of carbohydrate from the SEC. In contrast with previous work [10], this result was found to be independent of the initial concentration of flour and of amylose content.

It is important to know if the loss of 18-23% carbohydrate (Table 3.1) is across the entire distribution, or the loss of a certain component of the HWSF. To quantify any difference in $\overline{X}_w$ pre- and post-SEC, Berry plots were obtained using MALLS for the HWSF of Doongara at both concentrations. Figure 3.4 shows a typical Berry plot. Table 3.1 shows that the $\overline{X}_w$ of the pre-SEC HWSF was approximately three times larger than that of the post-SEC HWSF for the 1.96% (w/w) preparation, and 3.5 times larger for the 3.85% (w/w) preparation. Given that the loss of carbohydrate measured directly after SEC was only about 20% (Table 3.1), this loss must have been predominantly from high molecular weight species, like amylopectin, to cause the large decrease in the $\overline{X}_w$ of the molecules in the sample. The λ_{max} of the starch-iodine complex of the HWSF collected pre-SEC and post-SEC, shown in Table 3.1, shows that λ_{max} of the HWSF post-SEC has shifted to an even higher λ_{max} (towards that of amylose) than the pre-SEC HWSF. While we cannot exclude the possibility that some components may not be recoverable, these data further indicate that the unrecovered high molecular weight material is likely to be amylopectin. The loss could be due to the poor solubility of the amylopectin [10,11], or because the 10 μm pore size of the UH500 column (Waters specifications) prevented high molecular weight material from passing through the column (note that this loss of material was observed when the SEC was run without a guard column). Fortuitously, the unrecovered material increases the proportion of amylose in the HWSF.

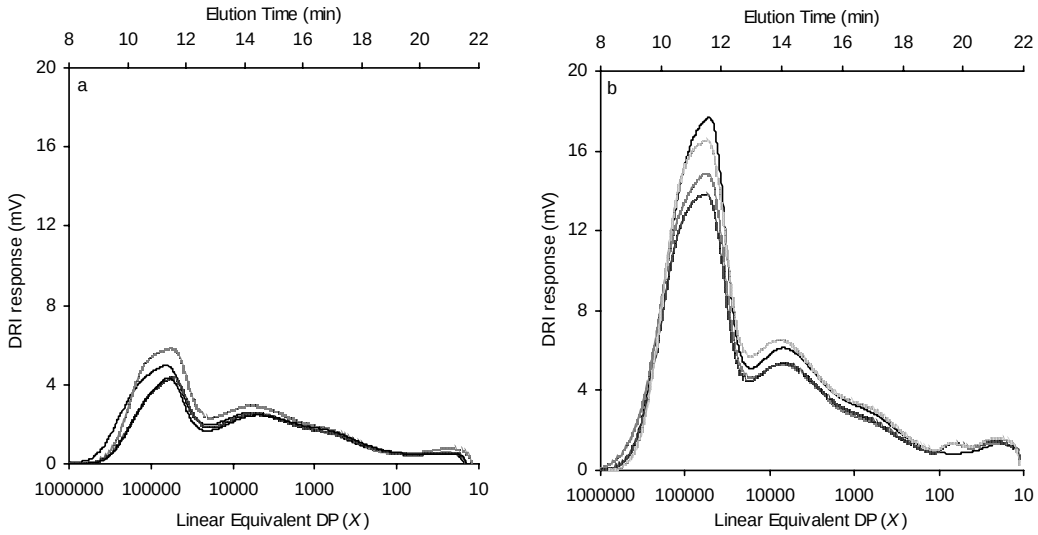

Figure 3.3. Reproducibility tests: SEC traces of the HWSF of flour of Amaroo prepared and analysed on four different occasions at both rice slurry concentrations: (a) 1.96 % (w/w) and (b) 3.85 % (w/w). These SEC traces were obtained from the Waters SEC system.

Table 3.1. Validation of the UH500/SEC system for analysis of the HWSF of flour. Recovery (%) of carbohydrate in the HWSF (from the three varieties at both concentrations) was determined. Values of $\overline{X}_w$ for the HWSF of Doongara prepared as determined from a Berry plots of MALLS data (an example of a Berry plot is in Figure 3.4). Absorption maxima, λ_{max} (nm), of starch-iodine complexes with HWSF from the two non-waxy varieties collected pre- and post-SEC.

Carbohydrate Recovery (%)	**Rice Flour Slurry 1.96%**	**Rice Flour Slurry 3.85%**
Shimizu Mochi	83.5	80.1
Amaroo	83.5	74.8
Doongara	79.3	78.3
Average ± SD	82.1 ± 2.4	77.7 ± 2.7
$\overline{X}_w$ – Doongara only	**Pre-SEC**	**Post-SEC**
Rice Flour Slurry 1.96%	$(7.5\pm2.0)\times10^5$	$(2.5\pm0.4)\times10^5$
Rice Flour Slurry 3.85%	$(1.5\pm0.5)\times10^6$	$(4.3\pm0.3)\times10^5$
λ_{max} (nm)	**Pre-SEC**	**Post-SEC**
Amaroo	611	630
Doongara	618	631

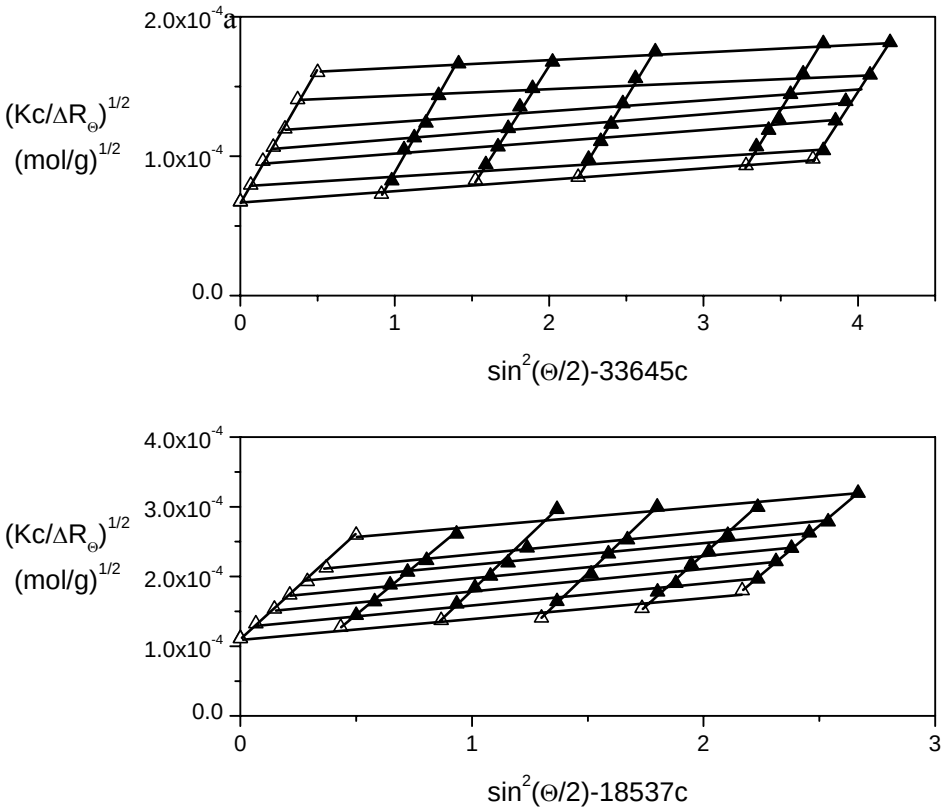

Figure 3.4. An example of a Berry plot prepared from MALLS data for Doongara HWSF (3.85 % (w/w)) prepared (a) pre- and (b) post-SEC.

3.3.2 Is debranching complete of the HWSF from flour?

Here we hope to solve the long-standing problem of apparent incomplete debranching of amylose [4,14,19]. In theory, linear amylose chains should be obtained by hydrolysing the α-(1,6) linkages with isoamylase. Some studies suggest that not all branch points are accessible to isoamylase, based on the molecular weight of the material remaining after incubations of amylose first with isoamylase, then with β-amylase [4,14,19]. Incomplete debranching would clearly have major implications for qualitative and quantitative interpretations of MWD data of amylose that was assumed to be debranched by isoamylase. The incubation of amylose with isoamylase and β-amylase is replicated in Figure 3.5, and in my hands, β-amylase completely digests the lower molecular weight chains of amylopectin (DP 10-100) in the debranched HWSF, but incompletely digests the higher molecular weight chains.

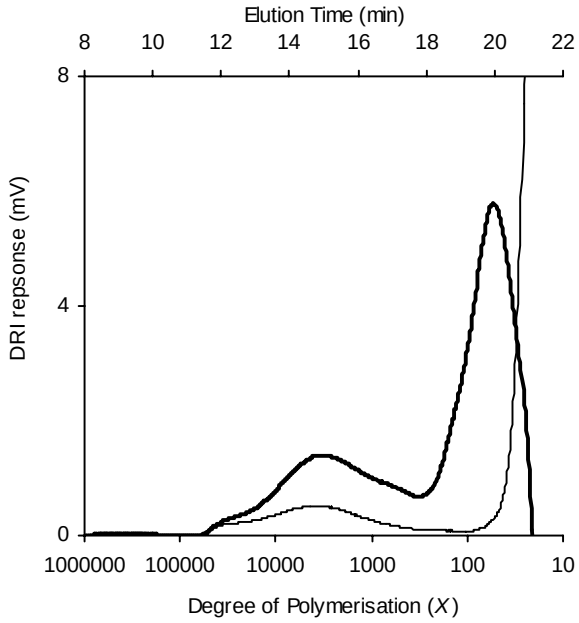

Figure 3.5. SEC traces of debranched HWSF (thick line) and debranched HWSF treated with β-amylase (thin line). These SEC traces were obtained from the Waters SEC system.

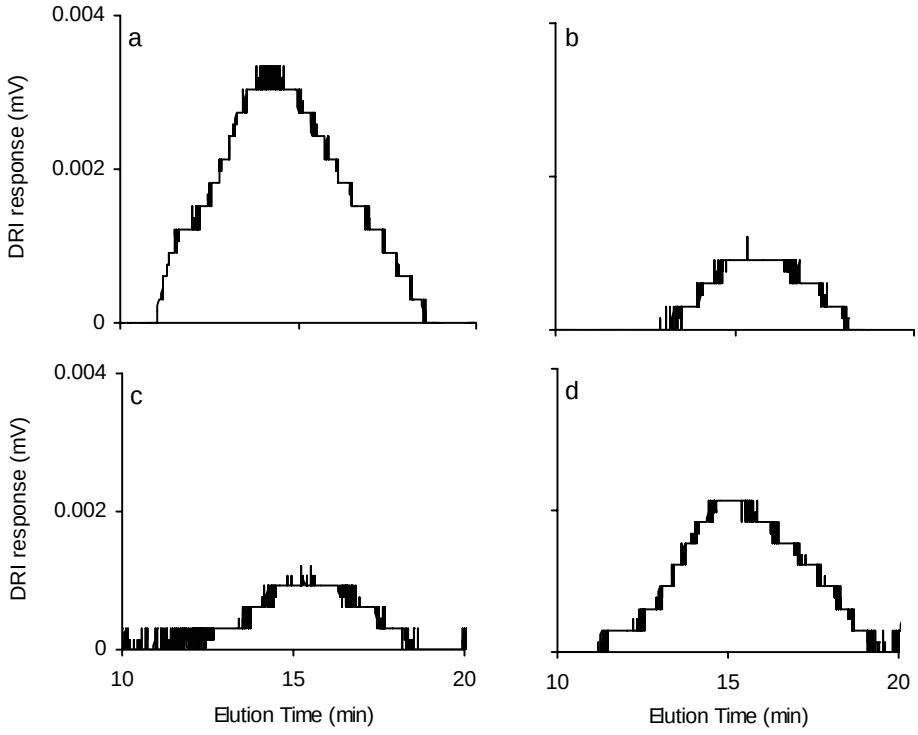

Figure 3.6. SEC traces of the HWSF of Doongara (1.96% (w/w) slurry) digested by isoamylase, then β-amylase, at pH 4 (a), pH 5 (b), pH 6 (c) and at the correct pH for each enzyme (d). These SEC traces were obtained from the Shimadzu SEC system.

In biological systems, pH affects the efficacy of catalytic sites of enzymes. Therefore, the effect of pH on successive incubations of isoamylase followed by *β*-amylase was examined across the range of pH suitable for these enzymes. Figure 3.6 shows that independent of pH, high molecular weight material remained. However as the pH became less acidic more of the higher molecular weight material was degraded. The remaining high molecular weight material, across the range of pH tested, reacted with iodine to form a blue colour, confirming the presence of long chains of starch. There are three possibilities: (i) that isoamylase does not hydrolyse all the *α*-(1,6) linkages, presenting a barrier to the action of *β*-amylase; (ii) that debranched chains associate, aggregate or retrograde, restricting the access and activity of *β*-amylase; or (iii) that *β*-amylase is much more efficient at digesting short chains, like the amylopectin chains that are completely digested in Figure 3.5.

The efficacy of hydrolysis of the *α*-(1,6) branch linkages of HWSF by isoamylase can be measured by ^{1}H NMR, which can distinguish the *α*-(1,6) and *α*-(1,4) linkages of starch, with a chemical shift of 5.40 for the *α*-(1,4) linkages, and 5.00 for *α*-(1,6) linkages [20]. In Figure 3.7 (panels a, c and e), the ^{1}H NMR spectra of HWSF show that branching frequency decreases with increasing amylose content (5.6 % for Shimizu Mochi, 2.5 % for Amaroo, and 1.3 % for Doongara). Upon debranching of the HWSF with isoamylase, the *α*-(1,6) peak disappears altogether, suggesting complete hydrolysis of all branch linkages (Figure 3.7, panels b, d and f). However, the lower limit of ^{1}H NMR detection of *α*-(1,6) linkages was found to be 0.5% (equating to 1 in 200 linkages), which is not sufficient to confirm complete hydrolysis of *α*-(1,6) linkages.

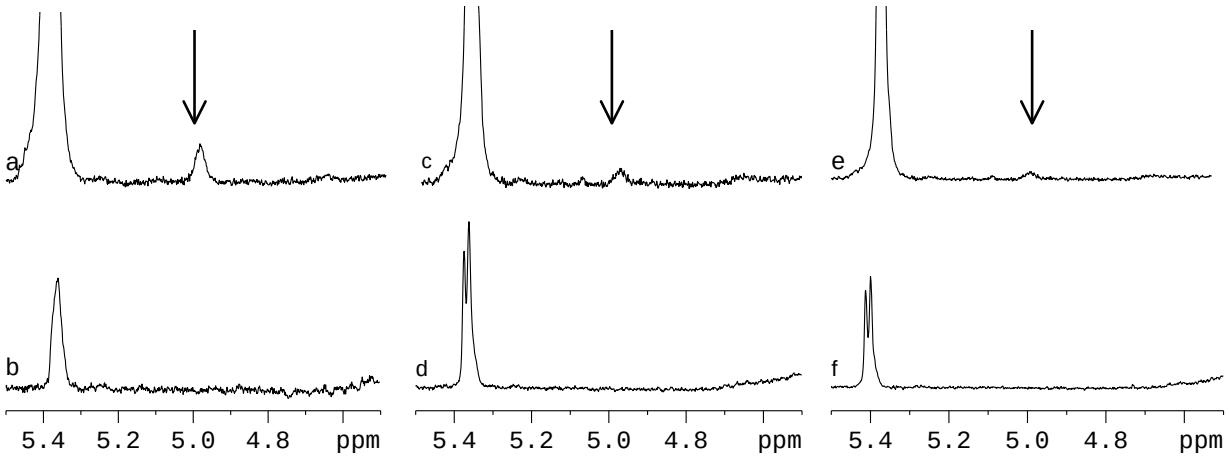

Figure 3.7. ^{1}H NMR spectra of HWSF (first row) and debranched HWSF (second row) from three varieties: Shimizu Mochi (panels a and b), Amaroo (panels c and d) and Doongara (panels e and f). The chemical shift for α-(1,4) linkages is 5.40, and 5.00 for α-(1,6) (as denoted by the arrows)[20]. ^{1}H NMR spectra is courtesy of Qunyu Gao.

Retrogradation, entanglement and association occur immediately after preparation of amylose solutions [11,13,31], and these have the potential to decrease the efficiency of isoamylase or *β*-amylase. Debranching of the HWSF (containing both amylose and amylopectin) theoretically produces chains that range from DP 6 (the shortest amylopectin chain[32]) up to several thousand [14]. The rate of retrogradation can be minimized [31], but rates of aggregation increase for chains around DP 50, and for small molecules (eg. DP ~ 110) [31,33]. This aggregation can be due either to chain entanglement, or to hydrogen bonding, between chains on different molecules (the latter is termed 'association' for this purpose). Association is favoured enthalpically, but entropic considerations show that dissociation of both aggregates and enthalpically-associated chains must be favoured if the solution is sufficiently dilute. This process can be quite slow: for example, it is well known that dissolution of long branched chains can take many days, an observation which can be rationalized in terms of reptation theory [34,35]. Thus, it is essential that the rate of this dissociation is over a reasonable time and temperature [31]. Here the SEC data were collected daily over 7 days at 50 °C. Normalized SEC traces of fresh and disassociated HWSF and debranched HWSF are shown in Figure 3.8. Comparing the SEC trace of fresh and disassociated HWSF (Figure 3.8a), the earlier elution of the fresh HWSF suggests some association in this sample. In contrast, the debranched HWSF (Figure 3.8b) showed no detectable evidence of association in the original sample. However, as isoamylase can hydrolyse the densely located branch linkages of amylopectin, and provided any associations do not involve the branch points, association might not affect isoamylase. The exo-hydrolysing *β*-amylase should be free to hydrolyse the disassociated debranched HWSF.

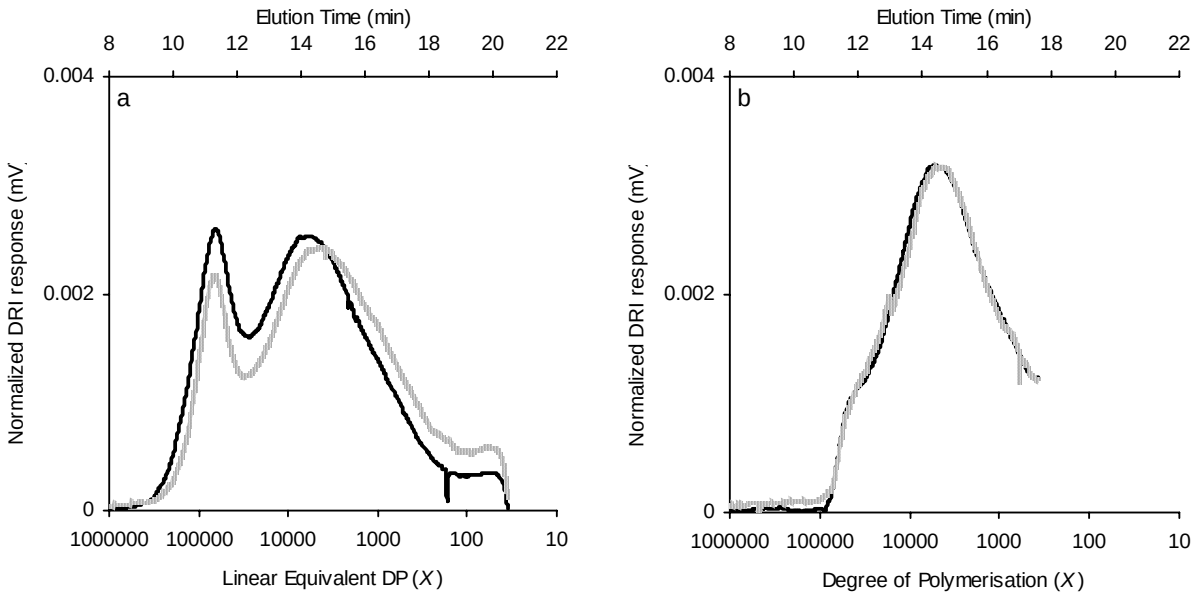

Figure 3.8. Association tests of the HWSF from Doongara flour 1.96 % (w/w) in the native (a) and debranched (b) state. Normalised SEC traces of the fresh HWSF (thick line) and the diluted trace (thin line) are presented. The vertical dashed lines show the limit of calibration for the UH500 column.

Figure 3.5 shows that *β*-amylase is much more able to digest shorter chains than longer ones, either because the shorter chains associate less [36], or because the shorter chain length provides a more suitable substrate for *β*-amylase. The addition of *α*-amylase to a solution of debranched chains will hydrolyse *α*-(1,4) linkages randomly, and decrease the average chain [37]. SEC traces of these digestions are shown in Figure 3.9. For each sample, including the negative control (no starch added), a peak eluted between 16 and 20 min (Figure 10). The material reacted with iodine to form a yellow colour, confirming absence of starch, and it absorbed strongly at 205 and 280 nm, indicating the presence of protein, probably residual enzyme. Thus *β*–amylase was able to digest all of the short chains in the α-amylase treated debranched solution, either because short chains provide a more suitable substrate or because short chains associate and aggregate more slowly [36].

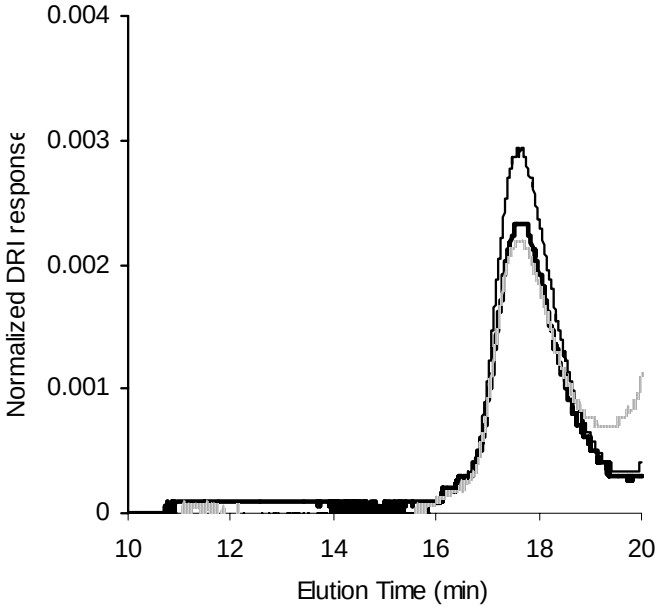

Figure 3.9. Normalized SEC traces of the HWSF of Doongara (1.96% (w/w) slurry) digested by isoamylase, then α-amylase and finally β-amylase, at pH 6 (bold line), at the correct pH for each enzyme (dashed line) and a blank of the 3 enzymes at pH 6 (thin line). These SEC traces were obtained from the Shimadzu SEC system.

The diversity of techniques employed here largely explains why the question of complete debranching of amylose by isoamylase has remained unanswered. To summarize, pH does not affect isoamylase efficiency, ^{1}H NMR used in isolation is not sufficient to answer this question, and *β*–amylase cannot digest debranched HWSF without a prior or concurrent incubation with *α*-amylase to decrease the size of chains. Taken together, these results strongly suggest that isoamylase does indeed completely debranch the starch in the HWSF of flour.

3.3.3 Characterizing starch in the HWSF from flour

The amorphous nature of amylose allows it to be relatively readily leached from the granules [38,39], and many studies that separate amylose from starch capitalize on this feature [23,38,40]. Purification of starch from flour carries the risk of damaging and losing amylose molecules [22]; this would make qualitative and quantitative interpretation impossible. Here, we attempt to leach an amylose-rich fraction from flour, thus avoiding the long time and other problems encountered when purifying starch from rice flour. The associated lipid-amylose complexes that may be leached will not contribute to the gel/paste of the cooked rice and as such not affect the eating quality, the investigation of which will in the future make use of the methods developed in the present paper. Figure 3.10 shows the debranched HWSF and HWIF from each variety separated on the UH250. This column elutes amylose chains in the void volume and separates amylopectin chains [16]. Figure 3.10 shows also that for the waxy variety, all the amylopectin chains elute below DP 100. Figure 3.10a shows that all the chains greater than DP 1000 are in the HWSF, many of the chains in the range of DP 100 – 1000 are in the HWSF and some chains of the order of

amylopectin are in the HWSF. Figure 3.10b shows that the HWIF contains no chains greater than DP 1000, but it does contain chains in the range of DP 100 – 1000. Thus the data indicate that some amylopectin is present in the HWSF and that some short amylose chains, or very long amylopectin chains, are within the HWIF. While it is possible for the long chains in the HWIF to be covalently linked to amylopectin molecules, given that amylose chains could be formed by extension of amylopectin chains [41], we first assume that they are derived from amylose.

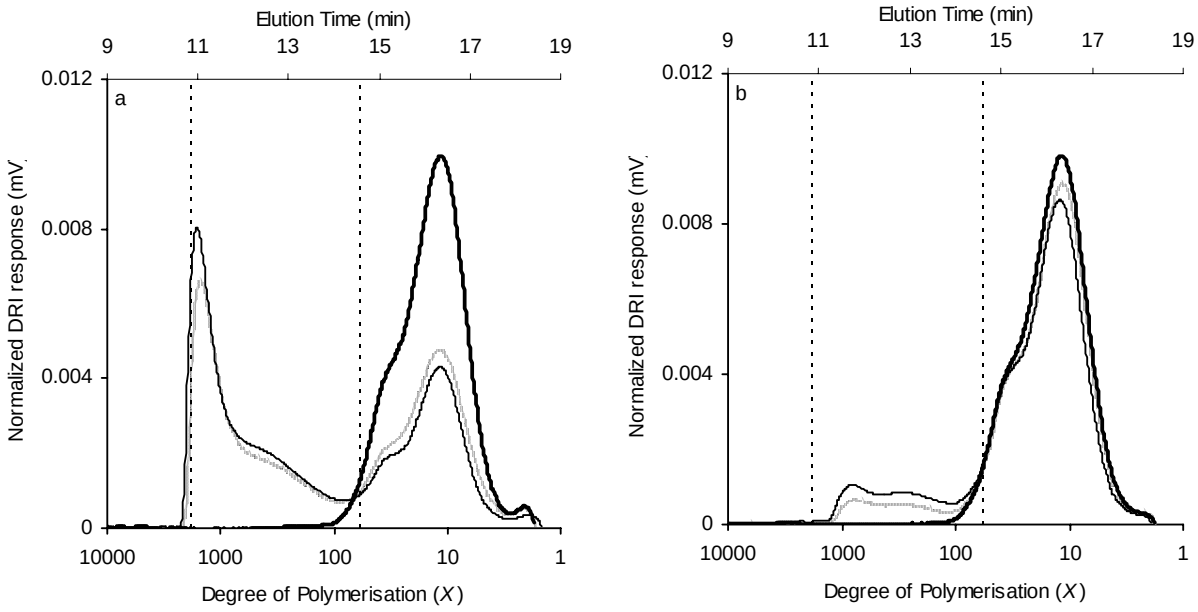

Figure 3.10. SEC distributions of (a) debranched starch in the HWSF of flour and (b) HWIF of flour of three varieties separated on a UH250 column: Shimizu Mochi (thick line), Amaroo (dotted line), and Doongara (thin line). These SEC traces were obtained from the Waters SEC system, and the vertical dashed lines show the limit of calibration for the UH250 column.

Table 3.2. Proportions in total rice flour (a) of HWSF, (b) of amylose in the HWSF, and (c) of amylose in the HWIF, for the three varieties prepared from a 1.96% (w/w) rice slurry.

Variety	**% Total Rice Flour**		
	HWSF	**Amylose in HWSF**	**Amylose in HWIF**
Shimizu Mochi	10.8	0.2	0.0
Amaroo	13.9	6.7	7.2
Doongara	17.4	9.7	11.1

To compare the separation of amylose from rice flour, the amount of amylose in the HWSF requires quantification. To do this, the yield of the dried HWSF of flour is measured, and the amylose within this fraction is determined by integrating the total intensity in the SEC traces (see e.g. [42] for an explanation as to why this yields the mass of chains). The chains between DP 100 and 1000 in Figure 3.10b are assumed to be (short) amylose chains for this calculation. Using Amaroo as the example from Table 3.2, 6.7% of flour comprises amylose in the HWSF, and 7.2 % of flour comprises short chains of amylose in the HWIF. In the only comparable study known to the authors, the yield of the HWSF from a starch source ranged from 4 – 6 %, and amylose within this HWSF accounted for only 7 – 35 % [23]; this equates to less than 2 % the starch being amylose in the separated fraction. So while there is slightly more amylose in the HWIF than HWSF using this method, the yield of amylose separated from flour is three to four times higher than that reported elsewhere [23]. Reasons to explain this discrepancy lie in the methodology of the earlier study. Specifically, (a) amylose was extracted by the butanol method from a starch, which was previously prepared by alkaline precipitation [23], both cause damage to starch, and (b) the leaching temperature of 80 °C was below the critical temperature of 85 °C [6], which would reduce the amount of amylose extracted.

Contamination of the HWSF by amylopectin seems inevitable, regardless of the separation technique [6,12,14,19]. There is a range of sizes of amylopectin molecules [44], and perhaps the smaller ones (DP 700-2100) solubilize more readily. Different speeds of centrifugation did not alter the amount of soluble amylopectin in the HWSF (data not shown). All other samples were centrifuged at 10^4 *g*, and other ways to maximize amylose in the HWSF were investigated.

Two concentrations of flour from each variety were tested to try and increase the proportion of amylose in the HWSF. The most conventional and simplest way to determine the composition of the HWSF and HWIF is to measure the maximum absorbance (λ_{max}) of the complex between starch in these fractions and iodine. The λ_{max} of this complex can be used to differentiate between amylose and amylopectin in the starch [45-47]. Table 3.3 shows the λ_{max} of the starch-iodine complex from gelatinized flour, from the HWSF, and from the solubilised HWIF of flour for all varieties and both concentrations. Amylose content is routinely measured at 620 nm (AACC 61-03) [27]. Table 3.3 shows that λ_{max} of the starch-iodine complex from gelatinized non-waxy flour is ~590 nm, and for the amylopectin-iodine complex from Shimizu mochi flour is 505 nm. Table 3.3 also shows that the maximum absorbance of HWSF is close to that of amylose (~615 nm), and that of HWIF is closer to that of amylopectin (~573 nm). These data indicate that the HWSF is amylose-rich and the HWIF is amylose-poor. Concentration does not affect λ_{max}, suggesting that concentration did not affect the proportion of amylose in the HWSF. SEC was used to analyse the hydrodynamic volume distribution of each fraction.

Table 3.3. Absorption maxima, λ_{max} (nm), of iodine complexes with starch in the rice flour, and the starch within the HWSF at two concentrations, and HWIF of flour prepared at the lower rice slurry concentration.

λ_{max} (nm)	Flour	HWSF – 3.85%	HWSF – 1.96%	HWIF – 1.96%
Shimizu Mochi	Plateau at 505	No plateau	No plateau	521
Amaroo	583	613	610	563
Doongara	601	620	621	583

Having shown that chromatograms of the molecules within the HWSF are reproducible and representative of the amylose (if not the amylopectin), the amylose in the HWSF can be examined with confidence. The chromatograms in Figure 3.11 show the bimodal SEC traces of the HWSF of flour, as separated by the UH500. The elution profile of Shimizu Mochi shows that amylopectin elutes first, and comparison with the other two varieties indicates that the broader second peak must be amylose (with a small amylopectin tail). In fact upon debranching, the narrow amylopectin peak is removed with all chains eluting below DP 100 (Figure 13). For all three varieties, the HWSF from the high concentration (3.85%) samples contained much more amylopectin than did the HWSF from the lower concentration (1.96%), even though some of the amylopectin molecules are removed during SEC. During preparation of the samples of the higher concentration, some resistance to the stirring of the paddle was noted (data not shown), suggesting that the samples experienced shear [39]. Shear assists the removal of outer layers of starch granules as they 'cook' [43], and at the higher concentration, greater interaction between molecules probably promoted more solubilization of the outer layers of the granule. Thus, an amylose-rich fraction can be separated from flour, and concentration of flour and degree of heating can be manipulated to minimize amylopectin and maximize amylose in the fraction.

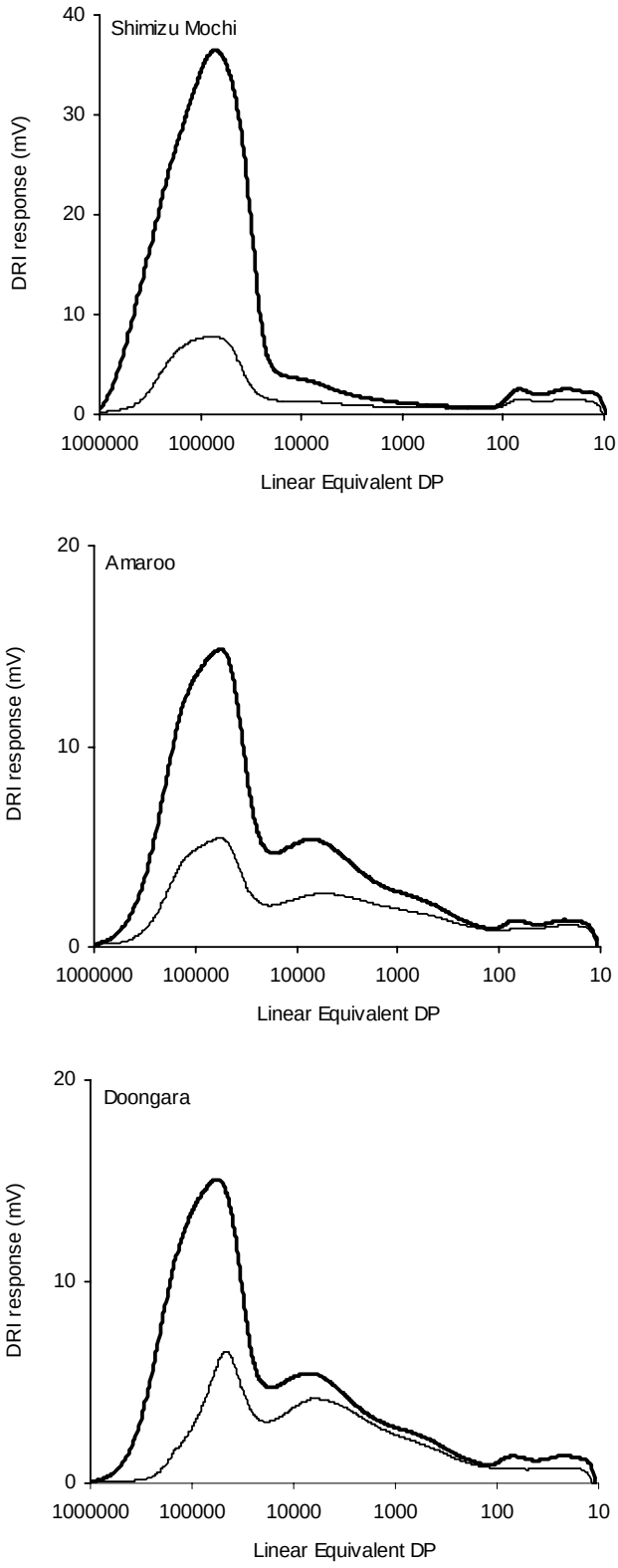

Figure 3.11. SEC traces of the HWSF of flour of Amaroo, Doongara and Shimizu Mochi rice flour separated on a UH500 column at two concentrations: 1.96% (thin line) and 3.85% (thick line). These SEC traces were obtained from the Waters SEC system.

The amylose-rich HWSF, both complete and debranched, for each variety were separated by the UH500 (Figure 3.12) (in which the abscissa show the equivalent molecular weight of linear starch with the same hydrodynamic volume – Figure 3.12a). For native amylose, the weight average molecular weight for the HWSF can only be determined by MALLS (Table 3.1), and the number-average cannot be determined by either SEC or MALLS. From the SEC data, the intensity of the DRI response in the amylose region of the native HWSF trace directly reflects the amylose content of the varieties (e.g. Doongara has both the highest intensity and amylose content). The $\overline{X}_W$ value for Doongara obtained by MALLS reported in Table 3, 7.5×10^5, is much larger than previous reports of 3000 for rice [12,48,49]. Post – SEC values for $\overline{X}_W$ are larger than those of other starches, 7.4×10^3 for cassava to 5.3×10^3 for maize [9]. The smallest sub-fractions of native starch range can range from 360 to 840, while the largest ranges between to 1.25×10^4 and to 5.2×10^3 [50]. Reasons for this discrepancy are discussed below.

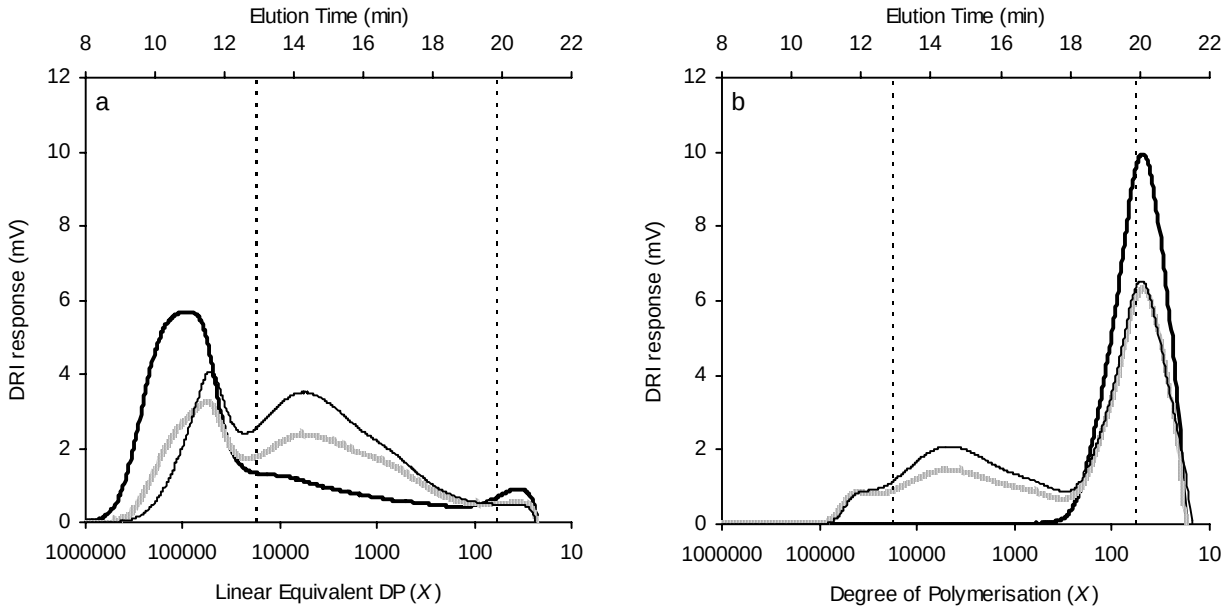

Figure 3.12. SEC traces of (a) native HWSF from the 1.96% (w/w) preparation and (b) molecular weight distributions of these HWSF, completely debranched by isoamylase, as separated by the UH500 column using the Waters system. Three varieties are presented Shimizu Mochi (thick line), Amaroo (dotted line), and Doongara (thin line), and the calibration limits of the Waters system used here are also presented.

The HWSF is completely debranched by isoamylase to produce linear starch chains and separated by a UH500. Here, the broad peak between DP 10^5 and 100 is the amylose peak, while the amylopectin elutes in the narrow peak lower than DP 100. The SEC distribution has not been corrected for band broadening, and although this is sufficiently small in modern SEC systems so as not to affect averages significantly, detailed shapes within the distribution may be affected [5,51]. SEC distributions of debranched HWSF are summarized in Figure 3.12b, and associated weight and number average degrees of polymerization ($\overline{X}_w$ and $\overline{X}_n$), and the polydispersity ($\overline{X}_w/\overline{X}_n$) are shown in Table 3.4. Thus for debranched amylose, MALLS data are not required. An $\overline{X}_w$ value of ~360 reported [12] in an earlier study of debranched amylose was determined by the modified Park-Johnson method and anthrone-sulfuric acid method[4] and can be directly compared to the $\overline{X}_n$ value of ~1800 reported here. The $\overline{X}_w$ value for debranched HWSF was found to be 0.61×10^4 for Amaroo and 1.26×10^4 for Doongara. There are no reports on a $\overline{X}_w$ value for debranched amylose from rice; however it has been reported that the $\overline{X}_w$ value from other starch sources can range from 1.03×10^3 to 4.28×10^3 [24].

Table 3.4. The ~~X~~n, ~~X~~w and polydispersity (Q) for debranched HWSF of flour (1.96% (w/w) from the non-waxy varieties.

HWSF	$\overline{X}_n$	$\overline{X}_w$	$Q = \overline{X}_w/\overline{X}_n$
Amaroo	1.82×10^3	0.61×10^4	3.4
Doongara	1.78×10^3	1.26×10^4	7.1

It is clear that a combination of sample preparation and advances in the understanding of the MWD theory can explain the discrepancies noted above. Amylose from previous studies was sourced from the precipitation of amylose from starch, after the starch itself was prepared from flour. It has been shown that incubation of flour in an alkaline solution [22], as part of the alkaline precipitation method, causes a significant decrease in the MWD of the amylose. In addition, the $\overline{X}_n$ and $\overline{X}_w$ for debranched amylose quoted here maybe slightly biased towards higher molecular weights, as the method to obtain an amylose-rich fraction preferentially leaches the larger amylose molecules, though it cannot be confidently assumed that the molecules of DP 100 -1000 in the HWIF are derived from amylose.

3.4 CONCLUSIONS

This chapter reports on improvements in key experimental techniques and analytical instrumentation for obtaining the most accurate hydrodynamic volume distribution for amylose molecules, and the MWD for debranched amylose. It is shown that the common practice of referring to molecular weights relative to pullulan greatly underestimates the actual molecular weight of the starch, and this practice can lead to errors. Analysis of an amylose-rich fraction by SEC, using conditions typical of those used widely in the literature, showed a 20 % loss of carbohydrate. By colourmetric analysis of the starch-iodine complexes and by determining $\bar{X}_w$ by MALLS, this loss was found to be predominately from residual amylopectin found in the amylose-rich fraction. Means of avoiding this loss are an important area for future work. With conditions used by many workers, it was shown that isoamylase does in fact hydrolyse all α-(1,6) branch linkages in the amylose-rich fraction to produce linear, α-(1,4) linked amylose chains. Amylose was separated directly from flour to avoid the starch degradation experienced by previous methods. Using RVA, a separation method was developed to extract an amylose fraction directly from flour, without causing any degradation to the starch. The $\bar{X}_w$ value for native amylose from Doongara is much larger than previous reports for rice. Similarly, the $\bar{X}_w$, $\bar{X}_n$ and polydispersity of debranched HWSF were also much larger. The combination of improved sample preparation and data treatment has yielded what are regarded as the most reliable MWDs of the amylose-rich fraction of rice flour.

3.5 REFERENCES

1. Ong, M. H. & Blanshard, J. M. V. Texture determinants of cooked, parboiled rice. II: Physicochemical properties and leaching behavior of rice. *J. Cereal Sci.* **21**, 261-9 (1995).
2. Ong, M. H. & Blanshard, J. M. V. Texture determinants in cooked, parboiled rice. I: Rice starch amylose and the fine structure of amylopectin. *J. Cereal Sci.* **21**, 251-60 (1995).
3. Fitzgerald, M. A. in *Rice Chemistry and Technology* (ed. Champagne, E. T.) (AACC, St Paul, Minnesota, 2004).
4. Hizukuri, S., Takeda, Y. & Yasuda, M. Multi-branched nature of amylose and the action of debranching enzymes. *Carbohydrate Research* **94**, 205-213 (1981).
5. Castro, J. V., Ward, R. M., Gilbert, R. G. & Fitzgerald, M. A. Measurement of the molecular weight distribution of debranched starch. *Biomacromolecules* **6**, 2260-70 (2005).
6. Roger, P. & Colonna, P. Molecular weight distribution of amylose fractions obtained by aqueous leaching of corn starch. *Int. J. Biological Macromolecules* **19**, 51-61 (1996).
7. Brun, Y. in *ACS Symposium Series - Multiple Detection in Size-Exclusion Chromatography* 281-301 (2005).
8. Sun, T., Chance, R. R., Graessley, W. W. & Lohse, D. J. A study of the separation principle in size exclusion chromatography. *Macromolecules* **37**, 4304-4312 (2004).
9. Roger, P. & Colonna, P. Evidence of aggregates contaminating amylose solutions. *Carbohydrate Polymers* **21**, 83-9 (1993).
10. Fishman, M. L. & Hoagland, P. D. Characterisation of starches dissolved in water by microwave heating in a high pressure vessel. *Carbohydrate Polymers* **23**, 175-83 (1994).
11. Chen, Y., Fringant, C. & Rinaudo, M. Molecular characterisation of starch by SEC: dependence of the performances on the amylopectin content. *Carbohydrate Polymers* **33**, 73-8 (1997).
12. Takeda, Y., Hizukuri, S. & Juliano, B. O. Purification and structure of amylose from rice starch. *Carbohydrate Research* **148**, 299-308 (1986).
13. Bello-Perez, L. A., Roger, P., Colonna, P. & Paredes-Lopez, O. Laser light scattering of high amylose and high amylopectin materials, stability in water after microwave dispersion. *Carbohydr. Polym.* **37**, 383-394 (1998).
14. Takeda, Y., Maruta, N. & Hizukuri, S. Structure of amylose subfractions with different molecular sizes. *Carbohydrate Research* **226**, 279-285 (1992).
15. Yokobayashi, K., Misaki, A. & Harada, T. Specificity of *Pseudomonas* Isoamylase. *Agric. Biol. Chem.* **33**, 625-7 (1969).
16. Batey, I. L. & Curtin, B. M. Measurement of amylose/amylopectin ratio by high-performance liquid chromatography. *Starch-Staerke* **48**, 338-344 (1996).
17. Banks, W. & Greenwood, C. T. Physicochemical studies on starches. XXXII. Incomplete *beta*-amylolysis of amylose. Discussion of its cause and implications. *Staerke* **19**, 197-206 (1967).
18. Takeda, Y., Maruta, N. & Hizukuri, S. Structures of indica rice varieties (IR48 and IR64) having intermediate affinities for iodine. *Carbohydrate Research* **187**, 287-94 (1989).
19. Takeda, Y., Maruta, N. & Hizukuri, S. Examining the structure of amylose by tritium labelling of the reducing terminal. *Carbohydrate Research* **227**, 113-120 (1992).
20. Gidley, M. J. Quantification of the structural features of starch polysaccharides by NMR spectroscopy. *Carbohydrate Research* **139**, 85-93 (1985).

21. Matheson, N. K. A comparison of the structures of the fractions of normal and high amylose pea seed starches prepared by precipitation with concanavalin A. *Carbohydrate Research* **199**, 195-205 (1990).
22. Chiou, H., Martin, M. & Fitzgerald, M. A. Effect of purification methods on rice starch structure. *Starch/Staerke* **54**, 415-20 (2002).
23. Mizukami, H., Takeda, Y. & Hizukuri, S. The structure of the hot-water soluble components in the starch granules of new Japanese rice cultivars. *Carbohydrate Polymers* **38**, 329-335 (1999).
24. Murugesan, G., Shibanuma, K. & Hizukuri, S. Characterisation of hot-water-soluble components of starches. *Carbohydrate Research* **242**, 203-215 (1993).
25. Chiou, H., Fellows, C. M., Gilbert, R. G. & Fitzgerald, M. A. Study of rice starch structure by dynamic light scattering in aqueous solution. *Carbohydrate Polymers* **61**, 61-71 (2005).
26. Castro, J. V., Dumas, C., Chiou, H., Fitzgerald, M. A. & Gilbert, R. G. Mechanistic information from analysis of molecular weight distributions of starch. *Biomacromolecules* **6**, 2248-59 (2005).
27. Juliano, B. O. in *Proceedings of the workshop on Chemical Aspects of Rice Grain Quality. Review of Methodolgy* 251-60 (International Rice Research Institute, 1979).
28. Teraoka, I. *Polymer Solutions: An Introduction to Physical Propertieties* (John Wiley, New York, 2002).
29. Chu, B. *Laser light scattering* (Academic, Boston, 1991).
30. Gallot-Grubisic, Z., Rempp, P. & Benoit, H. Universal calibration for gel permeation chromatography. *J. Polym. Sci., Polym. Lett. Ed.* **5**, 753-9 (1967).
31. Lu, T.-J., Jane, J.-L. & Keeling, P. L. Temperature effect on retrogradation rate and crystalline structure of amylose. *Carbohydrate Polymers* **33**, 19-26 (1997).
32. Morell, M. K., Samuel, M. S. & O'Shea, M. G. Analysis of starch structure using fluorophore-assisted carbohydrate electrophoresis. *Electrophoresis* **19**, 2603-2611 (1998).
33. Gidley, M. J. & Bulpin, P. V. Crystallisation of malto-oligosaccharides as models of the crystalline forms of starch: Minimum chain-length requirement for the formation of double-helices. *Carbohydrate Research* **161**, 291-300 (1987).
34. de Gennes, P. G. Kinetics of diffusion-controlled processes in dense polymer systems. II. Effects of entanglements. *J. Chem. Phys.* **76**, 3322 (1982).
35. McLeish, T. C. B. & Milner, S. T. Entangled dynamics and melt flow of branched polymers. *Adv. Polymer Sci.* **143**, 195-256 (1999).
36. Gidley, M. J. & Bulpin, P. V. Aggregation of amylose in aqueous systems: the effect of chain length on phase behavior and aggregation kinetics. *Macromolecules* **22**, 341-6 (1989).
37. Maeda, I., Kiribuchi, S. & Nakamura, M. Digestion of barley starch granules by the combined action of alpha- and beta-amylases purified from barley and barley malt. *Agric. Biol. Chem.* **42**, 259-67 (1978).
38. Tsai, M.-L. & Lii, C.-Y. Effect of hot-water-soluble components on the rheological properties of rice starch. *Starch/Staerke* **52**, 44-53 (2000).
39. Nguyen, C. C., Martin, V. J. & Pauley, E. P. in *PCT Int. Appl.* 103 pp. ((Penford Products Co., USA). Wo, 1990).
40. Bhattacharya, K. R., Sowbhagya, C. M. & Indudhara Swamy, Y. M. Importance of insoluble amylose as a determinant of rice quality. *J. Sci. Food and Agriculture* **29**, 359-64 (1978).

41. van de Wal, M., D'Hulst, C., Vincken, J. P., Buleon, A., Visser, R. & Ball, S. Amylose is synthesised in vitro by extention of and cleavage from amylopectin. *J. Biol. Chem.* **273**, 22232-22240 (1998).
42. Clay, P. A., Gilbert, R. G. & Russell, G. T. Molecular weight distributions in free-radical polymerizations. 2. Low-conversion bulk polymerizations. *Macromolecules* **30**, 1935-46 (1997).
43. Davey, M. J., Landman, K. A., McGuinness, M. J. & Jin, H. N. Mathematical modeling of rice cooking and dissolution in beer production. *AIChE Journal* **48**, 1811-26 (2002).
44. Takeda, Y., Shibahara, S. & Hanashiro, I. Examination of the structure of amylopectin molecules by fluorescent labeling. *Carbohydr. Res.* **338**, 471-475 (2003).
45. Takeda, Y. & Hizukuri, S. Structures of rice amylopectins with low and high affinities for iodine. *Carbohydrate Research* **168**, 79-88 (1987).
46. Ramesh, M., Ali, S. Z. & Bhattacharya, K. R. Structure of rice starch and its relation to cooked-rice texture. *Carbohydrate Polymers* **38**, 337-347 (1999).
47. Banks, W., Greenwood, C. T. & Khan, K. M. The interaction of linear amylose oligomers with iodine. *Carbohydrate Research* **17**, 25 - 33 (1971).
48. Hizukuri, S. Starch: analytical aspects. *Food Science and Technology* **74**, 347-429 (1996).
49. Takeda, Y., Tomooka, S. & Hizukuri, S. Structures of branched and linear molecules of rice amylose. *Carbohydrate Research* **246**, 267-272 (1993).
50. Hizukuri, S. & Takagi, T. Estimation of the distribution of molecular weight for amylose by the low-angle laser-light-scattering technique combined with high-performance gel chromatography. *Carbohydrate Research* **134**, 1 - 10 (1984).
51. van Berkel, K. Y., Russell, G. T. & Gilbert, R. G. Molecular weight distributions and chain-stopping events in the free-radical polymerization of methyl methacrylate. *Macromolecules* **38**, 3214-24 (2005).

Chapter 4

Impact of temperature on rice quality

4.1 INTRODUCTION

Higher global temperatures are forecast to threaten both our food security [1] and food quality in the future. For example, over the past 50 years, Australia's rice-growing region, the Murrumbidgee Irrigation Area (MIA), has experienced an average increase in the minimum temperature of 0.03 °C per annum, and of the maximum temperature by 0.01°C/yr (Bureau of Meteorology), a trend consistent with global changes in air temperature [2]. In general, grain-filling in rice occurs during the summertime, and seasonal fluctuations of 6 °C within a higher range of temperatures can increase the number of days over 30 °C during the Australian summer. These irregularities in air temperature can interrupt the grain-filling period, by shortening the duration of grain-filling, thereby having a negative impact on accepted and expected qualities of rice [3-6]. In order to maintain established variety-specific traits of quality in the future, the inevitable effects of climate change on rice quality must be determined. Only then can rice breeders begin to implement strategies to ensure that the quality of any variety of rice is predictable and stable in a changing environment.

Most of the rice grown around the world is non-waxy, which means that it contains the functional form of the protein Granule Bound Starch Synthase I (GBSSI), which synthesises amylose [7,8]. It is the amylose content and structure that largely defines quality of non-waxy rice, so understanding how high temperature during grain-filling affects amylose is integral to understanding these effects on grain quality. Amylose molecules are generally lightly branched and long ($\overline{X}_n$ value of 1.8 x 10^3, $\overline{X}_w$ value of 0.6-1.3 x 10^4) [9], and amylose content [10] and amylose structure can be easily determined [9]. Amylose content and structure can provide a direct link to both the functional properties of rice [11], and to the synthesis of amylose in the endosperm. For example, when rice experiences high temperatures between flowering and maturity, the phenotypic response, in many varieties, is a decrease in amylose content [4,12], which in turn, changes many of the functional properties of the flour [13]. However, the relationship between amylose content and amylose synthesis in high temperature has been the subject of only a few studies and has not been clearly established across the different germplasm classes of rice [14,15]. Therefore the objective here is to combine the function to structure relationship with the relationship between amylose structure and synthesis to provide options for securing amylose-based elements of rice quality in an increasingly warmer climate in all germplasm classes: *temperate japonica*, *tropical japonica* and *indica*.

With the sequence of the rice genome now available, and the rapid advancements in cataloguing allelic variability, it is becoming simpler to relate genetic variation at known loci to allelic function. Amylose is synthesised by the *waxy* gene (GBSS), and two alleles have been described at that locus, Wx^a and Wx^b. Prior to the availability of genotyping technology, these were defined on the basis of the amount of GBSS1 protein expressed at high temperature [7]. With the availability of genotyping technology, these are now defined by a G

→ T polymorphism at the 5` splice site of the leader intron 1 (+1) [16] which post-transcriptionally alters the expression of the GBSSI protein [17]. In varieties carrying the AGgt sequence, mRNA of 2.3 kB is produced and transcribed [18]. Varieties carrying the AGtt sequence use at least six different splicing patterns to generate a proportion of correctly and incorrectly spliced 2.3 kB GBSSI mRNA, some of which can be translated [19]. Those varieties also accumulate an incompletely spliced transcript of 3.3 kB, which contains intron 1, and cannot be translated [18]. This molecular information all suggests that ultimately it is amount of 2.3 kB transcript that determines the amount of GBSSI protein, and thus amylose, produced. The efficiency of splicing at the authentic splice site is compromised with different environmental stimuli. Nepalese Wx^{op} varieties have a G at +1 and are influenced by photoperiodism [20]. Varieties with a T at +1 can produce more GBSSI at cooler temperatures [3,15,17] which led to the conclusion that the authentic splice site at +1 is favoured at the cooler temperature [15].

Aside from the G/T polymorphism or Wx^a / Wx^b classification, there is a dinucleotide CT repeat unit located 55 bp upstream from the 5`-leader splice site within exon 1 [21,22]. The number of CT repeats ranges from 8 to 20 and can account for 83% of variance in amylose content, particularly amongst the medium and low amylose contents of Wx^b varieties [21-23]. The number of CT repeats, in combination with the G/T polymorphism, has been used to classify the amylose content of rice varieties as either sensitive or tolerant to high temperatures. In one study, varieties carrying the AGgt with CT 11 and 20 were classified as tolerant and those carrying AGtt with CT 17 and 18 as sensitive to high temperatures [15]. More weight is placed on the role of the polymorphism at the 5` splice site of intron 1 than the CT repeat as an indicator of temperature tolerance [15] .

This chapter demonstrates that varieties carrying the Wx^a allele are not all tolerant , in terms of amylose content and structure, to high temperature during grain filling. We systematically show that functional properties controlled by amylose, amylose content, structure and synthesis are all affected by high temperature in some varieties carrying the Wx^a allele. Further, data in this chapter we show another SNP in intron 1 of GBSS1 that correlates very strongly with temperature tolerance, and mechanisms are proposed to explain the seasonal variability in amylose content in Wx^a carriers and the basis of temperature sensitivity in some Wx^a carriers.

4.2 MATERIALS AND METHODS

4.2.1 Materials

Twelve varieties of rice (*Oryza sativa* L.), 2 from each of 6 CT_n classes, and from 5 origins were used in this study (Table 4.1). The CT_n classification was determined as part of the routine analyses of the Rice Improvement Program in Australia, using the microsatellite marker reported by Bligh et al. (1995) and the methods reported by [23].

Seeds of each variety were placed in pots filled with clay loam, then covered with sand. Once germinated, the plants were thinned to five per pot. All plants were grown at temperatures with a daily average of 28 °C throughout the vegetative stage, in a growth room with natural light. Panicles were tagged with the flowering date when the top half of the panicle was flowering. When at least three panicles in a pot reached five - eight days after flowering, the pot was transferred to one of three temperature-controlled glasshouses. In the first glasshouse the day/night temperature was 26/17 °C, in the second it was 36/17 °C, and in the third it was 36/27 °C. The glasshouses were lit with natural irradiance, and the rice was continually flooded until 10 days before maturity. Data loggers were placed in each glasshouse at a height of 10 cm above panicles to monitor consistency of performance of the temperature controls.

Grain was harvested at maturity, dehulled (THU35A 250V 50Hz Test Husker, Satake, 23-25 Marigold Street, Revesby, PO Box 4065, Milperra, NSA, 1891, Australia), milled (No.2 Mill, McGill, Seedburo Equipment Company, 1022 W Jackson Blvd, Chicago, IL 60607, USA) and then ground (Cyclotec 1093 Sample Mill, Tecator AB, Box 70 S-263 01, Hoeganaes, Sweden) to pass through a 0.5 mm sieve. All experimental work was conducted in duplicate and within 6 months of harvesting.

4.2.2 Methods

Viscosity curves were used to indicate a functional response to high temperatures. Curves were generated by Rapid Visco Analysis (Newport Scientific, Unit 1, 2 Apollo Street, Warriewood, NSW, 2102, Australia) using the standard method for rice (AACC Method 61-02). Since amylose is most likely to affect the change in viscosity from the trough to the final [11], we focus on this parameter of the curve, and use the term immediate retrogradation to describe it.

Amylose content was determined by iodine binding [10]. The molecular weight distribution (MWD) of debranched amylose was measured according to Chapter 3 [9]. SEC was performed on a Waters system consisting of an Alliance (2695) and Differential Refractive Index Detector (Waters 2410) with Waters software (Empower®) to control the pump, and to acquire and process data. The UH500 column used in this system was calibrated using

pullulan standards, the Mark-Houwink-Sakurada equation and universal calibration [24]. The Mark-Houwink parameters used for this conversion, with ammonium acetate (0.05 M, pH 5.2) as the solvent, and the column at 60 °C were recently found to be K = 0.00126 mL g^{-1} and α = 0.733 for pullulan, and K = 0.0544 mL g^{-1} and α = 0.486 for linear starch [24]. From the MWD of debranched amylose, the number- and weight- average degree of polymerisation ($\overline{X}_n$ and $\overline{X}_w$, respectively) and polydispersity ($Q = \overline{X}_w / \overline{X}_n$) were calculated [9,24].

To determine any relationship between immediate retrogradation and structural parameters, significance of the correlation (r) was determined from a Pearsons two-tailed critical values table. To determine the effect of temperature on these parameters, an ANOVA was performed (SAS program Version 9.1 (SAS Institute Inc., Cary, N.C., U.S.A.)).

GBSSI protein was extracted from mature grain [8] and separated using SDS-polyacrylamide gel electrophoresis (SDS-PAGE). SDS-PAGE was carried out with a Hoeffer 10 x 8 cm Mighty Small, using a 10% gel as described in the Operator Manual (Hoeffer Pharmacia Biotech Inc. 654 Minnesota Street, San Francisco, CA, 94107, USA). Gels were dried (Hoeffer Easy Breeze) after staining with Coomassie Blue R-250. GBSSI protein was identified by sequencing the excised band (Biomolecular Research Facility, Newcastle Protein, LS3-16, Life Sciences Building, University of Newcastle, University Drive, Callaghan NSW 2308, Australia).

The forward and reverse primers used to amplify the desired part of the *Wx* gene were, 5′-TAAAATGTGTTGCGGGAGGGA and 5′ TCCTTTGACCAACTCGGCTACTAA. The PCR cocktail (2.5 mmol $MgCl_2$, 0.2 mmol primers, 1x Gibco PCR buffer, 200 mmol of total dNTP, 1U PlatinumQ Taq DNA polymerase (Gibco BRLQ)) was mixed with 10 ng of DNA template. The PCR profile used was 94˚C for 2 min, followed by 30 cycles of denaturation at 94 ˚C for 30 s, annealing 60 ˚C for 30 s and polymerization 72 ˚C for 60 s, finishing at 72 ˚C for 7 min. PCR was performed using a Perkin-Elmer, Gene Amp PCR system 9700. The sequence of the amplified product was determined at a commercial laboratory. The program BioEdit was used to align sequences and translate the RNA [25].

4.3 RESULTS AND DISCUSSION

The identification and screening of varieties tolerant to high temperatures is necessary to secure grain quality in the future. The G→T polymorphism at the splice site of leader intron 1 of the *Wx* gene has been proposed to classify varieties as sensitive or tolerant to temperature during grain-filling [15]. However the claim was supported only by amylose content. In this chapter this classification is re-assessed by delving beyond amylose content, and exploring functional properties controlled by amylose, amylose structure, and GBSS1 protein expression. Larkin et al. (1999) used a narrow gene pool and a limited number of samples; both factors make it difficult to generalise widely from their findings. In this study, twelve rice varieties were sourced from five countries across six CT_n classes, Rexmont, Dawn and Bluebelle are further defined as long grain *tropical japonicas*, and Koshihikari is defined as a *temperate japonica* subspecies [26]. The G/T polymorphism at the 5′ splice site of leader intron 1 was used to define temperature tolerance [15] in the selection of varieties. Based on this definition, six of the varieties putatively grouped as temperature tolerant, carrying AGgt, and six grouped as temperature sensitive carrying AGtt (Table 4.1).

Table 4.1. Summary of the CT class, polymorphism at +1, origin, and predicted sensitivity to growth temperature [15].

Variety	CT Class	SNP	Origin	Temperature
I-Geo-Tze	11	G	Taiwan	Tolerant
Rexmont	11	G	USA	Tolerant
Doongara	14	G	Australia	Tolerant
Dawn	14	G	USA	Tolerant
IR64	17	G	Philippines	Tolerant
Bluebelle	20	G	USA	Tolerant
Koshihikari	17	T	Japan	Sensitive
Opus	17	T	Australia	Sensitive
Millin	18	T	Australia	Sensitive
Pelde	18	T	Australia	Sensitive
Amaroo	19	T	Australia	Sensitive
Langi	19	T	Australia	Sensitive

Viscosity curves are commonly used by food scientists and rice breeders as an index of functional properties of the grain and flour (Figure 4.1. Typically the difference between peak and final viscosity, or setback is reported [11], however setback is influenced by both protein and amylose [11,27]. A more meaningful parameter for this amylose-based assessment of temperature- induced alterations in rice quality could be immediate retrogradation, defined as the cooling period between trough and final viscosity. A correlation study (Table 4.2), shows that the viscosity parameter of immediate retrogradation is significantly correlated (r = 0.875, $P < 0.0001$) with amylose content as well as with $\overline{X}_n$, $\overline{X}_w$ and polydispersity. This is not surprising as it is the long amylose chains that, upon cooling, entangle and interact at multiple points to cause gelation [28-30]. Thus, the immediate retrogradation of the twelve varieties grown at the three temperatures is presented in Table 4.3. For all varieties carrying AGtt, when grain-filling occurred at either 36/17 °C or 36/27 °C, immediate retrogradation was significantly lower than when grain-filling occurred at 26/17 °C (Table 4.3). The parameter of immediate retrogradation was not significantly different between the three temperatures for three of the varieties carrying AGgt, but for the other three AGgt varieties, immediate retrogradation followed the same pattern with temperature as for the AGtt varieties (Table 4.3). This suggests that not all the AGgt varieties are tolerant to high temperatures during the grain filling period. There was no relationship between immediate retrogradation and the number of CT repeats.

Figure 4.1. The parameter of the viscosity trace are defined by the peak (P), trough (T) and final (F) vicosity, and the setback (SB) defined by the difference between the peak and final vicosity, and by immediate retrogradation (IR) which is the difference between the trough and final viscosity.

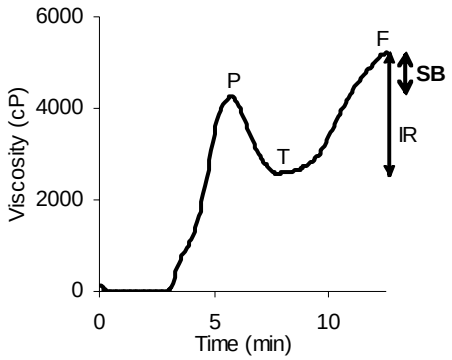

Table 4.2. Correlation of immediate retrogradation with amylose content, $\overline{X}_n$, $\overline{X}_w$ and Q of all varieties at every growth temperature. The probability is based on a two-tailed critical value for Pearsons r.

Parameter	**r**	***P***
Amylose	0.895	<0.0001
$\overline{X}_n$	0.731	<0.0001
$\overline{X}_w$	0.644	<0.0001
Q	-0.386	0.0199

Table 4.3: Immediate retrogradation (cP, final minus tough viscosity) of each variety grown at 26/17 °C, and the difference in immediate retrogradation presented as a percent difference to the 26/17 °C trial.

SNP	CT Repeat Class	Variety	26/17 °C (cP)	36/17 °C (% difference)	36/27 °C (% difference)
G	11	I-Geo-Tze	2646	17	21
G	11	Rexmont	2323	19	9
G	14	Doongara	2043	39	57
G	14	Dawn	1824	36	45
G	17	IR64	1353	17	30
G	20	Bluebelle	2118	54	62
T	17	Koshihikari	1338	46	42
T	17	Opus	1375	50	48
T	18	Millin	1497	57	57
T	18	Pelde	1728	56	53
T	19	Amaroo	1491	54	54
T	19	Langi	1761	79	52

The amylose contents of the twelve varieties grown in the three temperatures are shown in Table 4.4. When grain-filling occurred at 26/17 °C, the amylose content of varieties carrying AGgt was above 25 % defining those as high amylose varieties, and for AGtt varieties the amylose content was below 25%. The varieties carrying AGtt are all either intermediate or low amylose. Given the correlation shown in Table 4.2, any changes in immediate retrogradation at high temperature should be reflected in the amylose content. At higher temperatures, the reduction in amylose content of ten varieties was matched by a reduction in immediate retrogradation of only nine varieties. IR64 showed no change in immediate retrogradation but a reduction is amylose content to clearly illustrate the danger of relying on just one parameter to categorise varieties. For example, Lemont, Rexmont and L202 where all considered as tolerant to growth temperature [15], but the intermediate amylose variety, Lemont, actually showed a decrease in amylose content of 3 % in that study.

Table 4.4: Amylose Content (%) of twelve varieties grown at one of three temperatures.

SNP	CT Class	Variety	26/17 °C	36/17 °C	36/27 °C
G	11	I-Geo-Tze	30.8	30.4	29.9
G	11	Rexmont	27.4	28.7	31.8
G	14	Doongara	27.8	17.9	15.6
G	14	Dawn	26.7	19.8	19.8
G	17	IR64	24.7	20.5	18.0
G	20	Bluebelle	27.5	21.8	15.6
T	17	Koshihikari	23.1	19.3	17.8
T	17	Opus	23.0	19.8	21.0
T	18	Millin	20.6	16.6	16.3
T	18	Pelde	22.1	16.8	15.7
T	19	Amaroo	16.5	14.7	14.3
T	19	Langi	23.9	15.4	17.2

The molecular weight distribution (MWD) of debranched amylose from grains of each variety, and each temperature of grain-filling, is presented in Figures 4.2 and 4.3. In this calibrated SEC system [24], amylose chains elute and are defined as those above 100 Degrees of Polymerisation (DP) (see Chapter 3). As the Differential Refractive Index (DRI) detector is mass sensitive, it can be seen that for the 26/17 ˚C treatment there are more chains across the distribution in the AGgt varieties than in the AGtt varieties. When grain-filling occurred at the two high temperatures, the debranched amylose of the AGtt varieties contained very few amylose chains above DP 100. For two AGgt varieties, there was little difference in the MWD of amylose between the three temperature treatments. However, for three AGgt varieties, there was a noticeable decrease in the amount amylose chains and a shift in the MWD towards a lower DP. For the sixth AGgt variety, IR64, the amount of chains was slightly reduced for the 36/17 ˚C treatment and noticeably reduced for the for the 36/27 ˚C treatment. A defatted MWD of IR64 (data not shown) shows that the variability of MWDs of IR64 was not caused by amylose-lipid complexes. Within varieties except IR64, there was no significant difference between the amount and the MWD of the amylose chains when grain-filling occurred at either 36/17 °C or 36/27 °C. For the SEC distributions to be used quantitatively, instead of qualitatively, the number- and weight- average degree of polymerisation ($\overline{X}_n$ and $\overline{X}_w$, respectively) and polydispersity (Q) were calculated from SEC distributions of debranched amylose (Table 4.5). Generally, the distribution of amylose chains from the AGtt varieties is more polydisperse than for the AGgt varieties.

The apparent disparity within the AGgt carrying varieties seen in the above qualitative analysis of immediate retrogradation and amylose structural data can be confirmed by statistical analysis. Table 4.6 shows the results of an analysis of variance comparing the relationship between temperature of grain-filling and immediate retrogradation and structural parameters of amylose in the AGtt varieties and the AGgt. It is expected, and shown, that all the AGtt varieties were significantly affected by growth temperatures during the grain-filling period. The AGgt varieties, as expected from the qualitative review of the data, show that immediate retrogradation, $\bar{X}_n$ and $\bar{X}_w$ are all susceptible to growth temperature. It is interesting to note that amylose content within the AGgt group of varieties was statistically not susceptible to temperature given the decrease in amylose content of several of these varieties. This suggests that amylose content alone is not an ideal measure of susceptibility to temperature. Further, the apparent susceptibility of IR64 based on the amylose content is dubious and given the immediate retrogradation and MWD data, IR64 will be considered a variety that is tolerant to temperature.

Table 4.6. Influence of growth temperature on the functional and structural properties of starch amongst the AGgt and AGtt varieties as analysed by ANOVA (Table 4.1).

Parameter	**AGgt Varieties**		**AGtt Varieties**	
	F value	**Pr > F**	**F value**	**Pr > F**
Immediate retrogradation	3.85	0.0448	75.28	<0.0001
Amylose	1.11	0.3538	7.10	0.0068
$\bar{X}_n$	5.91	0.0128	20.49	<0.0001
$\bar{X}_w$	4.60	0.0027	14.13	0.0004
Q	0.17	0.8454	1.64	0.2262

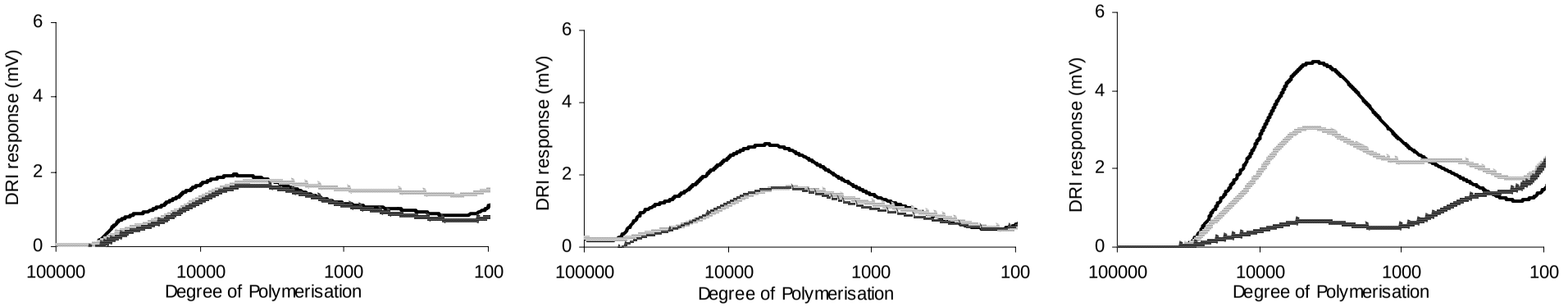

Figure 4.2a: Molecular weight distributions of debranched HWSF of flour from Rexmont, I-Geo-Tze and IR64. Growth temperature treatments are 26/17 °C (solid line), 36/17 °C (black dots) and 36/27 °C (black line with white dots).

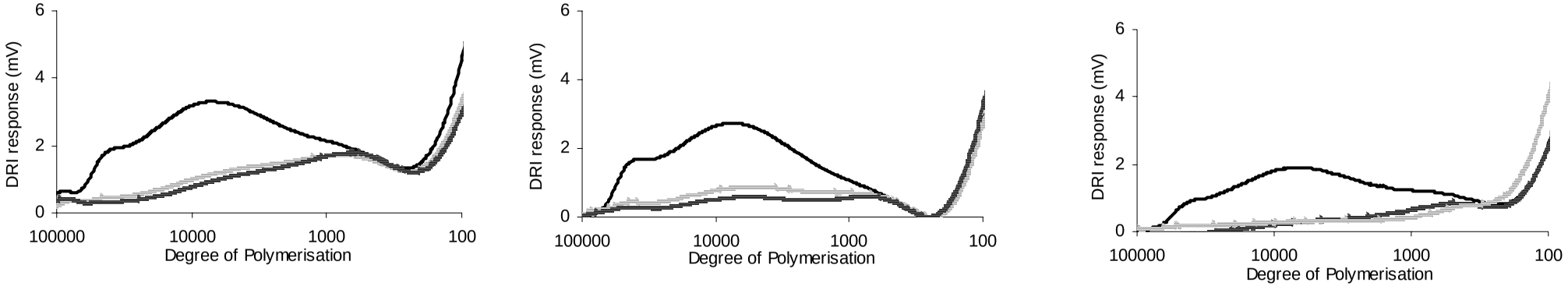

Figure 4.2b: Molecular weight distributions of debranched HWSF of flour from Doongara, Dawn and Bluebelle (left to right). Growth temperature treatments are 26/17 °C (solid line), 36/17 °C (black dots) and 36/27 °C (black line with white dots).

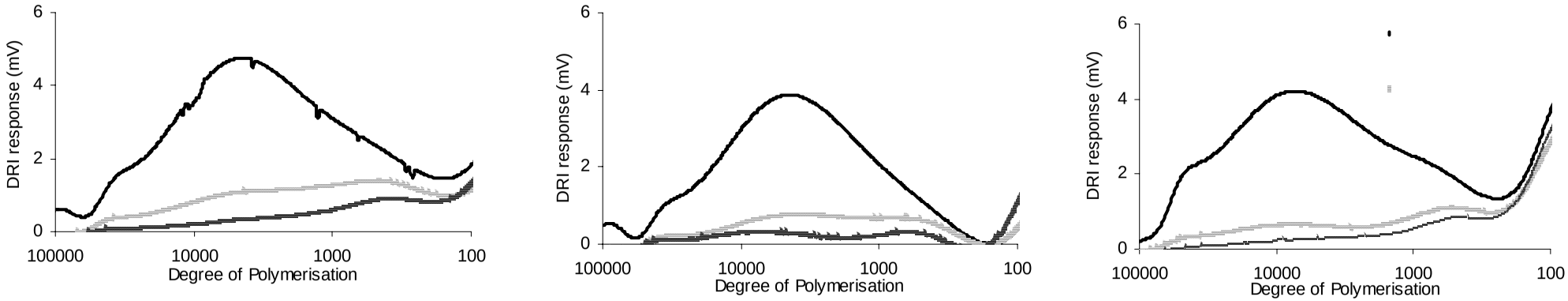

Figure 4.3a: Molecular weight distributions of debranched HWSF of flour from Koshihikari, Opus and Millin (left to right). Growth temperature treatments are 26/17 °C (solid line), 36/17 °C (black dots) and 36/27 °C (black line with white dots).

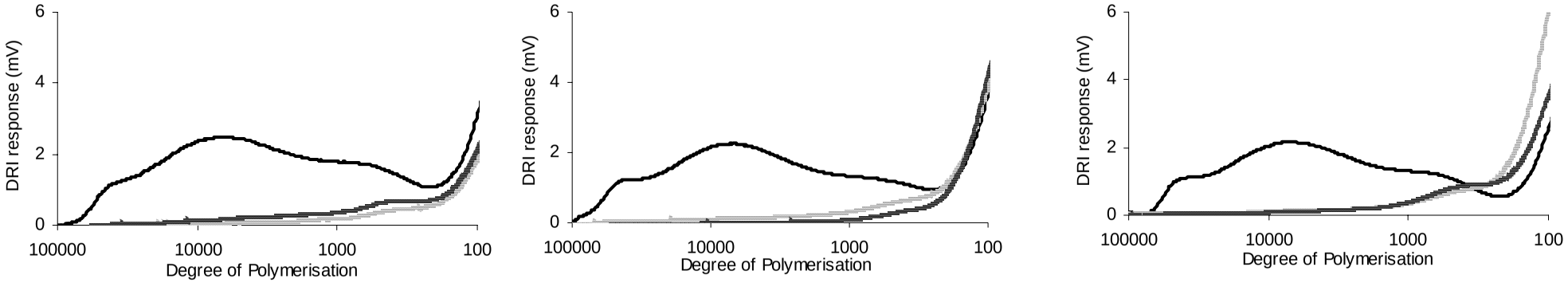

Figure 4.3b: Molecular weight distributions of debranched HWSF of flour from Pelde, Amaroo and Langi. Growth temperature treatments are 26/17 °C (solid line), 36/17°C (black dots) and 36/27 °C (black line with white dots).

Table 4.5. The number- and weight-average degree of polymerisation ($\bar{X}_n$ and $\bar{X}_w$, respectively) and the polydispersity ($Q = \bar{X}_w / \bar{X}_n$) from the number and weight distribution of debranched HWSF from twelve varieties grown at three temperatures during the reproductive period.

Temperature Trt		**26/17 °C**			**36/17 °C**			**36/27 °C**		
CT Class	**Variety**	$\bar{X}_n$	$\bar{X}_w$	***Q***	$\bar{X}_n$	$\bar{X}_w$	***Q***	$\bar{X}_n$	$\bar{X}_w$	***Q***
11	I-Geo-Tze	1242	11079	8.9	930	6692	7.2	820	7000	8.5
11	Rexmont	766	8746	11.3	580	6309	10.9	745	7860	10.5
14	Doongara	925	8715	9.4	546	4389	8.0	361	3143	8.7
14	Dawn	1690	11253	6.7	931	8913	9.6	596	7334	12.3
17	IR64	873	4153	4.8	596	3519	5.9	329	2350	7.2
20	Bluebelle	810	10529	13.0	377	5725	15.2	277	3507	12.7
17	Koshi	673	11017	16.4	464	6919	14.9	461	7796	16.9
17	Opus	1032	10481	10.2	523	7877	15.1	363	7411	20.4
18	Millin	659	8329	12.6	350	3373	9.6	233	3742	16.0
18	Pelde	683	8455	12.4	237	2319	9.8	287	3446	12.0
19	Amaroo	618	10218	16.5	218	4052	18.6	194	3330	17.2
19	Langi	749	11422	15.3	189	2362	12.5	187	2870	15.3

The final measure of the response of growth temperature to the grain-filling is the expression of Granule Bound Starch Synthase I at each temperature regime. Figure 4.4 shows the amount GBSSI protein in 10 mg of mature grain. For the 26/17 °C treatment, the amount of GBSSI from grain of the AGgt varieties is greater than that from the AGtt varieties. Only grains of three of the AGgt varieties express the same amount of protein independent of the temperature of grain-filling. The other nine varieties show a substantial decrease in the expression of GBSS1 protein in endosperms that developed at 36/17 °C or 36/27 °C compared with those that developed at 26/17 °C. The amount of GBSS1 is not confounded by the protein content of the grain, as the protein content actually decreases by 2 % in high growth temperatures (data not shown).

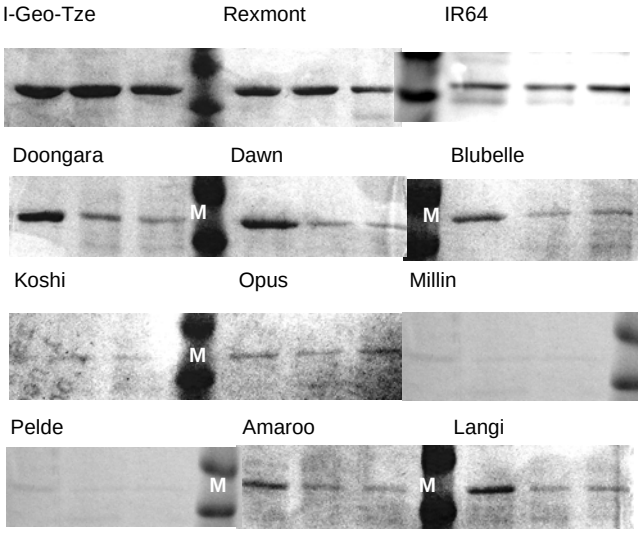

Figure 4.4. GBSSI per 10 mg of rice flour from each variety grown at 26/17 °C (left), 36/17 °C (middle), and 36/27 °C (right). Molecular markers are of weight 66 kDa and 55 kDa (white M).

The temperature during grain-filling can, in some varieties (Table 4.6), alter the structural properties of amylose [3,6,13]. Within the twelve varieties that spanned two polymorphisms and 6 CT classes, three distinct responses were noted. In all AGtt varieties, when grain-filling occurred in cool temperatures, long chains of amylose were present (Figure 4.3), and immediate retrogradation occurred (Table 4.3). When grain-filling occurred at high temperatures, the amount, number and weight average of amylose chains were significantly decreased (Figure 4.3, Table 4.5), and immediate retrogradation did not occur (Table 4.3). Amongst AGtt varieties this result is expected, but the replication of this result in 2 AGgt varieties and a decrease in amylose content for IR64 and no change in immediate retrogradation was not expected. The decrease in

amylose content is explained by the decrease in the expression of GBSS1 protein (Figure 4.4) in the AGtt varieties, and the decrease in immediate retrogradation is likely to be because short chains of amylose do not contribute to the formation of strong gels [29,30]. All AGtt varieties consistently show sensitivity to temperature during the grain-filling period. Of the AGgt varieties, I-Geo-Tze and Rexmont are tolerant to temperature in each of the characterisations. Although at 36/27 °C the amylose content and structure is altered, the viscosity trace and amount of GBSS1 suggests that IR64 is tolerant to temperature. The remaining AGgt varieties, Doongara, Dawn and Bluebelle, show sensitivity to temperature across all characterisations. The AGgt varieties are now separated into Group 1 (tolerant) and the Group 2 (responding like the AGtt varieties).

The difference in amylose content between AGtt and AGgt varieties has been shown to relate specifically to the SNP at the splice site of intron 1 [18] whereby the leader intron is correctly spliced in the AGgt varieties, giving mRNA of 2.3 kB [16,18,19]. However, in AGtt varieties, intron 1 can be retained, giving a transcript of 3.3 kB [18]. The lesser amount of the GBSS1 expression and lesser amount of amylose that accumulates in AGtt varieties is explained by the use of at least six different splicing patterns that remove intron 1, producing a small amount of correctly spliced GBSS mRNA (2.3 kB) [19]. High temperatures during grain-filling affect the use of the cryptic splice sites in AGtt varieties leading to even less mature mRNA, GBSS1 and amylose in high temperatures [15,17]. Figure 4.4 shows that expression of the GBSS1 protein in the Group 1 AGgt varieties did not decrease at high temperature, consistent with the discussion above, but in Group 2 AGgt varieties, it did decrease, in the same way as the AGtt varieties. Further, the systematic investigation of the amylose structure, function and protein expression in the AGgt varieties places the temperature sensitivity of the Group 2 AGgt varieties at either the transcriptional or the translational level. Revisiting the sequence of the *Wx* gene to account for the three phenotypes that have emerged revealed another SNP in the leader intron 1 (Figure 4.5). At +85 upstream from the authentic splice site of intron 1, the a in the Group 1 AGgt varieties is replaced by a g in the Group 2 AGgt and all AGtt varieties. This SNP changes the surrounding sequence from caaata (in the Group 1 AGgt varieties) to caagta in the Group 2 AGgt and all AGtt varieties.

Without the opportunity for rigorous experimental analysis, the second SNP at +85 allows speculation for the possible causes for the interruption of the translation or transcription mechanism that resulted in an interruption to amylose synthesis in Group 2 AGgt varieties. Often a trait can be the result of an entire gene network, such a that for grain size [31], whereby a SNP in one allele is complemented by a secondary allele. It is possible that the combination of SNPs within exon 1 of Rexmont and I-Geo-Tze in Group 1 AGgt varieties, and the Group 2 AGgt varieties are complemented by another allele in the gene network. For IR64 and Lemont, there maybe no compensation and as noted in this chapter a change in the trait is seen. Perhaps

Group 1 AGgt

	+1				+85
I Geo Tze	AG**G**tatacatatatgtttat	aattctttgtttcccctctt	attcagatcgatcacatgc	atctttcattgctcgttttt	ccttacaa**a**tagtctcattac
Rexmont	AG**G**tatacatatatgtttat	aattctttgtttcccctctt	attcagatcgatcacatgc	atctttcattgctcgttttt	ccttacaa**a**tagtctcattac
IR64	AG**G**tatacatatatgtttat	aattctttgtttcccctctt	attcagatcgatcacatgc	atctttcattgctcgttttt	ccttacaa**a**tagtctcattac

Group 2 AGgt

Bluebelle	AG**G**tatacatatatgtttat	aattctttgtttcccctctt	attcagatcgatcacatgc	atctttcattgctcgttttt	ccttacaa**g**tagtctcattac
Doongara	AG**G**tatacatatatgtttat	aattctttgtttcccctctt	attcagatcgatcacatgc	atctttcattgctcgttttt	ccttacaa**g**tagtctcattac
Dawn	AG**G**tatacatatatgtttat	aattctttgtttcccctctt	attcagatcgatcacatgc	atctttcattgctcgttttt	ccttacaa**g**tagtctcattac
Lemont	AG**G**tatacatatatgtttat	aattctttgtttcccctctt	attcagatcgatcacatgc	atctttcattgctcgttttt	ccttacaa**g**tagtctcattac
Labelle	AG**G**tatacatatatgtttat	aattctttgtttcccctctt	attcagatcgatcacatgc	atctttcattgctcgttttt	ccttacaa**g**tagtctcattac

Group 2 AGtt

Millin	AG**T**tatacatatatgtttat	aattctttgtttcccctctt	attcagatcgatcacatgc	atctttcattgctcgttttt	ccttacaa**g**tagtctcattac
Pelde	AG**T**tatacatatatgtttat	aattctttgtttcccctctt	attcagatcgatcacatgc	atctttcattgctcgttttt	ccttacaa**g**tagtctcattac
Koshihikari	AG**T**tatacatatatgtttat	aattctttgtttcccctctt	attcagatcgatcacatgc	atctttcattgctcgttttt	ccttacaa**g**tagtctcattac
Opus	AG**T**tatacatatatgtttat	aattctttgtttcccctctt	attcagatcgatcacatgc	atctttcattgctcgttttt	ccttacaa**g**tagtctcattac
Amaroo	AG**T**tatacatatatgtttat	aattctttgtttcccctctt	attcagatcgatcacatgc	atctttcattgctcgttttt	ccttacaa**g**tagtctcattac
Langi	AG**T**tatacatatatgtttat	aattctttgtttcccctctt	attcagatcgatcacatgc	atctttcattgctcgttttt	ccttacaa**g**tagtctcattac

Figure 4.5: DNA sequence of part of exon 1 and part of intron 1 of the *Wx* gene.

the secondary structure of the DNA maybe altered by the SNP preventing transcription, a mechanism proposed for the SNP at +1 [7,18]. Further in cooler temperatures, the secondary structure may be suitable for the binding of the transcription factor. It is the possibility that the SNP at +85 creates an alternate transcription start site is a mechanism that can be easily explored without experiment using bio-software programs.

According to the GT/AG intron rule [32], for the nine varieties carrying the polymorphism, the caagta sequence could be utilised as either a donor splice site (caa↓gta) or an acceptor splice site (ca↓agta) (Figure 4.6). It is already known that aa↓gt is one of the splice donor sites utilised in intron 1 of the *Wx* gene [19]. If the SNP at +85 is recognised as a donor site, the first 85 base pairs of intron 1 would be included in the transcript to produce mRNA of 2.4 kB. If recognised as an acceptor site, then only 85 base pairs would be removed during transcription leaving the remaining 1039 base pairs of leader intron 1 within the mRNA to yield the 3.3 kB mRNA.

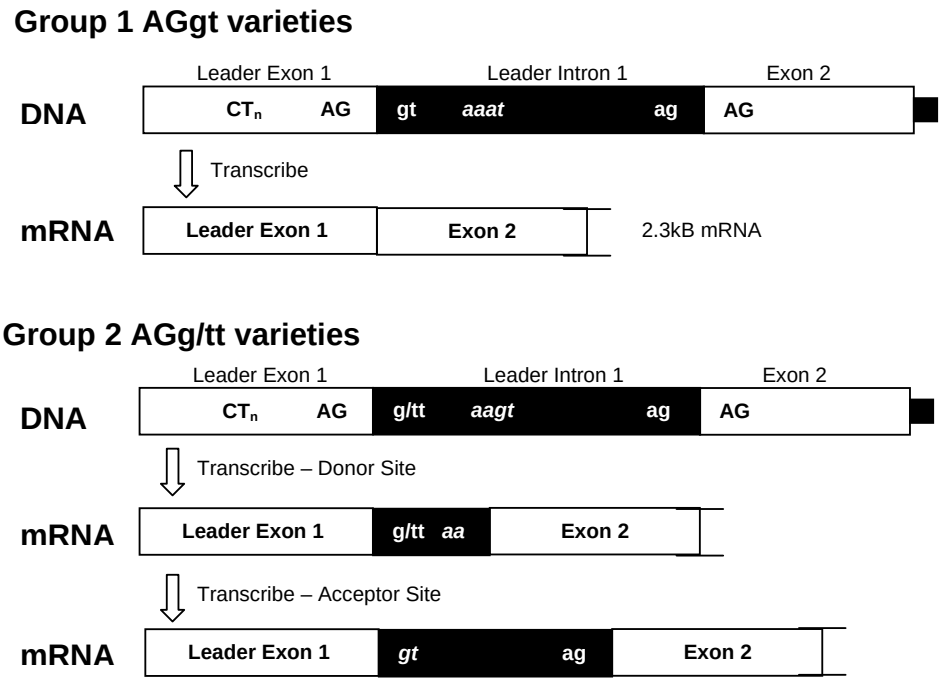

Figure 4.6. Diagram of the possible splice site mechanisms of the *Wx* gene.

In theory it is plausible for Group 2 AGgt varieties to process a GBSS transcript of 3.3 kB if the SNP at +85 acts as a splice acceptor site, yet no study has ever noted GBSS transcript of 3.3 kB for AGgt varieties. In one particular study, three AGgt varieties were examined for the effects of high temperature on the processing of GBSSI transcripts [15]. Of these varieties, the amylose content of Lemont fell about 3% in the high temperature treatment of 32 °C - 4 °C below the maximum temperature used in this work. Examination of the sequence of GBSS1 of Lemont (www.ncbi.nlm.nih.gov) shows that Lemont belongs to Group 2 AGgt. When Lemont was grown at low and high temperatures during grain filling, the mRNA was 2.3 kB at each of the three temperatures, and no other transcripts of GBSS were evident [15]. In another study [16], it can be seen that Labelle carries a G at both +1 and +85, and again only transcripts of 2.3 kB are processed. Extrapolating from these data, the SNP at +85 is unlikely to act as a splice acceptor site. In addition, the high temperature work showed that the amount of mRNA did not decrease at high temperatures for Lemont [15], which is not consistent with the amount of GBSS1 protein detected in Group 2 AGgt varieties in high temperature in this work (Figure 4.4). The other possibility is that the SNP acts as a splice donor site (Figure 4.6). In this case, it would only retain 85 bases of intron 1 and a band at 2.3 kB would contain a mixture of correctly and incorrectly spliced GBSS transcript. Thus, in Group 2 AGgt varieties, we propose that splicing occurs at both the authentic splice site and at the site created by the SNP at +85, resulting in transcript of 2.3 kB that contains a mixture of correctly and incorrectly spliced transcript, and at higher temperatures, the proportion of incorrectly spliced transcript increases, consistent with the decrease in both the expression of GBSS1 protein (Figure 4.4) and accumulation of amylose (Table 4.4).

The inclusion of the extra 85 bases in the incorrectly spliced GBSS transcripts in Group 2 AGgt varieties adds two translation start sites (TSS) upstream of the authentic TSS, one at +10 and one at +53. If translation begins at +10, the authentic TSS is not in frame, and the 140th codon is a stop codon, UGA (Figure 4.7a). If translation begins at +53 (Figure 4.7b), the authentic TSS is in frame, but the 20th codon is a stop codon, which is 3 codons upstream of the authentic TSS. Therefore it is unlikely that incorrectly spliced transcript, arising from splicing at the SNP at +85, is translated. Therefore, within the normal range of temperatures in a variable season, the proportion of correctly processed of GBSS transcript would vary, and this would explain why all Group 2 AGgt varieties are of intermediate amylose. If high temperatures increase the proportion of incorrectly spliced GBSS transcript, this would explain why the amount of mRNA at 2.4 kB does not change in the work of Larkin and Park, and since the incorrectly spliced transcript cannot be translated, this explains the significant decrease in expression of GBSS protein in the Group 2 AGgt varieties at high temperature.

a

```
1     AUG UUU AUA AUU CUU UGU UUC CCC UCU UAU UCA GAU CGA UCA CAU   45
1      M   F   I   I   L   C   F   P   S   Y   S   D   R   S   H    15

46    GCA UCU UUC AUU GCU CGU UUU UCC UUA CAA UGC AGA GAU CUU CCA   90
16     A   S   F   I   A   R   F   S   L   Q   C   R   D   L   P    30

91    CAG CAA CAG CUA GAC AAC CAC Cau guc ggc ucu cac cac guc cca   135
31     Q   Q   Q   L   D   N   H   H   V   G   S   H   H   V   P    45

136   gcu cgc cac cuc ggc cac cgg cuu cgg cau cgc cga cag guc ggc   180
46     A   R   H   L   G   H   R   L   R   H   R   R   Q   V   G    60

181   gcc guc guc gcu gcu ccg cca cgg guu cca ggg ccu caa gcc ccg   225
61     A   V   V   A   A   P   P   R   V   P   G   P   Q   A   P    75

226   cag ccc cgc cgg cgg cga cgc gac guc gcu cag cgu gac gac cag   270
76     Q   P   R   R   R   R   R   D   V   A   Q   R   D   D   Q    90

271   cgc gcg cgc gac gcc caa gca gca gcg guc ggu gca gcg ugg cag   315
91     R   A   R   D   A   Q   A   A   A   V   G   A   A   W   Q   105

316   ccg gag guu ccc cuc cgu cgu cgu gua cgc cac cgg cgc cgg cau   360
106    P   E   V   P   L   R   R   R   V   R   H   R   R   R   H   120

361   gaa cgu cgu guu cgu cgg cgc cga gau ggc ccc cug gag caa gac   405
121    E   R   R   V   R   R   R   R   D   G   P   L   E   Q   D   135

406   cgg cgg ccu cgg uga
136    R   R   P   R   *
```

b

```
1     AUG CAU CUU UCA UUG CUC GUU UUU CCU UAC AAU GCA GAG AUC UUC   45
1      M   H   L   S   L   L   V   F   P   Y   N   A   E   I   F    15

46    CAC AGC AAC AGC UAG ACA ACC ACC aug
16     H   S   N   S   *   T   T   T   M
```

Figure 4.7. Amino acid sequences after translation of the 3.37 kDa mRNA which includes 85 base pairs of intron 1. Translation could begin at the first Transition Start Site at +10 (a), or from the second Transition Start Site at +53 (b). Capitals here are the introns, and the exons are in small letters, and the stop codon is in bold.

Before genotyping became accessible, two alleles of the *Wx* gene were described based on the amount of GBSS1 protein expressed [7]. The Wx^a allele was defined as expressing the same amount of GBSS1 protein across all temperatures, and the Wx^b allele as expressing less protein at higher temperatures [7]. As genotyping technology became available, the Wx^a allele was associated with a G at the splice site of intron 1, and the Wx^b allele associated with the T [17]. In this study, a third genotype defined by a second SNP in intron 1 challenges those associations. The Group 1

AGgt varieties exhibit all the qualities of the Wx^a allele defined by Sano [7], and the Group 2 AGgt and the AGtt varieties are consistent with the definition of the Wx^b allele [7]. Thus to acknowledge the common traits of Wx^a and Wx^b alleles in Group 2 AGgt varieties carrying the 'g' at +85, we propose a third allele with the nomenclature Wx^{ab}, whereby the *a* symbolises the G at +1 and the *b* symbolises the g at +85. Classification of the *Wx* alleles in this way defines amylose content of only the Wx^a varieties as tolerant to high temperature.

Selection of amylose alleles in a breeding program [23] or in a pedigree analysis [22] has focused more on using the CTn in exon 1 rather than the G/T polymorphism. The CTn has been adapted for cost-efficient, high-throughput analysis [23]. While this polymorphism is useful for screening progeny of a known cross, its utility even for that is limited. CT_{17} and CT_{19} occur in both the Wx^a and Wx^b alleles [22,33]. Thus, as our capacity develops to detect differences at the molecular level, and to ascribe functionality to those differences, our ability to develop varieties with expected and predictable amylose content will improve. The SNP at +85 described here, may provide a mechanism to select within the Wx^a varieties for temperature tolerant amylose content. Therefore in an increasingly warmer and unstable climate, coupling knowledge of the three *Wx* alleles with improvements in predictive weather and climate tools, will give rice breeders a powerful tool to choose varieties suitable both to their growing conditions and to market requirements.

The discussion so far has focused on the impact of high temperatures during the grain filling phase has on the accepted synthesis pathway for amylose using malto-oligosaccharides (MOS) as a primer [34]. An alternate pathway proposed is that amylose is the product of an extended, and subsequently cleaved amylopectin chain that is used a a primer for extension by GBSS1 [35]. In the MWDs of Group 2 AGgt, AGtt varieties and in IR64 there is a peak at 1000 DP in the two hotter temperature treatments. The data is of the MWD of debranched HWSF so it is impossible to know if the chains originate from soluble amylopectin (which is made more soluble by a long chain), or simply a small amylose that is the product of GBSS1 using MOS as a primer. If the chains do originate from amylopectin, there is evidence for the precursor of amylose to be a cleaved extension of amylopectin. In high temperatures in the Group 2 AGgt and AGtt varieties, the long amylopectin chain is either not extended by the low amount of GBSS1, or the mechanism to cleave the long chain from amylopectin is hampered. The peak at 1000 DP for IR64 grown at 36/17 °C together with a high expression of GBSS1 suggests that the cleavage mechanism is a probable cause for the amylose not being extended.

4.4 CONCLUSIONS

As global air temperatures continue to climb steadily, it is important that, alongside with maintaining yield, grain quality is maintained. Focusing on amylose, and following the pathway from function to structure to synthesis, non-waxy varieties can be categorised into three groups on the basis of the phenotypic response to growth temperature in the reproductive stage. Two of these groups are temperature sensitive and one is temperature tolerant. These phenotypic responses are supported by a polymorphism located in leader intron 1, 85 base pairs downstream from the authentic leader exon 1 – leader intron 1 splice site. In temperature sensitive varieties, this a → g polymorphism probably offers an alternate splice site, and while the mechanism is not understood, it is thought that in temperature sensitive varieties this splice site is accidentally utilised at high temperatures to yield untranslatable mRNA that includes 85 base pairs of leader intron 1. The subsequent low amylose of grains from high growth temperatures yields poorer quality grains with lower uncharacteristic viscosity parameters, lower amylose content and an odd amylose structure. Screening varieties based on this a → g polymorphism will allow a predictive tool to appreciate the performance of non-waxy varieties under high temperatures. Coupling this knowledge with improved technologies for predicting weather enables rice growers the opportunity to control the quality of rice, and thus market price of rice coming from their land.

4.5 REFEREENCES

1. Peng, S., Huang, J., Sheehy, J. E., Laza, R. C., Visperas, R. M., Zhong, X., Centeno, G. S., Khush, G. S. & Cassman, K. G. Rice yields decline with higher night temperature from global warming. *PNAS* **101**, 9971 - 9975 (2004).
2. Karl, T. R., Kukla, G., Razuvayev, V. N., Changery, M. J., Quayle, R. G., Heim, R. R. & Easterling, D. R. Global warming: Evidence for asymmetric diurnal temperature change. *Geophys. Res. Lett.* **18**, 2253 - 2256 (1991).
3. Asaoka, M., Okuno, K., Sugimoto, Y., Kawakami, J. & Fuwa, H. Effect of environmental temperature during development of rice plants on some properties of endosperm starch. *Starch/Starke* **36**, 189 - 193 (1984).
4. Asaoka, M., Okuno, K. & Fuwa, H. Effect of environmental temperature at the milky stage on amylose content and fine structure of amylopectin of waxy and nonwaxy endosperm starches of rice (*Oryza sativa L.*). *Agric. Biol. Chem.* **49**, 373 - 379 (1985).
5. Umemoto, T., Nakamura, Y. & Ishikura, N. Activity of Starch Synthase and the Amylose Content in Rice Endosperm. *Phytochemistry* **40**, 1613 - 1616 (1995).
6. Lisle, A., Martin, M. & Fitzgerald, M. A. Chalky and translucent rice grains differ in starch composition and structure and cooking properties. *Cereal Chemistry* **77**, 627 - 632 (2000).
7. Sano, Y. Differential regulation of waxy gene expression in rice endosperm. *Theor. Appl. Genet.* **68**, 467-473 (1984).
8. Echt, C. S. & Schwartz, D. Evidence for the inclusion of controlling elements within the structural gene at the waxy locus in maize. *Genetics* **99**, 275 - 284 (1981).
9. Ward, R. M., Gao, Q., de Bruyn, H., Gilbert, R. G. & Fitzgerald, M. A. Improved methods for the structural analysis of the amylose-rich fraction from rice flour. *Biomacromolecules* **7**, 866 - 876 (2006).
10. Juliano, B. O. Amylose analysis in rice - a review. *Proceedings of the workshop on Chemical Aspects of Rice Grain Quality. Review of Methodolgy*, 251 - 260 (1979).
11. Juliano, B. O., Cagampang, G. B., Lourdes, J. C. & Santiago, R. G. Some Physicochemical properties of rice in southeast Asia. *Cereal Chemistry* **41**, 275 - 286 (1964).
12. de la Cruz, N., Kumar, I., Kaushik, R. P. & Khush, G. S. Effect of temperature during grain development on stability of cooking quality components in rice. *Japan J. Breed.* **39**, 299 - 306 (1989).
13. Zhong, L.-j., Cheng, F.-m., Wen, X., Sun, Z. X. & Zhang, G. P. The deterioration of eating and cooking quality caused by high temperature during grain filling in early-season *indica* rice cultivars. *Journal of Agronomy and Crop Science* **191**, 218 - 225 (2005).
14. Sano, Y., Maekawa, M. & Kicuchi, H. Temperature effects on the *Wx* protein level and amylose content in the endosperm of rice. *J. Hered.* **6**, 221 -222 (1985).
15. Larkin, P. D. & Park, W. D. Transcript accumulation and utilisation of alternate and non-concensus splice sites in rice granule-bound synthase are temperature-sensitive and controlled by a single-nucleotide polymorphism. *Plant Molecular Biology* **40**, 719-727 (1999).

16. Isshiki, M., Morino, K., Nakajima, M., Okagaki, R. J., Wessler, S. R., Izawa, T. & Shimamoto, K. A naturally occurring functional allele of the rice waxy locus has a GT to TT mutation at the 5` splice site of the first intron. *The Plant Journal* **15**, 133 - 138 (1998).
17. Hirano, H.-Y., Eiguchi, M. & Sano, Y. A single base change altered the regulation of the *Waxy* gene at the posttranscriptional level during the domestication of rice. *Molecular Biology and Evolution* **15**, 978 - 987 (1998).
18. Wang, Z.-Y., Zheng, F.-Q., Shen, G.-Z., Gao, J.-P., Snustad, D.-P., Li, M.-G., Zhang, J.-L. & Hong, M.-M. The amylose content in rice endosperm is related to the post-transcriptional regulation of the *waxy* gene. *Plant Journal* **7**, 613 - 622 (1995).
19. Cai, X.-L., Wang, Z.-Y., Xing, Y.-Y., Zhang, J.-L. & Hong, M.-M. Aberrant splicing of intron 1 leads to the heterogeneous 5` UTR and decreased expression of *waxy* gene in rice cultivars of intermediate amylose content. *The Plant Journal* **14**, 459-465 (1998).
20. Mikami, I., Aikawa, M., Hirano, H.-Y. & Sano, Y. Altered tissue-specific expression at the Wx gene of the opaque mutants in rice. *Euphytica* **105**, 91 - 97 (1999).
21. Bligh, H. F. J., Till, R. I. & Jones, C. A. A microsatellite sequence closely linked to the *waxy* gene of *Oryza sativa*. *Euphytica* **86**, 83-85 (1995).
22. Ayres, N. M., McClung, A. M., Larkin, P. D., Bligh, H. F. J., Jones, C. A. & Park, W. D. Microsatellites and a single-nucleotide polymorphism differentiate apparent amylose classes in an extended pedigree of US rice germ plasm. *Theoretical and Applied Genetics* **94**, 773 - 781 (1997).
23. Bergman, C. J., Delgado, J. T., McClung, A. M. & Fjellstrom, R. G. An improved method for using a microsatellite in the rice waxy gene to determine amylose class. *Cereal Chemistry* **78**, 257-260 (2001).
24. Castro, J. V., Ward, R. M., Gilbert, R. G. & Fitzgerald, M. A. Measurement of the molecular weight distribution of debranched starch. *Biomacromolecules* **6**, 2260 - 2270 (2005).
25. Hall, T. A. BioEdit: a user-friendly biological sequence alignment editor and analysis program for Windows 95/98/NT. *Nucl. Acids. Symp. Ser.* **41**, 95 - 98 (1999).
26. Lu, H., Redus, M. A., Coburn, J. R., Rutger, J. N., McCouch, S. R. & Tai, T. H. Population structure and breeding patterns of 145 U.S. rice cultivars based on SSR marker analysis. *Crop Science* **45**, 66-76 (2005).
27. Fitzgerald, M. A., Martin, M., Ward, R. M., Park, W. D. & Shead, H. J. Viscosity of rice flour: A rheological and biological study. *Journal of Agricultural and Food Chemistry* **51**, 2295-2299 (2003).
28. Bhattacharya, K. R. & Sowbhagya, C. M. Pasting behaviour of rice: A new method of viscography. *Journal of Food Science* **44**, 797 - 804 (1979).
29. Gidley, M. J. Molecular mechanisms underlying amylose aggregation and gelation. *Macromolecules* **22**, 351 - 358 (1989).
30. Philpot, K., Martin, M., Burtado Jr., V., Willoughby, D. & Fitzgerald, M. A. Environmental factors that affect the ability of amylose to contribute to retrogradation in gels made from rice flour. *J. Agric. Food Chem.* **54**, 5182-5190 (2006).
31. McCouch, S. R., Sweeney, M., Li, J., Jiang, H., Thomson, M., Septiningsih, E., Edwards, J., Moncada, P., Xiao, J., Garris, A., Tai, T., Martinez, C., Tohme, J., Sugiono, M., McClung, A. M., Yuan, L. P. & Ahn, S.-N. Through the genetic bottleneck: *O. rufipogon* as a source of trait-enhancing alleles for *O. sativa*. *Euphytica* **154**, 317-339 (2006).

32. Mount, S. M. A catalogue of splice junction sequences. *Nucleic Acids Res.* **10**, 459 - 472 (1982).
33. Prathepha, P. & Baimai, V. Variation of *Wx* microsatellite allele, waxy allele distribution and differentiation of chloroplast DNA in a collection of Thai rice (*Oryza sativa* L.). *Euphytica* **140**, 231-237 (2004).
34. Denyer, K., Clarke, C. J., Hylton, C. M., Tatge, H. & Smith, A. M. The elongation of amylose and amylopectin chains in isolated starch granules. *Plant Journal* **10**, 1135-1143 (1996).
35. Ball, S. G., van de Wal, M. & Visser, R. Progress in understanding the biosynthesis of amylose. *Trends in Plant Science* 3, 462 - 467 (1998).

Chapter 5

Impact of carbon dioxide and temperature on grain quality

5.1 INTRODUCTION

The quality of rice defines its market price primarily because quality is so easily recognized by the consumer. Physical qualities, such as grain shape and the chalky appearance (white spots) of milled rice are easy to identify in the market place, and these are the parameters used to grade, and thus value, rice. Physical properties are simple to measure and are part of every rice breeding program. Cooking qualities of the rice are also important to the consumer since they often determine the nature of the meal and suitability for processing. Cooking qualities are much harder to define and depend entirely upon the structure of the components of the rice grain at the multiple levels of organization found within the cereal endosperm. Significant variability in the metrics of the traits of quality can be found in the rice germplasm. However, while genotype defines the capacity of the plant to express particular metrics of the traits of quality, the environmental effect on genetic expression changes the metrics of many of these traits, by changing the amounts and/or structures of the components of the grain. For example, the *Waxy* gene is responsible for amylose synthesis [1] and one of its alleles [2] is sensitive to high temperatures [3]. Protein content affects cooking properties [4] and in elevated atm-CO_2, the physiology of N metabolism and remobilization is altered [5]. Lipids also affect cooking properties by complexing with amylose molecules [6], and environmental conditions affect the relationship between amylose and lipids [7]. Agriculture, particularly food production, is the most climate-sensitive of all economic sectors [8], and for much of the developing world, this means rice. As the world becomes warmer, and as stocks of greenhouse gases accumulate in the atmosphere, it is becoming urgent and essential to know how the drivers of climate change will affect rice grain quality, and to identify current and potential genetic options to protect the quality of rice.

Global air temperatures are increasing at 0.02 ˚C per year and carbon dioxide levels are increasing by 1.5 ppm each year; climate change has real potential to impact on the world's rice industries [8]. Elevated atm-CO_2 decreases the amount and activity of rubisco (ribulose-1,5-biphosphate carboxylase) [9,10], which suppresses photorespiratory loss of carbon and thus enhances net photosynthesis [11]. During development this increased amount of carbohydrate (which occurs up to a limit of 500 ppm atm-CO_2 [12]) is directed towards the tiller after the third leaf instead of the usual case, which is after the emergence of the fifth or sixth leaf, resulting in more tillers and fewer, but larger, leaves [13 14]. A increasing trend exists between leaf area and the number of juvenile spikelets [15], presenting one mechanism whereby elevated CO_2 could increase yield potential [14]. In elevated atm-CO_2, the temperature of the canopy increases slightly [16]. Slight increases in canopy temperature have been associated with a decrease in yield [17,18]. The rate of stomatal conductance of plants, for which genetic variability exists, is able to modulate the

temperature of the canopy sufficiently to affect the final number of fully formed, mature grains [17]. Price differentials of traded rice are defined by the physical quality of rice – fully formed mature grains and grains that are not chalky (white spots in endosperm). Fully formed, mature grains are unlikely to break during milling whereas chalky and immature grains are highly likely to break during milling [19]. Thus, exploring genetic variability for traits that increase yield is likely to increase physical quality, thus marketability, of rice. However, any yield advantage potentially gained from elevated atm-CO_2 could be counteracted by high night-time temperatures, since these are reported to decrease yield [18]. The relationship between night-time temperature and yield is reported for only one variety of rice; since genetic variability exists for other physiological yield determinants, it is not unreasonable to assume that it also exists for tolerance to increased night-time temperatures.

The effect on quality from the combination of elevated atm-CO_2 and temperature is both unknown, and, given the discussion above, it is difficult to predict. Many studies have explored the impact of temperature on grain quality [13,20-23]. Elevated atm-CO_2 alters plant physiology in ways that present intuitive options for ameliorating some of the negative effects of high temperature on quality. However, only a few studies have considered the effect of varying atm-CO_2 levels on rice quality [24-26], and none have considered the combined effect on rice quality when both temperature and atm-CO_2 levels are elevated.

Climate change will adversely affect the landscape, agricultural industries, and economies of developing countries [8]. This is significant because these countries (i) rely on rice for up to 79 % of the calorific needs of their populations [27], and (ii) must purchase rice on the international market to meet shortfalls between production and consumption. It is critical to focus on the effect of climate change on the most important commodity of developing countries, rice, and to identify options to ameliorate the effects of climate change on rice production. Recognizing that increases in temperature and atm-CO_2 are the two immediate threats of climate change to agriculture, and that quality drives the market price for rice, this study aims to provide the first comprehensive analysis of the impact of climate change on the quality of rice using the newest technologies and analytical techniques.

5.2 MATERIALS AND METHODS

5.2.1 Materials

Rice (*Oryza sativa* L.) sourced from the Department of Primary Industries of Yanco, was grown in growth chambers at the University of Western Sydney, Richmond during the 2003/04 season. Rice varieties chosen for this study are Amaroo (Australia and 19 % amylose), IR64 (IRRI Philippines and 24 % amylose), Taipei 309 (Taiwan and 17 % amylose) and Shimizu mochi (Japan and 0% amylose). Seeds were grown in 6 kg of soil sourced from Mt.Annan, with approximately 430 kg N ha^{-1} added per pot [28]. Plants were grown in one of two concentrations of carbon dioxide - ambient (380 ppm) and elevated (780 ppm) [28]. Five days after anthesis, plants within each atmospheric carbon dioxide (atm-CO_2) treatment were further divided into two temperature treatments with day/night temperatures of either 25/19 °C or 30/20 °C (Note: the growth chambers were only capable of cooling so the maximum temperature reached depended on solar radiation). In order to avoid any spatial and room effects, pots were circulated each week both within a growth chamber and between chambers that were programmed to the same conditions. Grains were harvested at maturity. At a paddy moisture content of 14%, the paddy of each was dehulled (THU35A 250V 50Hz Test Husker, Satake), milled (McGill No.2 Mill) and a sub-sample was ground (Cyclotec 1093 sample mill, Tecator) to pass through a 0.5 mm sieve.

Isoamylase (derived from *Pseudomonas* sp.) was obtained from Megazyme and used as supplied. Pullulan standards (Shodex) were used for calibration of Size Exclusion Chromatography (SEC), using universal calibration [29,30]. The fluorescence label for Capillary Electrophoresis (CE), 8-amino-1,3,6-pyrene trisulfonic acid (APTS) was obtained from Sigma. High purity water (MilliQ) was used for all SEC experiments. All chemicals used were reagent grade.

5.2.2 Methods

Most quality parameters were measured on grain from each of the seven pots in the trial, and reported as the average and standard error. For SEC and Capillary Electrophoresis, starches from two pots were analysed to ensure repeatability, but only one is reported.

5.2.2.1 Effect of Temperature and Carbon Dioxide on the Physical Properties of Rice

The length and width of the grain was measured by capturing the image of the grain with Image Analysis and then analysed by Sigmascan software. The proportion of grains with 0-10 % chalk, 10-25 %, and above 25 % (attract price penalty) were measured with a Cervitec 1625 Grain Inspector (FOSS) that was calibrated using artificial neural network technology.

5.2.2.2 Effect of Temperature and Carbon Dioxide on the Composition of Rice Grains

5.2.2.2.1 Protein

The protein content of the milled endosperm from each variety was commercially determined by the Dumas method (ASTM E191-64).

5.2.2.2.2 Amylose

The molecular weight distribution (MWD) of debranched amylose was determined as described previously [30]. SEC was performed on a Waters system consisting of an Alliance (2695) and Differential Refractive Index Detector (Waters 2410) with Waters software (Empower®) to control the pump, and to acquire and process data. The Ultrahydrogel 500 column used in this system was calibrated using pullulan standards, the Mark-Houwink-Saturada equation and universal calibration [29]. From the MWD of debranched amylose, the number- and weight-average degree of polymerization ($\bar{X}_n$ and $\bar{X}_w$, respectively) and polydispersity ($Q = \bar{X}_w / \bar{X}_n$) were calculated (see Chapter 2) [29,30].

Granule Bound Starch Synthase (GBSS1) protein was extracted from mature grain [31] and separated using SDS-polyacrylamide gel electrophoresis (SDS-PAGE). SDS-PAGE was carried out with a Hoeffer 10 x 8 cm Mighty Small, using a 10 % gel as described in the Operator Manual (Hoeffer Pharmacia Biotech Inc. 654 Minnesota Street, San Francisco, CA, 94107, USA). Gels were dried (Hoeffer Easy Breeze) after staining with Coomassie Blue R-250. GBSSI protein was identified by sequencing the excised band (Biomolecular Research Facility, Newcastle Protein, LS3-16, Life Sciences Building, University of Newcastle, University Drive, Callaghan NSW 2308, Australia).

Two functional alleles of GBSS1 are encoded by the *Waxy* locus [1] and are characterized by a single nucleotide polymorphism (SNP) at the splice site of intron 1 [2]. In order to classify the alleles for the varieties used here, DNA was extracted from unpolished grains using the cTAB method [32] and the SNP was detected on an agarose gel (1.2 %), following the polymerase chain reaction (PCR) and *Acc*I digestion of PCR products, exactly as described by Han (2004)[33].

5.2.2.2.3 Amylopectin

The number distribution of amylopectin chains was obtained by debranching amylopectin with isoamylase [34], and tagging the reducing end of each chain with APTS [35]. The tagged amylopectin chains were analysed by Capillary Electrophoresis (CE, Beckman Coulter P/ACE™ MDQ Capillary Electrophoresis System), controlled with 32 Karat Software.

5.2.2.3 Effect of Temperature and Carbon Dioxide on the Cooking Properties of Rice

Viscosity curves were determined using the AACC Method 61-02 using the Rapid Visco Analyzer (RVA, Newport). Three metrics of the viscosity curve were recorded: peak, trough and final viscosity.

For the measurement of gelatinization temperature, a mixture of flour and water, at a ratio of 1:2, was heated under pressure from 25-120˚C at increments of 10 ˚C min^{-1} using a Differential Scanning Calorimeter (DSC, Mettler Toledo $DSC822_e$). Gelatinisation temperature was determined as the peak of the endotherm.

Rheological properties such as shear storage modulus (G′) and temperature of the G'_{max} were determined by rheometry (Advanced Rheometer 2000, TA Instruments) using a mixture of flour and water at a ratio of 1:2, with a 1 Hz frequency and a heating rate of 10 ˚C min^{-1}, which is equivalent to the heating rate of the RVA and DSC.

Hardness of gels was measured on retrograded gels [7]. Briefly, gels were prepared using the RVA with the standard heating and holding conditions for rice flour (AACC 61-02), and then covered and stored overnight at 4 °C. The following morning gels were warmed to room temperature and the force required to puncture the gel was measured. The probe was a round-ended, tempered plastic cylinder (17 mm diameter) attached to a 5 N load cell, fitted to a Lloyd Tensile Tester. The probe travelled at 100 mm min^{-1} to a distance of 65 mm (30 mm of gel). Nexygen software (Version 7.61) was used to control the probe and the load cell, and to collect the data.

5.3 RESULTS AND DISCUSSION

5.3.1 Effect of Temperature and Carbon Dioxide on the Physical Properties of Rice

The traits of grain length and width, weight and the chalky appearance of grains are the properties that define preliminary consumer appeal for rice in both domestic and international markets. The dimensions of the rice grains grown in the four environments are shown in Table 5.1. The four varieties used in this study differ in their length and width. Quantitative Trait Loci that affect grain dimensions and weight in rice have been mapped on seven chromosomes [36] suggesting that allelic variability at multiple loci defines grain dimensions, and explaining the enormous variability that exists for the dimensions and weight of rice grains found in domesticated germplasm. Table 5.1 shows clearly that in an environment where either temperature or atm-CO_2 are individually elevated, and in an environment where both are elevated, neither the dimensions of the grain, nor the weight of the grain was affected. This suggests either that none of the alleles in the seed-size pathway in these varieties are sensitive to elevated temperature or atm-CO_2, or that these four networks of alleles can compensate if one or more of the elements of the pathway is affected. The weight and shape of grains is the first quality trait that breeders select for in rice improvement programs, so identifying networks of alleles for these traits that are resistant to the drivers of climate change will assist rice breeding programs to maintain their objectives to satisfy consumer demands for grain size and shape.

Table 5.1. The physical properties of paddy and whole grain rice. Values are the means and standard error (*n*=7).

Parameter	Temperature	25/19°C	25/19°C	30/20°C	30/20°C
	Carbon Dioxide	380ppm	780ppm	380ppm	780ppm
Paddy Weight (mg)	Amaroo	24.6 ± 0.9	23.7 ± 0.5	23.3 ± 0.9	23.5 ± 1.4
	IR64	22.6 ± 1.1	23.8 ± 0.9	23.2 ± 1.7	24.0 ± 0.8
	Taipei 309	23.9 ± 0.8	24.0 ± 0.5	24.5 ± 0.4	24.6 ± 0.6
Brown Grain Weight (mg)	Amaroo	22.4	21.7	20.0	20.2
	IR64	19.8	20.3	20.6	21.2
	Shimizu Mochi	20.9	21.3	20.7	20.2
	Taipei 309	22.3	22.1	24.0	22.6
Length (mm)	Amaroo	5.53 ± 0.34	5.43 ± 0.33	5.37 ± 0.36	5.35 ± 0.38
	IR64	6.39 ± 0.59	6.51 ± 0.62	6.41 ± 0.53	6.50 ± 0.53
	Shimizu Mochi	4.74 ± 0.16	4.71 ± 0.17	4.70 ± 0.18	4.68 ± 0.17
	Taipei 309	4.88 ± 0.27	4.80 ± 0.31	4.78 ± 0.30	4.80 ± 0.27
Width (mm)	Amaroo	2.75 ± 0.16	2.71 ± 0.16	2.75 ± 0.17	2.68 ± 0.18
	IR64	2.14 ± 0.17	2.18 ± 0.26	2.21 ± 0.21	2.20 ± 0.16
	Shimizu Mochi	2.66 ± 0.15	2.69 ± 0.16	2.69 ± 0.16	2.67 ± 0.16
	Taipei 309	2.91 ± 0.16	2.87 ± 0.21	2.95 ± 0.21	2.89 ± 0.21

Chalk is the opaque or white belly of the rice grain whereby a grain is typically defined as chalky if more than 25 % of its belly is opaque [19]. Chalk is an undesirable aesthetic property that affects the price that rice fetches in international and domestic marketplaces. The grades of the international rice market are defined by increments of chalky and broken grain. The difference between samples of 2 % and 6 % chalk is US$15–25/ton. In domestic markets in the Philippines, China and Vietnam, it is our observation that farmers face a 25% decrease in price for chalky grain, and in Thailand grain samples that exceed 10% chalk are outside the specifications for any export grade. In Table 5.2, the weight-average percent of chalk is presented, together with the distribution of the proportion of grains containing less than 10 % chalk, 10-25 % chalk and greater than 25 % chalk. Chalkiness of a grain is known to increase with high temperature [21,37] and Table 2 shows that this is the case, especially for IR64. Even though it is challenging to estimate the economic impacts of climate change [8], chalk is one of two parameters that define market grade, so as the climate changes, and incidences of temperature volatility punctuate grain-filling more regularly, chalk represents a certain and significant economic risk for countries that trade in rice.

Table 5.2. The weight average chalk percent of rice grains, and the percent of grains that have < 10 % chalk per grain, 10-25 % chalk per grain, and more than 25% chalk per grain. Values are the means and standard error (*n*=7).

Variety	Temperature	25/19°C	25/19°C	30/20°C	30/20°C
	Carbon Dioxide	380ppm	780ppm	380ppm	780ppm
Amaroo	Total Chalk	15 ± 5	12 ± 3	13 ± 5	13 ± 2
	< 10% Chalk	59 ± 6	59 ± 6	56 ± 8	45 ± 4
	10-25% Chalk	27 ± 3	34 ± 4	38 ± 6	49 ± 2
	> 25% Chalk	13 ± 3	7 ± 2	7 ± 3	6 ± 2
IR64	Total Chalk	8 ± 1	8 ± 2	13 ± 4	11 ± 1
	< 10% Chalk	78 ± 3	77 ± 4	51 ± 5	66 ± 3
	10-25% Chalk	21 ± 3	23 ± 4	45 ± 4	33 ± 3
	> 25% Chalk	1 ± 0	0 ± 0	4 ± 2	1 ± 0
Shimizu Mochi	Total Chalk	73 ± 2	74 ± 5	74 ± 2	76 ± 2
	< 10% Chalk	0 ± 0	0 ± 0	0 ± 0	1 ± 1
	10-25% Chalk	0 ± 0	0 ± 0	0 ± 0	0 ± 0
	> 25% Chalk	100 ± 0	100 ± 0	100 ± 0	99 ± 1
Taipei 309	Total Chalk	8 ± 2	8 ± 1	10 ± 1	9 ± 1
	< 10% Chalk	80 ± 4	83 ± 2	75 ± 2	76 ± 3
	10-25% Chalk	18 ± 3	15 ± 3	19 ± 2	20 ± 3
	> 25% Chalk	2 ± 1	2 ± 1	6 ± 2	4 ± 1

Total chalk (and the distribution of chalk) did not change significantly for the two temperature treatments for Amaroo and Taipei 309, perhaps because these varieties are adapted to the warmer and drier environments of the temperate rice-growing regions of Australia and Taiwan. However, when *temperate japonica* rice varieties experience temperatures of about 35 °C regularly through grain-filling, grains show a significant increase in chalk [21]. The genetic cause of chalk has never been identified but the phenotype of chalk is smaller starch granules [21] that are poorly packed [37]. Thus, the genetic cause of chalk can probably be safely mapped to the network of regulatory and synthetic genes that leads to mature starch granules. The data presented here, together with the data reported by Lisle et al. (2000), suggest that the network of alleles driving the pathway to starch granules in *temperate japonica* germplasm can withstand higher temperatures than the network driving the same pathway in tropical germplasm. Active selection for adaptation of rice germplasm to a hot dry climate presumably involves capturing networks of alleles, including those that regulate stomatal conductance, that lead to panicles of fully matured, translucent grains. Thus, the *temperate japonica* germplasm adapted to regions like Australia could represent

a source of temperature-tolerant alleles for protecting tropical germplasm – which accounts for most of the world's rice [38] - against the effects of global warming on chalk.

The degree of chalkiness in response to atmospheric carbon dioxide levels, either alone or in combination with growth temperature, has not been previously explored. As shown in Table 5.2, in comparison with the ambient atm-CO_2 treatment, plants grown in elevated atm-CO_2 have more grains with <10 % chalk and 10–25 % chalk, and less with chalk above 25 % - a trend independent of temperature and a trend that increases the proportion of marketable grains. Due to the more intense temperature stress experienced by IR64 (as suggested above), the effect of carbon dioxide on the chalk distribution in IR64 is even more pronounced (Table 5.2). In elevated atm-CO_2 the plant fixes more carbon [5,39] and in higher temperatures, the duration of grain-filling is shorter [40]. Perhaps when both temperature and atm-CO_2 are elevated, and the amount of chalk is marginally improved (Table 5.2), the supply of carbon to the grain increases slightly in coordination with the faster maturation associated with increased temperatures. Overall, a reduction in chalk at elevated atm-CO_2 will increase the yield of marketable rice for both whole grain consumption and industrially suitable grain. Thus, increasing concentrations of CO_2 could ameliorate, to some degree, the effect of global warming on the degree of chalk for rice farmers and traders, especially those dealing in tropical germplasm.

5.3.2 Effect of Temperature and Carbon Dioxide on the Composition and Cooking Properties of Rice

Considerable resources have been invested in discovering the impact of temperatures during the grain-filling stage on the traits of grain quality. Very little research has focused on the effects of carbon dioxide levels on grain quality and even less on the combined effects of temperature and carbon dioxide. The query here is to determine whether the increase in atmospheric carbon dioxide levels can counteract the negative effects on grain quality that occur as a direct result of increased temperatures.

5.3.2.1 Protein

The amount and timing of nitrogen accumulation from the soil into the rice plant are critical for the determination of tiller number in the rice plant [5]. In a low nitrogen soil (40 kg N ha^{-2}) there is no difference in the accumulation of N between different CO_2 treatments. The only effect of atm-CO_2 on nitrogen accumulation in the plant is when there is sufficient N in the soil to meet the larger N requirement of a greater number of tillers per unit area [5]. With a N application of 120 kg N ha^{-1} in elevated atm-CO_2, the rate of nitrogen uptake before panicle initiation (PI) is faster, which increases the number of tillers [5,13]. However, after anthesis, there was no difference in the rate of N uptake between CO_2 treatments, suggesting that the plants in elevated CO_2 had depleted

the supply of available N in the soil, and were experiencing a level of N deficiency [5]. Thus, if N nutrition is not adjusted to meet the larger need of a larger plant, during grain filling, plants grown in elevated atm-CO_2 are forced to remobilise endogenous sources of N acquired before PI, leading to earlier senescence, rather than delivering to grains the N acquired directly from the soil [5]. In other studies where plants were grown in elevated atm-CO_2, the net effect is an overall reduction in N per grain [25,26].Therefore, to ensure that N uptake by the plant is not limited by availability of N in the soil, a nutrient mix equivalent to 430 kg N ha^{-1} [24] was applied to the plants grown for this study. Taking into account the rate of N application also ensures that any change in the suite or content of protein in the grain is a reflection of the controlled temperature and atm-CO_2 treatments imposed on the plants rather than nutrient availability [4,41,42]. For each variety, the protein content (%) of the milled grains from all four treatments was not significantly different (Table 5.3), indicating that, for the plants used in this study, the source-sink dynamics for N operating during grain-filling were not affected by the availability of N in the soil. The data in Table 1 also indicate that protein content of grains is not likely be altered by climate change, at least when N nutrition adjusted. However, to take advantage of the benefits of climate change of increased yield and nutrient uptake, the increased requirement for N fertilization will increase the cost of rice production which will inevitably pass onto consumers and thus add to the cost of climate change [8].

The protein content of a rice endosperm affects functional properties such as viscosity [4] and milling quality [43,44]. Protein content specifically affects the viscosity parameter of setback as defined by the difference between peak and final viscosity [45]. In increased temperature, setback is reported to decrease [21]. In elevated atm-CO_2, setback is reported to increase for the variety Jarrah [24], which was grown with high nitrogen (430 kg N ha^{-1}), but setback decreased for the variety Akitakomachi [26]. For all the varieties used in this study, setback was not affected by atm-CO_2 (Table 5.4). The changes in setback reported by Seneweera et al. (1996) and Terao et al. (2005) were due to changes in the peak viscosity rather than the final viscosity, and changes in peak viscosity are generally due to changes in protein content [4]. Figure 5.1 presents data from a number of studies [24,26,46] and shows a negative correlation between peak viscosity and protein content of the endosperm. Further, Figure 5.1 shows that [CO_2] has no effect on the relationship between N content and peak viscosity. Nitrogen nutrition increases the proportion of insoluble proteins [42] which changes the hydration kinetics and swelling of gelatinized flour, which changes the peak viscosity [4]. In this study, and in the study reported by Seneweera et al (1996), high N nutrition led to high peak viscosities, thus the effect seen here and in Seneweera's work is a response to high N nutrition. So, rather than differences in peak viscosity being attributed to variety [26], it is more likely that the changes observed across the three studies are dominated by

the interaction between N availability and the nutritional requirements of plants that are physiologically altered by the drivers of climate change.

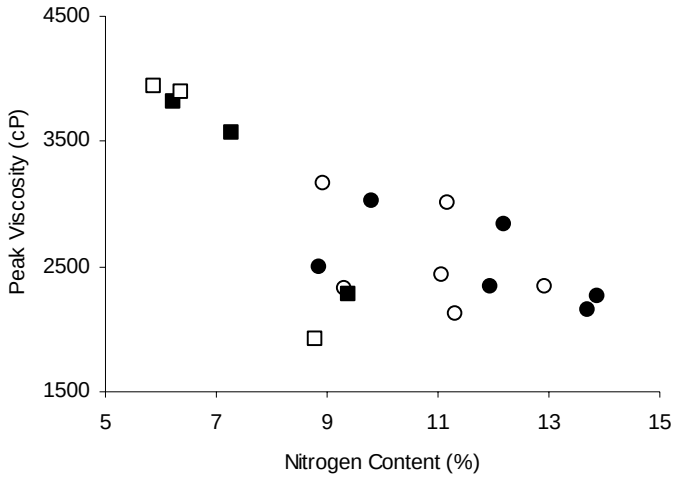

Figure 5.1. Relationship between protein content (%) and peak viscosity of milled rice grown in ambient (filled symbols) and elevated atm-CO_2 (empty symbols). The circle symbols are data from literature [24,26,46], and square symbol represents data from this study (r = -0.74).

Table 5.3. Chemical traits of varieties grown across the four growth treatments. Data is presented as mean and Standard Error of the Mean (n = 7).

Treatment	Temperature	25/19 °C	25/19 °C	30/20 °C	30/20 °C
	Carbon Dioxide	380 ppm	780 ppm	380 ppm	780 ppm
Parameter	Variety				
Amylose Content (%)	Amaroo	16.6 ± 0.3	17.1 ± 0.4	15.4 ± 0.3	14.0 ± 0.2
	IR64	24.7 ± 0.2	24.1 ± 0.6	21.3 ± 0.2	22.5 ± 0.2
	Taipei 309	16.1 ± 0.4	16.9 ± 0.2	16.7 ± 0.5	16.7 ± 0.3
Amylopectin Content (%)	Amaroo	71.5	71.8	72.4	74.8
	IR64	61.6	64.6	64.8	64.6
	Shimizu mochi	89.3	89.9	89.4	90.4
	Taipei 309	75.0	73.8	73.5	74.4
Protein Content (%)	Amaroo	11.9	11.1	12.2	11.2
	IR64	13.7	11.3	13.9	12.9
	Shimizu mochi	10.7	10.1	10.6	9.6
	Taipei 309	8.9	9.3	9.8	8.9
$\bar{X}_n$	Amaroo	730 ± 10	980 ± 40	510 ± 20	500 ± 0
	IR64	850 ± 30	950 ± 10	800 ± 10	790 ± 10
	Taipei 309	970 ± 10	970 ± 10	810 ± 10	800 ± 10
$\bar{X}_w$	Amaroo	6200 ± 0	7400 ± 100	4500 ± 40	4900 ± 50
	IR64	6200 ± 200	6400 ± 70	5200 ± 170	5300 ± 200
	Taipei 309	7200 ± 120	7000 ± 90	5200 ± 200	5800 ± 160
Q	Amaroo	8.5 ± 0.1	7.6 ± 0.2	8.9 ± 0.4	9.6 ± 0.1
	IR64	7.2 ± 0.0	6.7 ± 0.1	6.5 ± 0.2	6.8 ± 0.0
	Taipei 309	7.4 ± 0.2	7.2 ± 0.1	6.5 ± 0.1	7.2 ± 0.1

5.3.2.2 Amylose

Amylose molecules are involved in every cooking property of non-waxy rice, and their contribution to these properties is generally estimated from viscosity profiles [21,45,47], hardness of gels [7,48] and rheological measurements [49,50]. Expression of Granule Bound Starch Synthase 1 protein is required for the synthesis of amylose [31]. GBSS1 protein is the product of the *Waxy (Wx)* locus [1]. Amylose chains are the product of GBSS1 [1,31], and are much longer than the longest chain from an amylopectin molecule [30]. There is a direct relationship between the amount of GBSS1 protein expressed and the amount of amylose that accumulates in the endosperm [22,23,51].

The amount of GBSS1 protein expressed in non-waxy varieties grown in the four controlled environments is shown in Figure 5.2. Overall, IR64 expresses more GBSS1 than Amaroo and Taipei 309, consistent with its higher amylose content. A comparison of the two temperature treatments shows a decrease in the amount of GBSS1 protein expressed in the warmer temperature treatment (Figure 5.2) for all three non-waxy rice. Given that the amount of GBSS1 correlates directly with the amount of amylose that accumulates in grains [20,22,23,51], the decrease indicates that amylose content is lowered in all three non-waxy rice at high temperatures. Elevated atm-CO_2 does not alter the amount of GBSS1 expressed (Figure 5.2), consistent with amylose contents reported in other studies using different varieties of rice [26 25].

Figure 5.2. Expression of GBSS1 protein of each variety grown at either 30/20°C (H) or 25/19°C (L), or ambient (A) or elevated atm-CO_2 (E).

The molecular weight distributions (MWD) of linear chains from debranched molecules of starch in the Hot Water Soluble Fraction (HWSF) of flour are shown in Figure 5.3. Starch in the HWSF is predominantly amylose [30]. Amylose chains are those that elute above 100 degree of polymerization (DP) [30]. In the 30/20 ˚C treatments there is a decrease in the proportion of high molecular weight chains for both atm-CO_2 treatments (Figure 5.3). The number-average degree of polymerization of amylose chains ($\overline{X}_n$), weight-average degree of polymerization ($\overline{X}_w$) and polydispersity (Q) were determined from the MWD of linear amylose, and are presented in Table 5.3. For all varieties, high temperatures during grain filling reduced the $\overline{X}_w$ values for debranched amylose. Since amylose chains are essentially linear [52] this result indicates that the amylose chains are shorter at high temperature. Within each temperature treatment, elevated atm-CO_2 has no influence on the MWD of amylose chains for all the varieties.

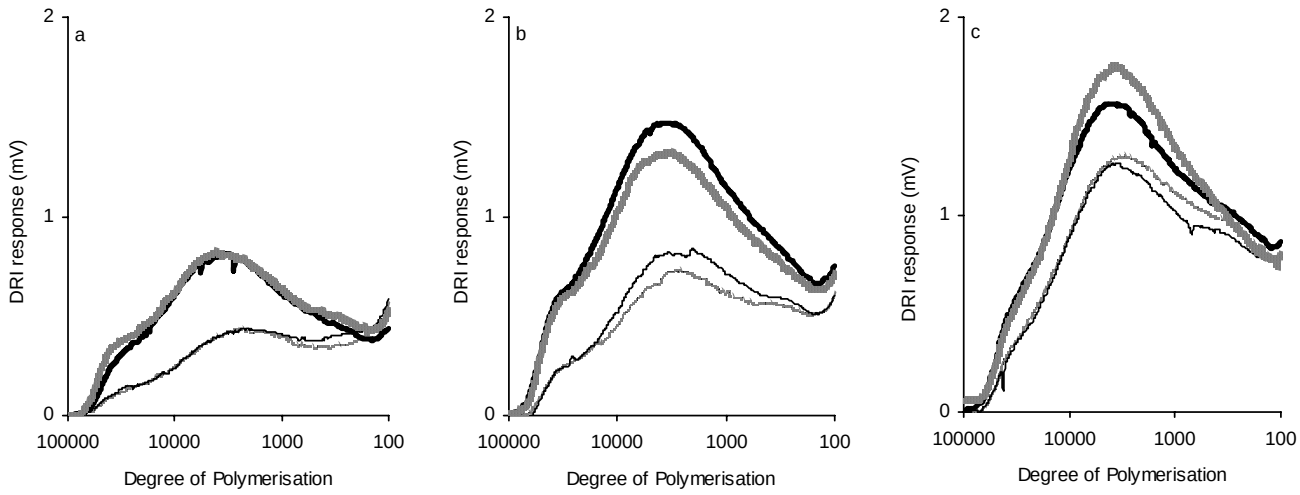

Figure 5.3. Molecular weight distributions of debranched amylose of the hot water soluble fraction from three varieties: (a) Amaroo, (b) Taipei 309 and (c) IR64. The four treatments include the 25/19 °C at 380 ppm atm-CO_2 (thick solid line), 25/19 °C at 780 ppm atm-CO_2 (thick dotted line), 30/20 °C at 380 ppm atm-CO_2 (thin solid line), and 30/20 °C at 780 ppm atm-CO_2 (thin dotted line).

The amount of amylose chains detected by SEC for the different treatments is consistent with the pattern of GBSS1 expression in Figure 5.2. A decrease in amylose is expected for Amaroo and Taipei 309, which both carry the Wx^b allele (Figure 5.4); expression of the Wx^b allele is known to be lower in high temperatures [3,51]. However, the decrease is completely unexpected for IR64 since it carries the Wx^a allele (Figure 5.4), which is reported to be unaffected by high temperatures [3]. This suggests that amylose is not the product of GBSS1 alone, but that transcription or translation of the Wx^a allele is regulated by some process that is susceptible to high temperatures, with a subsequent effect on the number and length of amylose chains. The differences in amylose content and structure will affect the way amylose contributes to cooking properties. Thus, a deeper level of knowledge of the factors that regulate amylose synthesis is necessary in order to maintain predictable cooking properties of rice as the world gets warmer.

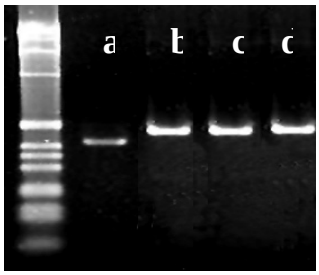

Figure 5.4. Agarose gel showing digested PCR product of the splice site of intron 1 of GBSS1. PCR product of IR64 (a) was digested, giving a band of 400 bp, indicating that it carries the Wx^a allele, and PCR product of Amaroo (b), Taipei 309 (c) and Shimizu mochi (d) was not digested, giving a band of 457 bp, indicating those varieties carry the *Wxb* allele. Image courtesy of Vito Burtado Jr (IRRI).

The viscosity trace shows three inflection points - the peak, trough and final viscosity - and the difference between trough and final viscosity defines the immediate retrogradation of the gel (Table 5.4). Immediate retrogradation describes the effect of the long linear chains of amylose on the formation of gel networks [48]. In the 30/20 ˚C treatments, the immediate retrogradation is smaller than for the 25/19˚C treatments (Table 5.4). This observation is simply attributed to the decrease in amylose chains, in particular the decrease in long chains which interact to form a gel on cooling [48]. Table 5.4 also shows that varying atm-CO_2 within a temperature, shows no difference in the trough and final viscosity and thus no difference in immediate retrogradation is observed. This result is consistent with the observed decrease in amylose chains, the $\overline{X}_w$ value of amylose chains, and expression of GBSS1 protein in higher temperatures, and the lack of effect of elevated atm-CO_2 on amylose and on these properties.

The structure of amylose also contributes to the hardness of rapidly retrograded gels [48 7]. Table 5.4 shows the hardness of retrograded gels made from rice flour from each treatment. There is no change in hardness for gel made from Shimizu mochi (which contains no amylose) in elevated temperature or elevated atm-CO_2, but for the other three varieties, there is a significant difference in hardness when made from grains from grown at elevated temperature (Table 5.4). Elevated atm-CO_2 did not affect hardness (Table 5.3). Again, the changes seen for the high temperature treatments are consistent with the decrease in GBSS1 protein and the decrease in synthesis of long chains of amylose in grains grown in elevated temperature.

The rheological changes that occur as a flour slurry becomes a gel relate to viscosity [53], HWS starch [50], gelatinization temperature and composition of the flour. The shear storage modulus (G′, or elastic modulus) is a direct measure of deformation because it is measured at constant stress. The visco-elastic nature of the sample is reflected in the phase angle (δ). The first change to occur is 10 ˚C below the gelatinization temperature when the samples move from a more viscous state (towards δ 90 ˚) to a more elastic state (towards δ 0 ˚). As gelatinization proceeds through the layers of the starch granules, G′ increases rapidly to maximum G′ (G'_{max}) and occurs within 10 ˚C of the gelatinization temperature (Table 5.4). G'_{max} is significantly higher for non-waxy rice

Table 5.4. The functional parameters of varieties grown across the four growth treatments with data presented as the Mean and Standard Error of the Mean (n = 7).

Parameter	Temperature	25/19°C	25/19°C	30/20°C	30/20°C
	Carbon Dioxide	380ppm	780ppm	380ppm	780ppm
Peak Viscosity (cP)	Amaroo	2334 ± 52	2438 ± 38	2839 ± 52	3000 ± 96*
	IR64	2152 ± 27	2117 ± 27	2254 ± 39	2334 ± 10
	Shimizu Mochi	1362 ± 49	1413 ± 41	1418 ± 63	1552 ± 24
	Taipei 309	2489 ± 37	2321 ± 50*	3019 ± 43	3157 ± 58
Trough Viscosity (cP)	Amaroo	1377 ± 37	1400 ± 24	1630 ± 43	1684 ± 67
	IR64	1236 ± 13	1265 ± 21	1440 ± 17	1468 ± 19
	Shimizu Mochi	661 ± 21	680 ± 24	785 ± 38	879 ± 14
	Taipei 309	1443 ± 29	1341 ± 55	1943 ± 34	1989 ± 62
Final Viscosity (cP)	Amaroo	2433 ± 47	2549 ± 34	2556 ± 42	2653 ± 71
	IR64	2744 ± 23	2806 ± 8	2847 ± 23	2885 ± 13
	Shimizu Mochi	701 ± 39	733 ± 18	633 ± 29	673 ± 21
	Taipei 309	2807 ± 45	2643 ± 77*	3135 ± 41	3194 ± 62
Gelatinization Temperature (˚C)	Amaroo	67.8 ± 0.3	67.8 ± 0.1	70.7 ± 0.2	71.1 ± 0.2
	IR64	73.4 ± 0.1	73.2 ± 0.1	76.3 ± 0.1	76.1 ± 0.1
	Taipei 309	65.8 ± 0.2	65.9 ± 0.5	69.5 ± 0.2	69.5 ± 0.3
	Shimizu Mochi	65.8 ± 0.1	65.8 ± 0.1	68.5 ± 0.1	68.4 ± 0.2
G'_{max}	Amaroo	40000 ± 400	37200 ± 3900	24800 ± 8600	31700 ± 700
	IR64	42300 ± 1700	46500 ± 11800	33500 ± 2500	36600 ± 2700
	Shimizu Mochi	3200 ± 400	3700 ± 200	2500 ± 140	3000 ± 600
	Taipei 309	39000 ± 2800	43800 ± 8800	36400 ± 5800	36000 ± 3500
Temperature of $G`_{max}$	Amaroo	78.5 ± 0.5	78.3 ± 0.4	78.9 ± 0.6	80.5 ± 0.9
	IR64	83.7 ± 1.3	83.7 ± 0.1	85.7 ± 0.1	83.0 ± 1.6
	Shimizu Mochi	72.6 ± 0.0	71.3 ± 1.3	74.0 ± 0.7	75.2 ± 0.9
	Taipei 309	76.7 ± 0.7	75.8 ± 1.2	77.1 ± 0.8	77.8 ± 1.6
Hardness (N)	Amaroo	0.74 ± 0.04	0.73 ± 0.03	0.59 ± 0.03	0.68 ± 0.02
	IR64	2.18 ± 0.05	1.95 ± 0.05	1.48 ± 0.05	1.63 ± 0.03
	Taipei 309	0.82 ± 0.06	0.77 ± 0.07	0.63 ± 0.03	0.59 ± 0.02
	Shimizu Mochi	0.13 ± 0.00	0.14 ± 0.00	0.16 ± 0.01	0.17 ± 0.01

* ANOVA, represents a significance to 5%

grown in cool temperatures than in elevated temperature (Table 5.4), despite the large standard errors; interaction between gelatinization and leaching events is reported to explain the large standard error of the G'_{max} measurement [53]. According to Hooke's Law of elasticity, the shear storage modulus is the inverse of strain or deformation, and as such, the higher the modulus the greater the resistance of the sample to deformation. The higher G'_{max} in the 25/19˚C treatment suggests that the paste/gel is more stable than that from the 20/30 ˚C samples, and highest in ambient than elevated atm-CO_2. This could be related to the longer amylose chains in the 25/19 ˚C treatment, since long chains aggregate and potentially stiffen the gel [48,50]. Also, grains from the 25/19 ˚C treatment are less chalky (Table 2); perhaps fully formed starch granules are more difficult to destroy than the immature starch granules found in chalky grains.

Thus, increasing concentrations of carbon dioxide are not likely to have any effect on either amylose synthesis, content or its functional properties. By contrast, global warming will decrease the ability of *temperate japonica* varieties to synthesize long amylose chains, with consequential impact on amylose content, structure and on the functional properties controlled by amylose. Unexpectedly, these data show that global warming could also affect amylose synthesis, with consequences for functional properties, in tropical germplasm. Given the contribution of amylose to functional properties, it becomes urgent to determine where the variability lies in temperature tolerance of either expression or regulation of the Wx^a allele. Combining elevated atm-CO_2 with elevated temperature did not counteract the effect of elevated temperature.

5.3.2.3 Amylopectin

The most informative method to understand amylopectin structure is to consider the metrics of a log-linear plot of the number distribution of debranched amylopectin as measured by capillary electrophoresis [54]. Figure 5.5 is an example of the log-linear plot which is independent of normalisation and the slops are defined by two non-random chain stoppage events, s_1 and s_3, and two random stoppage events s_2 and s_4 [54].

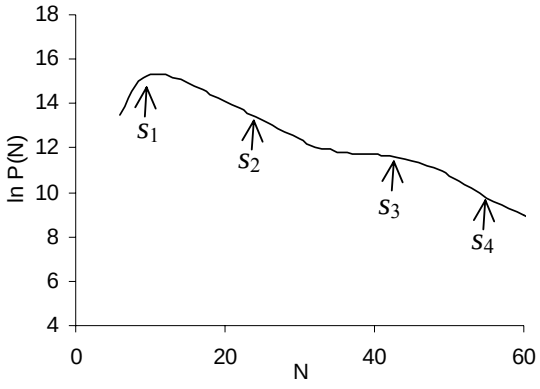

Figure 5.5. An example of a log-linear plot derived from data collected from a Capillary Electrophoresis. The labels denote the slope metrics of the plot.

The metrics derived from the plot for Taipei 309 grown in the four environments will be discussed (Table 5.5 and Figure 5.6). When Taipei 309 was grown in high temperature during grain-filling the value of s_3 and s_4 is larger than that grown at ambient temperatures (Table 5.5). There is no change in the metrics between atm-CO_2 treatments within a temperature trial. A change in the s_3 metric is suggestive of an interruption in the synthesis of chains that extend across two lamellae, that is, across region 2 and 4. Therefore, the non-random event, chain-length dependent that is defined by s_3 metric is implicated in the crystallisation of single clusters in the amylopectin molecule [54]. A more positive value for s_3 indicates that the magnitude of the non-random control is higher [54], and so indicates that the processes driving crystallization of the cluster differ when amylopectin synthesis occurs in high temperature. In high temperatures, the proportion of B chains on amylopectin are reported to increase [20] but the value of s_2, which describes the kinetics of synthesis of chains within a cluster, DP12 – 30, is not affected by high temperature (Table 5.5). This indicates that the activity of the network of alleles that produces single-cluster chains is either unaffected by elevated temperature or can compensate if part of the network is affected. The enzyme that synthesizes short chains on amylopectin, starch synthase I (SSI) is reported to be sensitive to high temperatures [55]. In SSI mutants of rice, the absence of SS1 activity increases chains DP 6-7, decreases chains of DP 8-12 and increases chains of DP 16-19 [56].

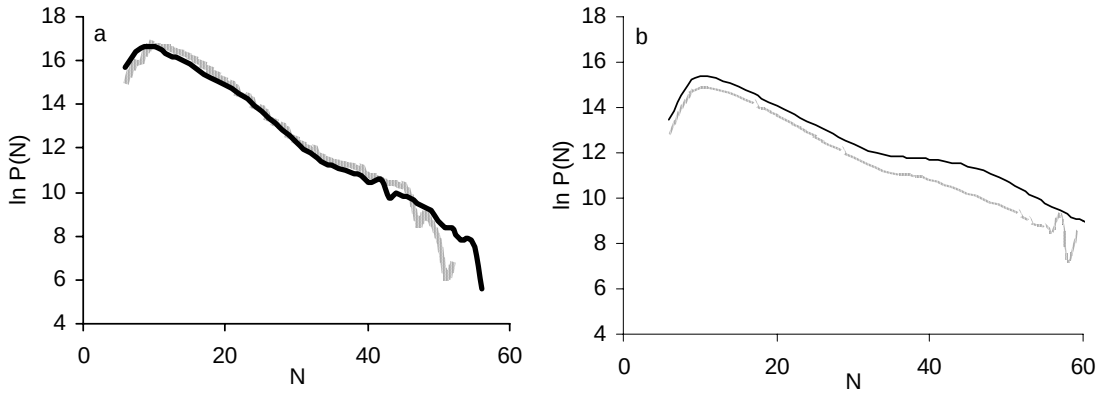

Figure 5.6 : Number distribution of debranched amylopectin from Taipei 309. The four treatments include (a) the 25/19 °C at 380 ppm atm-CO_2 (thick solid line) and 25/19 °C at 780 ppm atm-CO_2 (thick dotted line) and (b) the 30/20 °C at 380 ppm atm-CO_2 (thin solid line) and 30/20 °C at 780 ppm atm-CO_2 (thin dotted line) treatments.

Table 5.5. The slope metrics for debranched amylopectin based on the plot in Figure 5.6.

Variety	Temperature	25/19 °C	25/19 °C	30/20 °C	30/20 °C
	Carbon Dioxide	380 ppm	780 ppm	380 ppm	780 ppm
Taipei 309	s_1	0.229	0.266	0.283	0.253
	s_2	-0.237	-0.248	-0.165	-0.181
	s_3	-0.159	-0.130	-0.048	-0.061
	s_4	-0.412	-0.574	-0.179	-0.252

The slope of the metric is a ratio of growth and stoppage events. The s_4 metric for Taipei 309 is steeper for the 25/19 °C than the 30/20 °C at both atm-CO_2 levels (Table 5.5). This indicates that at 25/19°C there is a greater ratio of stoppage events which suggests that few chains extend to the second lamellae and there would be more chains per cluster [54]. In the 30/20 °C treatment, there are comparatively more growth events suggesting that chains do extend into the second lamellae to create amylopectin molecules with more than one cluster [57].

Gelatinisation temperature (GT) is an important trait of grain quality that defines the temperature that starch crystals melt, the temperature granules lose their macro structure, and the suitability of grains for industrial processes. In essence, GT defines cooking time [19]. Power emissions contribute 24 % of greenhouse gas emissions (Stern Review 2006), therefore adopting selection practices for shorter-cooking rice is another way that rice improvement programs can contribute to minimizing and remediating the effect of climate change. Table 5.4 shows that there are no differences in GT between atm-CO_2 treatments, but high growth temperatures increase GT by 3 °C - a result seen in many studies [20,23], and which would lengthen cooking time [19]. The increase in GT is consistent with the observed increase in the value of s_3, which is related to the processes that regulate crystallization [54]. Starch synthase IIa (SS11a) is an enzyme whose activity contributes significantly to GT. Four haplotypes of SS11a have been described [58], two that consistently segregate with low GT and two that consistently segregate with high GT [58-61]. Analysis of the data in those studies shows that low GT alleles are sprinkled throughout temperate and tropical germplasm. For varieties carrying low GT alleles, high temperature causes GT to rise to an intermediate value (Table 5.5); intermediate GT is actively selected for in rice improvement programs for tropical germplasm [45]. Therefore, genetic options are already possible for avoiding the effect of global warming on this trait.

5.4 CONCLUSION

This is the first study that comprehensively explores the potential impact of climate change on the parameters of rice grain quality, from structure of the grain at several levels through to the functional properties and potential economic impact. The data indicate that the effect of global warming will be negative on almost all rice quality traits. In increased temperatures during the grain-filling period chalkiness increases, the starch composition and structure are damaged which leads to unexpected functional properties of the grain such as viscosity and gelatinisation temperature. Elevated atm-CO_2 neither affects quality alone, nor counteracts many of the effects of elevated temperatures. The distribution of chalk is decreased in elevated atm-CO_2. Allelic options that are currently available to protect the economically and functionally important traits of quality against the effects of climate change have been identified, particularly in germplasm that has actively been selected for adaptation to hot dry climates, and allelic options that require discovery have also been identified.

5.5 REFERENCES

1. Sano, Y. Differential regulation of waxy gene expression in rice endosperm. *Theor. Appl. Genet.* **68**, 467-473 (1984).
2. Wang, Z.-Y., Zheng, F.-Q., Shen, G.-Z., Gao, J.-P., Snustad, D.-P., Li, M.-G., Zhang, J.-L. & Hong, M.-M. The amylose content in rice endosperm is related to the post-transcriptional regulation of the *waxy* gene. *Plant Journal* **7**, 613 - 622 (1995).
3. Larkin, P. D. & Park, W. D. Transcript accumulation and utilisation of alternate and non-concensus splice sites in rice granule-bound synthase are temperature-sensitive and controlled by a single-nucleotide polymorphism. *Plant Molecular Biology* **40**, 719-727 (1999).
4. Martin, M. & Fitzgerald, M. A. Proteins in rie gains influence cooking properties. *J. Cereal Sci.* **36**, 285 - 294 (2002).
5. Kim, H. Y., Lieffering, M., Miura, S., Kobayashi, K. & Okada, M. Growth and nitrogen uptake of CO_2-enriched rice under field conditions. *New Phytologist* **150**, 223-229 (2001).
6. Morrison, W. R. Starch lipids and how they relate to starch granule structure and functionality. *Cereal Foods World* **40**, 437 (1995).
7. Philpot, K., Martin, M., Burtado Jr., V., Willoughby, D. & Fitzgerald, M. A. Environmental factors that affect the ability of amylose to contribute to retrogradation in gels made from rice flour. *J. Agric. Food Chem.* **54**, 5182-5190 (2006).
8. Stern, N. *Stern Review: The Economics of Climate Change* (Cambridge University Press, Cambridge, 2006).
9. Rowland-Bamford, A. J., Baker, J. T., Allen Jr, L. H. & Bowes, G. Acclimation of rice to changing atmospheric carbon dioxide concentration. *Plant, Cell and Environment* **14**, 577 - 583 (1991).
10. Nakano, H., Makino, A. & Mae, T. The effect of elevated partial pressure of carbon dioxide on the relationship between photosynthetic capacity and N content in rice leaves. *Plant Physiol.* **115**, 191-198 (1997).
11. Amthor, J. S. Perspective on the relative insignificance of increasing atmospheric CO_2 concentration to crop yield. *Fields Crop Research* **58**, 109-127 (1998).
12. Jitla, D. S., Rogers, G. S., Seneweera, S. P., Basra, A. S., Oldfield, R. J. & Conroy, J. P. Accelerated early growth of rice at elevated CO2: is it related to developmental changes in the shoot apex ? *Plant Physiol.* **115**, 15 - 22 (1997).
13. Yoshida, S. *Fundamentals of Rice Crop Science* (International Rice Research Institute, Los Banos, Laguna, 1981).
14. De Costa, W. A. J. M., Weerakoon, W. M. W., Herath, H. M. L. K. & Abeywardena, R. M. I. Response of growth and yield of rice (*Oryza sativa*) to elevated atmospheric carbon dioxide in the subhumid zone of Sri Lanka. *J. Agronomy and Crop Science* **189**, 83 - 95 (2003).
15. Sheehy, J. E., Dionora, M. J. A. & Mitchell, P. L. Spikelet numbers, sink size and potential yield in rice. *Fields Crop Research* **71**, 77- 85 (2001).
16. Yoshimoto, M., Oue, H. & Kobayashi, K. Energy balance and water use efficiency of rice canopies under free-air CO_2 enrichment. *Agricultural and Forest Meteorology* **133**, 226 - 246 (2005).

17. Horie, T., Matsuura, S., Takai, T., Kuwasaki, K., Ohsumi, A. & Shiraiwa, T. Genetic difference in canopy diffusive conductance measured by a new remote-sensing method and its association with the difference in rice yield potential. *Plant Cell and Environment*, 1-8 (2005).

18. Peng, S., Huang, J., Sheehy, J. E., Laza, R. C., Visperas, R. M., Zhong, X., Centeno, G. S., Khush, G. S. & Cassman, K. G. Rice yields decline with higher night temperature from global warming. *PNAS* **101**, 9971 - 9975 (2004).

19. Juliano, B. O. *Rice: Chemistry and Technology* (ed. Juliano, B. O.) (St. Pauls, Minnesota, 1985).

20. Asaoka, M., Okuno, K., Sugimoto, Y., Kawakami, J. & Fuwa, H. Effect of environmental temperature during development of rice plants on some properties of endosperm starch. *Starch/Starke* **36**, 189 - 193 (1984).

21. Lisle, A., Martin, M. & Fitzgerald, M. A. Chalky and translucent rice grains differ in starch composition and structure and cooking properties. *Cereal Chemistry* **77**, 627 - 632 (2000).

22. Jiang, H., Dian, W. & Wu, P. Effect of high temperature on the fine structure of amylopectin in rice endosperm by reducing the activity of the starch branching enzyme. *Phytochemistry* **63**, 53 - 59 (2003).

23. Zhong, L.-j., Cheng, F.-m., Wen, X., Sun, Z. X. & Zhang, G. P. The deterioration of eating and cooking quality caused by high temperature during grain filling in early-season *indica* rice cultivars. *Journal of Agronomy and Crop Science* **191**, 218 - 225 (2005).

24. Seneweera, S. P., Blakeney, A., Milham, P., Basra, A. S., Barlow, E. W. R. & Conroy, J. P. Influence of rising atmospheric CO_2 and phosphorus nutrition on the grain yield and quality of rice (*Oryza sativa* cv. Jarrah). *Cereal Chemistry* **73**, 239 - 243 (1996).

25. Ziska, L. H., Namuco, O., Moya, T. & Quilang, J. Growth and yield response of field-grown tropical rice to increasing carbon dioxide and air temperature. *Agron. J.* **89**, 45- 53 (1997).

26. Terao, T., Miura, S., Yanagihara, T., Hirose, T., Nagata, K., Tabuchi, H., Kim, H.-Y., Lieffering, M., Okada, M. & Kobayashi, K. Influence of free-air CO_2 enrichment (FACE) on the eating quality of rice. *J. Sci. Food Ag.* **85**, 1861 - 1868 (2005).

27. *Rice Almanac* (eds. Maclean, J. L., Dawe, D. C., Hardy, B. & Hettel, G. P.) (International Rice Research Institute, 2002).

28. Seneweera, S. P. & Conroy, J. P. Growth, grain yield and quality of rice (*Oryza sativa* L.) in response to elevated CO_2 and phosphorus nutrition. *Soil Sci. Plant Nutr.* **43**, 1131-1136 (1997).

29. Castro, J. V., Ward, R. M., Gilbert, R. G. & Fitzgerald, M. A. Measurement of the molecular weight distribution of debranched starch. *Biomacromolecules* **6**, 2260 - 2270 (2005).

30. Ward, R. M., Gao, Q., de Bruyn, H., Gilbert, R. G. & Fitzgerald, M. A. Improved methods for the structural analysis of the amylose-rich fraction from rice flour. *Biomacromolecules* **7**, 866 - 876 (2006).

31. Echt, C. S. & Schwartz, D. Evidence for the inclusion of controlling elements within the structural gene at the waxy locus in maize. *Genetics* **99**, 275 - 284 (1981).

32. Fulton, T. M., Chunwongse, J. & Tanksley, S. D. Microprep protocol fpr extraction of DNA deom tomato and other herbaceous plants. *Plant Molecular Biology Rep.* **13**, 207-209 (1995).

33. Han, Y., Xu, M., Liu, X., Yan, C., Korban, S. S., Chen, X. & Gu, M. Genes coding for starch branching enzymes are major contributors to starch viscosity characteristics in waxy rice (*Oryza sativa* L.). *Plant Science* **166**, 357 - 364 (2004).

34. Batey, I. L. & Curtin, B. M. Measurement of amylose/amylopectin ratio by high-performance liquid chromatography. *Starch* **48**, 338-344 (1996).

35. O'Shea, M. G., Samuel, M. S., Konik, C. M. & Morell, M. K. Fluorophore-assisted carbohydrate electrophoresis (FACE) of oligosaccharides: efficiency of labelling and high-resolution separation. *Carbohydrate Research* **307**, 1 - 12 (1998).

36. McCouch, S. R., Sweeney, M., Li, J., Jiang, H., Thomson, M., Septiningsih, E., Edwards, J., Moncada, P., Xiao, J., Garris, A., Tai, T., Martinez, C., Tohme, J., Sugiono, M., McClung, A. M., Yuan, L. P. & Ahn, S.-N. Through the genetic bottleneck: *O. rufipogon* as a source of trait-enhancing alleles for *O. sativa*. *Euphytica* **154**, 317-339 (2006).

37. Tashiro, T. & Wardlaw, I. F. The effect of high temperature on kernel dimensions and the type and occurence of kernel damage in rice. *Aust. J. Agric. Res.* **42**, 485-496 (1991).

38. Childs, N. W. in *Rice: Chemistry and Technology* (ed. Champagne, E. T.) 1 - 23 (AACC, St. Paul, Minnesota, 2004).

39. Baker, J. T., Allen Jr, L. H., Boote, K. J. & Pickering, N. B. Rice responses to drought under carbon dioxide enrichment. 2. Photosynthesis and evapotranspiration. *Global Change Biology* **3**, 129 - 138 (1997).

40. Jenner, C. F. Starch synthesis in the kernel of wheat under high temperature conditions. *Aust. J. Plant Physiol.* **21**, 791 - 806 (1994).

41. Resurreccion, A. P., Hara, T., Juliano, B. O. & Yoshida, S. Effect of temperature during ripening on grain quality of rice. *Soil Sci. Plant Nutr.* **23**, 109 - 112 (1977).

42. Tamaki, M., Ebata, M., Tashiro, T. & Ishikawa, M. Physio-ecological studies on quality formation of Rice Kernel. I. Effects of nitrogen top-dressed at full heading time and air temperature during ripening period on quality of rice kernel. *Japanese Journal of Crop Science* **58**, 653 - 658 (1989).

43. Juliano, B. O. Factors affecting nutritional properties of rice protein. *Transactions of the National Academy of Science and Technology, Republic of the Philippines* **7**, 205 - 216 (1985).

44. Leesawatwong, M., Jamjod, S., Kuo, J., Dell, B. & Rerkasem, B. Nitrogen fertilizer increases seed protein and milling quality of rice. *Cereal Chemistry* **82**, 588-593 (2005).

45. Juliano, B. O., Cagampang, G. B., Lourdes, J. C. & Santiago, R. G. Some Physicochemical properties of rice in southeast Asia. *Cereal Chemistry* **41**, 275 - 286 (1964).

46. Ziska, L. H., Manalo, P. A. & Ordonez, R. A. Intraspecific variation in the response of rice (*Oryza sativa* L.) to increased CO_2 and temperature: growth and yield reponse of 17 cultivars. *J. Experimental Botany* **47**, 1353 - 1359 (1996).

47. Fitzgerald, M. A., Martin, M., Ward, R. M., Park, W. D. & Shead, H. J. Viscosity of rice flour: A rheological and biological study. *Journal of Agricultural and Food Chemistry* **51**, 2295-2299 (2003).

48. Gidley, M. J. Molecular mechanisms underlying amylose aggregation and gelation. *Macromolecules* **22**, 351 - 358 (1989).

49. Nguyen, Q. D., Jensen, C. T. B. & Kristensen, P. G. Experimental modelling studies on the flow properties of maize and waxy maize starch pastes. *Chemical Engineering Journal* **70**, 165 - 171 (1998).

50. Tsai, M.-L. & Lii, C.-y. Effect of Hot-water-soluble Components on the Rheological Properties of Rice Starch. *Starch* **52**, 44 - 53 (2000).

51. Sano, Y., Maekawa, M. & Kicuchi, H. Temperature effects on the *Wx* protein level and amylose content in the endosperm of rice. *J. Hered.* **6**, 221 -222 (1985).

52. Hizukuri, S., Takeda, Y., Yasuda, M. & Suzuki, A. Multi-branched nature of amylose and the action of de-branching enzymes. *Carbohydrate Research* **94**, 205 - 213 (1981).

53. Svegmark, K. & Hermansson, A.-M. Changes induced by shear and gel formation in the viscoelastic behaviour of potato, wheat and maize starch dispersions. *Carbohydrate Polymers* **15**, 151 - 169 (1991).

54. Castro, J. V., Dumas, C., Chiou, H., Fitzgerald, M. A. & Gilbert, R. G. Mechanistic information from analysis of molecular weight distributions of starch. *Biomacromolecules* **6**, 2248-59 (2005).

55. Keeling, P. L., Banisadr, R., Barone, L., Wasserman, B. P. & Singletary, G. W. Effect of temperature on enzymes in the pathway of starch biosynthesis in developing wheat and maize grain. *Aust. J. Plant Physiol.* **21**, 807-827 (1994).

56. Fujita, N., Yoshida, M., Asakura, N., Ohdan, T., Miyao, A., Hirochika, H. & Nakamura, Y. Function and characterisation of starch synthase I using mutants in rice. *Plant Physiology* **140**, 1070 -1084 (2006).

57. Takeda, Y., Shibahara, S. & Hanashiro, I. Examination of the structure of amylopectin molecules by fluorescent labelling. *Carbohydrate Research* **338**, 471 - 475 (2003).

58. Waters, D. L. E., Henry, R. J., Reinke, R. F. & Fitzgerald, M. A. Gelatinization temperature or rice explained by polymorphisms in starch synthase. *Plant Biotechnology Journal* **4**, 115 - 122 (2006).

59. Umemoto, T., Aoki, N., Lin, H., Nakamura, Y., Inouchi, N., Sato, Y., Yano, M., Hirabayashi, H. & Maruyama, S. Natural variation in rice starch synthase IIa affects enzyme and starch properties. *Functional Plant Biology* **31**, 671 - 684 (2004).

60. Umemoto, T. & Aoki, N. Single-nucleotide polymorphisms in rice starch synthase IIa that alter starch gelantinisation and starch association of the enzyme. *Functional Plant Biology* **32**, 763 - 768 (2005).

61. Nakamura, Y., Francisco Jr., P. B., Hosaka, Y., Sato, A., Sawada, T., Kubo, A. & Fujita, N. Essential amino acids of starch synthase SSIIa differentiate amylopectin structure and starch quality between *japonica* and *indica* rice varieties. *Plant Molecular Biology* **58**, 213 - 227 (2005).

Chapter 6

Potential impact of temperature and carbon dioxide on rice quality

The increase in global temperatures and carbon dioxide levels has the potential to threaten the rice industry with a decrease in yield already noted in literature. Of the little information known about the impact of temperature on grain quality, no measures to maintain accepted qualities in the long term are in place. Very little is known about the potential impact of carbon dioxide alone or with increased temperature. Thus the major objectives of this thesis were to fill these gaps in knowledge. Grain quality is largely governed by the structure of starch, yet the methods to characterise starch have not been revised alongside advances in technology and theories to understand molecular weight distribution (MWD). As such, the first objective of this thesis became a re-evaluation of the characterisation of starch.

Starch is a natural polymer that is governed by the molecular weight theories of polymer chemistry, yet these theories are not usually applied to the hydrodynamic volume distributions obtained from the separation of starch by Size Exclusion Chromatography (SEC). Chapter 2 began with an explanation of the error associated with the current presentation of SEC data throughout literature; in particular the need to calibrate the SEC became apparent. With an understanding of the molecular weight distribution theory, it was shown that the MWD of debranched amylopectin was considerably underestimated without universal calibration. Further, the ability to extract quantitative rather than qualitative information from the SEC distribution was highlighted. This has lead to the ability to have a more accurate means to characterise debranched amylopectin.

The structure of amylose is believed to largely define many quality traits of rice. Amylose is difficult to characterise because it is impossible to isolate without causing structural damage, amylose is unstable in aqueous solutions and not known to be completely debranched by isoamylase, and the analysis of amylose by SEC has not been assessed. In Chapter 3, a hot water soluble fraction of flour containing an amylose-rich fraction was used to assess these problems. Analysis of the HWSF was found to be reproducible by SEC, but a loss of 20% carbohydrate identified as high molecular weight by both iodine binding and multi-angle laser light scattering during analysis is extremely worrying and is the focus of urgent work. Similar to the analysis of debranched amylopectin in Chapter 2, it was found that the MWD of debranched amylose is underestimated without the appropriate calibration of the SEC system. Furthermore, it was resolved that isoamylase can completely debranch amylose and that it was inappropriate analytical techniques that lead to the contrary belief. Overall this work improved the accuracy and confidence in the characterisation of amylose.

With the much needed revision of the methods to characterise starch, it became possible to explore the potential impacts of increased temperature and carbon dioxide on rice quality. Twelve rice varieties were grown in each of three temperature regimes, and at maturity analysed for a

range of amylose based quality traits including the expression of Granule Bound Starch Synthase I (GBSSI), amylose content and structure, and a parameter of viscosity. On this basis, the phenotypes of the twelve varieties response to temperature could be divided into three categories. Group 1 maintained the same phenotype across all temperature regimes, Group 2 showed sensitivity to high temperature by yielding a poor grain quality at high temperatures, and a third group shared the phenotype of Group1 varieties at lower temperatures and Group 2 varieties in warmer temperatures. A single nucleotide polymorphism at the splice site of intron 1 was thought to explain the difference between Group 1 and Group 2 varieties, but is unable to explain the third group. In this study, a secondary polymorphism within intron 1 of the *Waxy* gene has been identified and a mechanism proposed to explain the origin of the third category of varieties. This second polymorphism needs to be tested amongst a broad dataset before it is routinely used. The designation of a single nucleotide polymorphism to explain a phenotype allows a molecular based screening process that can analyse more than 90 samples per day, and provide breeders with valuable information about the performance of current and new rice cultivars in the future climate.

After temperature, carbon dioxide is another abiotic stress with the potential to impact on the rice industry. A broad range of quality traits were examined after varieties were grown in a range of temperature and carbon dioxide regimes. In general the varieties showed a decrease in the overall quality of the grain, with carbon dioxide doing very little to alleviate the loss in grain quality. Interestingly, the distributions of chalk improved in conditions of elevate carbon dioxide with more grains showing less chalk; a result worthy of further work. This work also highlighted the need to repeat the same experiment in a range of soil nitrogen levels to understand the real contribution of nitrogen to the growth dynamic of elevated temperature and carbon dioxide levels.